Shigeko Haruyama · Toshihiko Sugai
Editors

Natural Disaster and Coastal Geomorphology

Springer

Natural Disaster and Coastal Geomorphology

Shigeko Haruyama · Toshihiko Sugai
Editors

Natural Disaster and Coastal Geomorphology

Springer

Editors
Shigeko Haruyama
Mie University
Tsu
Japan

Toshihiko Sugai
The University of Tokyo
Tokyo
Japan

ISBN 978-3-319-33812-5 ISBN 978-3-319-33814-9 (eBook)
DOI 10.1007/978-3-319-33814-9

Library of Congress Control Number: 2016940115

Printed on acid-free paper

This Springer imprint is published by Springer Nature
The registered company is Springer International Publishing AG Switzerland

Preface

Flooding, tsunami, and earthquake are important natural disaster issues for local people to understand the disaster process and to make evacuation method and reconstruction method in discussion in each local participant. The disaster mitigation research is needed for us to continue to better living together in nature. The geographers have been discussing natural disaster science and finding out the appropriate methodology of disaster mitigation program with disaster risk assessment and hazard mapping or risk mapping. Utilizing geographical information system and satellite remote sensing, the current situation of hazardous regions has been clarified and visualized in the global scale and the resuscitation or restoration process in local scale after natural disaster has been discussed with geographical views.

In geographical view, natural disaster should be dealt with more comprehensive between human dimensions, including social science, human science, psychology under natural disaster, gender, and minority science in natural disaster, and physical dimensions including geomorphology, climatology, vegetation geography, and hydrology in integration. Human dimension of disaster science is the important analysis process for clarification toward future regional planning both urban and rural coupling for disaster mitigation. Thus, the substantial reduction of disaster risk and losses in lives has been discussed for long period but the quality of natural disaster has been rapidly changed with transformation for growth to immense under the global environmental change in specific Asia region. The recent rapid land use change and land cover change are the other factors for a tendency toward great size in disaster in the world because of human disturbance on earth surface.

Geomorphology tried to explain that the natural disaster process continues on the specific locations in land forming and repeated damage in selected sites. Also, geomorphology should make to understand the natural disaster occurrence nature-oriented process on each site. If we have an appropriate information or knowledge of geomorphology of coastal and fluvial plains in each living region, the disaster mitigation planning should be more harmonious with nature in future. The hazard map and risk map are now open for all in several Web sites of local

government offices in Japan, but these were not used for understanding the study for place features before natural disaster. After natural disaster occurrence, these maps are remembered for confirmation of disaster location and the knowledge of natural disaster process. The knowledge of geomorphology would support evacuation on site and lifestyle before disaster occurrence.

In January 2015 and March 2015, the Tokyo Conference on International Study for Disaster Risk Reduction and Resilience was held in Tokyo and the 3rd World Conference on Disaster Risk Reduction was held in Sendai city, respectively. In the two international disaster risk reduction symposiums, the importance of science and technology for future disaster mitigation was discussed for future sustainability.

We, all of authors contributed this book chapters, are desirous of conveying a mitigation message in the voice of coastal and fluvial geomorphology in Japan. Geomorphologic knowledge is connected to professional reciters of natural disaster. 2011 Eastern Japan Earthquake was one of the historical memorized natural disasters in Japan, and we should convey several messages and lessons for future mitigation and prevention action. In this publication, we tried to explain coastal geomorphology related to natural disaster in specific tsunami, and in the final, all of regional planners should make a challenge to future suitable regional planning in the study area with offering up a silent prayer for disaster area in Eastern Japan coastal area. Still now, the discussion between residents and government with distinguished academic experts has been continued and we should present geomorphologic data for these discussion.

We express our thanks the opportunity for conveying message from geomorphologic narration by Springer.

Shigeko Haruyama
Toshihiko Sugai

Acknowledgments

We express our thanks to local offices that provided statistical data for analysis and to local people who participated in the field survey with questionnaire of disaster damage and evacuation system in the community level activities. We also thank the JSPS (KAKENHI Grant Nos. A 24240114, A 24248039, B15H04565, B26282078, and B26750106 for young scientist), International Research Institute of Disaster Science, Tohoku University, and Japan Geographic Data Center for the financial support.

Shigeko Haruyama
Toshihiko Sugai

Contents

Editors and Contributors

About the Editors

Shigeko Haruyama Professor Dr. of Department of Environmental Science and Technology, Graduate School of Bioresources, Mie University. She got Ph.D., Department of Agricultural Engineering, Graduate School of Agriculture, the University of Tokyo. Graduated from the University of Tokyo, she worked as as associate professor in the Department of Geography of the Faculty of Education, Waseda University, and then moved to graduate school of frontier science, the University of Tokyo, as an associate professor. She is working IGU chair of commission on hazard and risk. The special field is fluvial geomorphology and natural disaster in monsoon Asia and the following books and papers are her main publications; S. Haruyama eds. (2013) "Coastal Geomorphology and Vulnerability of Disaster towards disaster risk reduction." TERRA PUB Publisher, S. Haruyama and Kay Thwe Hliang (2013) "Morphometroic Analysis of the Bago River Basin." TERRAPUB Publisher. S. Haruyama and T. Shiraiwa (2014) "Environmental Change and the Social Response of the Amur River Basin", Springer.

Toshihiko Sugai Professor, Department of Natural Environmental Studies, Graduate School of Frontier Sciences, the University of Tokyo. He got BA in 1987, Ph.D. in 1994 from Department of Geography, Faculty of Science, The University of Tokyo (UT). Assistant Professor of Department of Human Geography, UT, 1993–96, Senior researcher, Active Fault Research Center, Geological Survey of Japan, 1996–99. He is a physical geographer and his interest is Quaternary environmental changes, fluvial and tectonic geomorphology. He published articles with his advisees in *Quaternary International, Bulletin of Seismological Society of America, Geomorphology, Marine Geology*, etc. Recent publication is Sugai T., Novenko, E.U. et al eds. "Environment evolution and human activity in the late Quaternary" in *Geographical Review of Japan* (2015)

Contributors

Tomoya Abe Postdoctoral Researcher, Marine Geology Research Group, Institute of Geology and Geoinformation, Geological Survey of Japan. He received Ph.D. in geography at Graduate School of Environmental Studies, Nagoya University, 2015. He is a physical geographer and his research focuses on sediment transport and landform change by extreme events such as tsunami storm and flood.

Shizuka Hashimoto Associate Professor, Dr. Graduate School of Agricultural and Life Sciences, the University of Tokyo. Graduated from the University of Tokyo (Ph.D., Agriculture). After graduation, he worked for the University of Tokyo, Massachusetts Institute of Technology, as a postdoctoral fellow granted by Japanese Society for Promotion of Sciences (JSPS), and for National Institute for Environmental Studies of Japan as a NIES special researcher, Kyoto University, as an associate professor, before joining the University of Tokyo. His research interests are on various issues associated with the sustainability of social and ecological production system, with special interests on the role of institutions and human behaviors, including land use planning, disaster management, and ecosystem management.

Keita Honda Teacher of the geography of Musashi high school and junior high school in Tokyo. He got Ph.D. from Department of Natural Environmental Studies, Graduate School of Frontier Sciences, the University of Tokyo, 2014. His interest is fluvial and coastal geomorphology and geographical education. His published paper is in *Transactions, Japanese Geomorphological Union* (2011).

Kazuaki Hori Associate Professor, Department of Geography, Graduate School of Environmental Studies, Nagoya University. He got BA from Department of Geography, Faculty of Science, the University of Tokyo, in 1996 and Ph.D. from Department of Earth and Planetary Science, Faculty of Science, the University of Tokyo, in 2001. His professional carrier includes a lecturer and an associate professor of Faculty of Science and Technology, Meijo University. He is a physical geographer and his research focuses on fluvial and coastal landform evolution and Quaternary environment change. He published many articles, for example, *Journal of Sedimentary Research* (2002), *Geophysical Research Letters* (2007) and is the author of "*Classification, Architecture, and Evolution of Large-river Deltas" in Large Rivers: Geomorphology and Management* (2008).

Yuichi Niwa Assistant Professor, Division of Disaster Science, International Research Institute of Disaster Science, Tohoku University. He got BA from Department of Geography, Faculty of Science, the University of Tokyo, in 2007 and Ph.D. from Department of Natural Environmental Studies, Graduate School of Frontier Sciences, the University of Tokyo, in 2012. He is a physical geographer and his interest is fluvial and coastal landform evolution and tectonic geomorphology. He published articles such as *Quaternary International* (2011) and *Bulletin of the Seismological Society of America* (2012).

Hiroshi Shimazu Professor, Department of Geography, Faculty of Geo-environmental Sciences, Rissho University. He got Ph.D. from the University of Tokyo in 1993. After graduation, he worked as an assistant professor, Department of History, at Kanazawa University. Since 1996, he has worked in Rissho University. He is physical geographer. His main subject is fluvial geomorphology and debris transport processes along the rivers in mountain region. His papers are published in the journal of *Transactions, Japanese Geomorphological Union*.

Chapter 1
Introduction—Overview of Natural Disasters and Coastal Landforms

Shigeko Haruyama

Abstract Asia and the Pacific regions are exposed to severe natural disasters because many densely populated cities are sited on coastal plains. The geomorphic features in coastal areas have a key role in defining the risk levels and the vulnerability to natural disasters of coastal regions. Rapid land-use changes in recent decades have forced a transformation in risk assessment to approaches that analyze and evaluate the relationship between social structures and natural disasters. Disaster resilience should incorporate more insight into social structures and more local community activities as the next advance in disaster mitigation. The 2011 East Japan (Tohoku Japan) earthquake has presented many lessons for consideration by regional land-use planners regarding the relationship between geomorphology and tsunami damage, and the appropriate activities of local communities. In this introduction chapter, the author illustrates the relationship between a natural disaster and coastal geomorphology by using the response of the lower Abukuma River basin to the tsunami that followed the 2011 East Japan earthquake. The damage caused by the earthquake and tsunami took different forms on each type of coastal landform and demanded specific responses from the relevant social structures, including evacuation activities. Future regional planning for disaster mitigation should incorporate scientific knowledge of coastal geomorphology.

Keywords Natural disaster · Coastal landform · Flood reduction · Regional planning

S. Haruyama (✉)
Graduate School of Bioresources, Mie University, 1577 Kurimachiyacho, Tsu, Mie 614-8507, Japan
e-mail: haruyama@bio.mie-u.ac.jp

S. Haruyama and T. Sugai (eds.), *Natural Disaster and Coastal Geomorphology*, DOI 10.1007/978-3-319-33814-9_1

1.1 Recent Natural Disasters in Asia

Asia–Pacific region is prone to natural disasters of many kinds. Its coasts are exposed to typhoons, the Baiu pattern of spring rains, cyclonic disturbances and monsoons, and Tsunami intrusion with earthquake. The great Nepal earthquake of 2015 was the latest reminder that the active tectonic environment of Himalayan range in Asia also threatens the region with geologic hazards with large number of victims. Several recent disasters have had strong connections to the fluvial and coastal geomorphology of Asia.

In 2004, the giant Sumatra–Andaman Islands earthquake caused widespread damage, and the ensuing tsunami inundated coastlines across the entire Indian Ocean basin (Umitsu and Takahashi 2007). Phuket Island in southern part of Thailand was suffered some of the most severe damage from tsunami intrusion, and a large number of foreign visitors and local residents living in the pocket beaches of Phuket resort areas fell victim because of their ignorance of tsunamis. The evacuation processes in each pocket beaches were different concerning with local community activities related with religious networking. The grappling of recovery and rehabilitation of each town located on pocket beaches of Phuket Island facing the Andaman Sea took a long time after tsunami disaster. However, the community-based activities and special religious community party were important roles of evacuation process and subsisting after destructive tsunami (Hayashi et al. 2007). Poor knowledge of tsunami brought local people to ignore the second high tsunami waves to secure from disaster. The micro-landform analysis of pocket beaches affected is very common vulnerable level of tsunami intrusion, and the other impacts were rapid land-use change along the coast for next stages of vulnerability. Because the recent accelerating land-use change along the coast brought high vulnerability, the damages and calamities were huge in 2004 tsunami in the southern part of Thailand (Haruyama and Hayashi 2013).

In 1995, the large Hanshin-Awaji earthquake struck the Kinki region in Japan. The port city of Kobe was strongly affected by shaking along with fault, and liquefaction caused extensive damage on the coastal plain. The geo-space of damage has been shown to be related to the fluvial and coastal landform, and alluvial fan and delta are different stage damage in Kobe City (Takahashi 1996). After this huge disaster, evacuation volunteer groups were promoted to be in each local government, and community-based activity for fighting disaster was advanced to wide area in Japan.

In 2008, the huge Nargis cyclone attacked the Bay of Bengal, and Ayeyarwady Delta was one of the disaster target areas. During 1947–2007, thirty-four cyclones crossed along Myanmar Coast zone with high storm surges; however, the local people did not know how to secure their lives from the Nargis cyclone. The Ayeyarwady Delta was usually submerged by flood water in monsoon season, but the cyclone brought the large-sized seawater inundation and tremendous inundation along the coast. In the southern part of the delta, some elevated zones such as natural levees along the rivers, sand dunes near the coast, sand ridges along the

rivers, and the specific Lower Holocene marine terraces near the coastal line were exposed to severe flooding damages. The inundation stages, direction of intrusion wave, and the period of inundation depend on the landform conditions of the fluvial and coastal plains. The local residents took a long fleeting to safety, and the evacuation activity and rescue process were delayed. The rehabilitation processes also had been very slowly done in delta after cyclone, and now, there are some cyclone shelters in the villages which were attacked by storm surges in 2007 (Hlaing et al. 2013).

In 2011, the central plain of Thailand was affected by a long-period flooding after monsoon season. The alluvial plains in Thailand were strongly suffered from great economic losses, and the incapacitation of the region had an impact on global supply chains in the world under the damage. The most severely flooded zones were deeper, and the deepest back marshes behind natural levees in the upper fluvial plain and the reclaimed former lagoons behind mud spits were particularly hard hit. In recently developed industrial zones on the fluvial plain near the historic city of Ayutthaya located on the lower Chao Phraya River, the long-period inundation triggered to stop production lines of industries and impacted economic loss in not only Thailand but also in global production network. In these respects, the natural disaster had a meaning of geomorphologic dimension of so-called geo-hazard in this alluvial plain. The urban flood and rural flood faced to different profiles in each landform and the accelerating land-use change with urban sprawl around the capital city of Bangkok brought the more severe flooding, long-period inundation. We need the appropriate regional planning for disaster mitigation and flood prevention on each landform based on understanding geomorphologic history on site in future (Haruyama 1993; Haruyama and Ramphing 2012).

The disaster risk assessment with future mitigation program of fluvial and coastal plain should be extremely important matter for protection in each local residence against natural disaster if the advancement of engineering works on the river basin. The coastal areas are usually in face of danger tsunami intrusion, high tide, and typhoon with storm surge and strong winds. The coastal erosion related with human-induced and natural-induced factors threatened the subsistence, local community network, and economic losses in the society in the coastal erosion zones of the Red River Delta. The lower part of Red River Delta is one of the target areas where coastal erosion occurred, and the emigration to other places because of lost lands has been taken place in the area. The land cover changes in the Red River watershed, riverbed dredging on the main river course, land-use change along the coastal plain, and dam with reservoir construction in the upper reaches of the Red River are impact on coastal erosion of the southern delta. Understanding the disaster risk of coastal erosion, and finding and preparing the coastal erosion risk index, the vulnerability index mapping would be very helpful instrumental for future regional planning toward to disaster mitigation (Murooka et al. 2015).

In 2015, the Kinu River basin in Japan was attacked by heavy rainfall and long-period inundation with a breach of embankment, and the residential area was rehabilitated and rebuilt after the disaster. The flooding and inundation area was in

correspondence with a hazard map published by local government. The hazard map and geomorphologic land classification map are useful information for understanding natural disaster of the fluvial and coastal plains. In future, geo-information should make a connection with prevention and evacuation process.

1.2 Coastal Landform Studies After the 2011 East Japan Earthquake

Eastern Japan was afflicted by a giant earthquake and tsunami in 2011. In the initial field surveys after the 2011 East Japan (Tohoku) earthquake, Haraguchi and Iwamatsu (2011) used aerial photographs taken by the Geographical Institute of Japan to compile detailed maps of tsunami flooding along the Pacific Ocean from the Shimokita Peninsula in Aomori Prefecture in northern Honshu to Chiba Prefecture in southern damaged area. They also surveyed each locality of tsunami inundation, collecting physical evidence of tsunami deposits, measuring tsunami run-ups using laser leveling instruments, and administering survey questionnaires to local residents. They also noted that the tsunami intruded to a high elevation in the narrow dissected valley plains along the Sanriku Coast, but the tsunami run-up was on the wider coastal plains in southern Miyagi Prefecture. In northern Iwate Prefecture, some villages were successfully shielded by large seawalls, but the other towns were devastated. Some elder residents living in these towns recalled the damage caused by the Chilean earthquake tsunami taken in 1960, and the tsunami handed down the generations in these local villages. Although tall seawalls, tidal embankments, and impoundments with sluice gates had been constructed along the Pacific Ocean coast of eastern Japan, some of these facilities were damaged by the earthquake, leaving the coastal plains less protected from future tsunamis.

Geoscientists with many different specialties tried to carry out urgent field studies immediately after the 3.11 earthquake and tsunami disaster. Umitsu (2011), a geomorphologist, looked for damage signs of the tsunami's inflow and outflow directions on different geomorphic landform units and artificial landforms with buildings on the Ishinomaki coastal plain. He found the artificial landforms and buildings were important roles for obstruction tsunami current and damage level. Koarai et al. (2011) examined the distribution of tsunami inundation depths and their relationship to structural damage and demonstrated that a tsunami inundation depth of 3 m was the threshold value for the complete building collapse. After the tsunami struck, inundation maps were quickly distributed on Web sites by Japanese geographers. These maps were important resources for emergency responders in ensuring supplies of food and drinking water, medical services, and lifeline recovery in the immediate aftermath.

The narrow valley plains of the Sanriku coast, a ria (sawtooth) coastline, suffered from the highest tsunami inundations. The small coastal plains on the Sanriku Coast also contained fishing villages. In Chaps. 2–5, tsunami and geomorphology with sedimentology would be discussed in each landform.

1.3 Human Dimension and Physical Dimension of 2011 Tsunami in Coastal Plain

Taresawa and Haruyama (2013) explained that the land use on each landform site showed different disaster risks in the 2011 tsunami and prepared geomorphologic land classification map of the southern part of the mouth of the Abukuma River that showed evidence of the relationship between tsunami inundation and coastal landforms. The above-mentioned study area was heavily damaged, and the dikes along the lower reaches were severely degraded. The lagoon and former lagoon area near the river mouth experienced extensive subsidence after the earthquake, and these areas were subjected to inundation by the tsunami and daily high tides afterward. The tsunami swept westward over the narrow coastal plain onto the fluvial plain, and the most strongly affected areas were as follows: (1) urbanized areas in and around the city of Sendai, (2) agricultural production areas in the central part of the coastal plains, and (3) small fishing villages along the coastline. However, several towns originated in medieval period of the historic *Rikuzen hamakaido* road, on the edge of a marine terrace, were spared from tsunami intrusion. Haruyama and Taresawa (2014) explained that the local community activities for evacuation and prevention under the 3.11 disaster had various ways originated from different community networks and location based on landform.

After conducting geomorphologic analysis of the southern part of the mouth of the Abukuma River, the author prepared a simplified geomorphologic land classification map, showing the fluvial–coastal plains of the lower Abukuma River basin after the study of Taresara and Haruyama (2013) (Fig. 1.1). Hillsides that had been cut or modified for residential use suffered from landslide damage. The narrow marine terraces around Mt. Abukuma escaped from tsunami inundation and liquefaction.

The lower Abukuma River basin contains the distinct former meander channels with natural levees, and the present branches are deflected to the south in response to coastal currents. All of these channels and branches have well-developed natural levees of 500–1,000 m wide, generally consisting of sand and reaching heights of 1–1.5 m. Although the natural levees were not inundated for long by the 2011 tsunami, they were affected by liquefaction caused by the earthquake. Photo 1.1 is one of the states of disaster in 2011 tsunami and the region near the mouth of the Abukuma River.

Several sand ridges are generally parallel to the coastline, and the swales between them were subject to tsunami intrusion and long-period stagnation (Figs. 1.1 and 1.2). The disaster risk levels of tsunami in each local administrative area show that the coastal landform was affected to explain each local scope of the disaster (Fig. 1.3). Under the severe tsunami 2011, the coastal plain was suffered from huge damage, and there were heavy loss of lives and sufferers. The deceased population attacked by tsunami was reported; the figure is produced using statistical data prepared by local administrations; and the ratio of deceased is dissimilar from each local community.

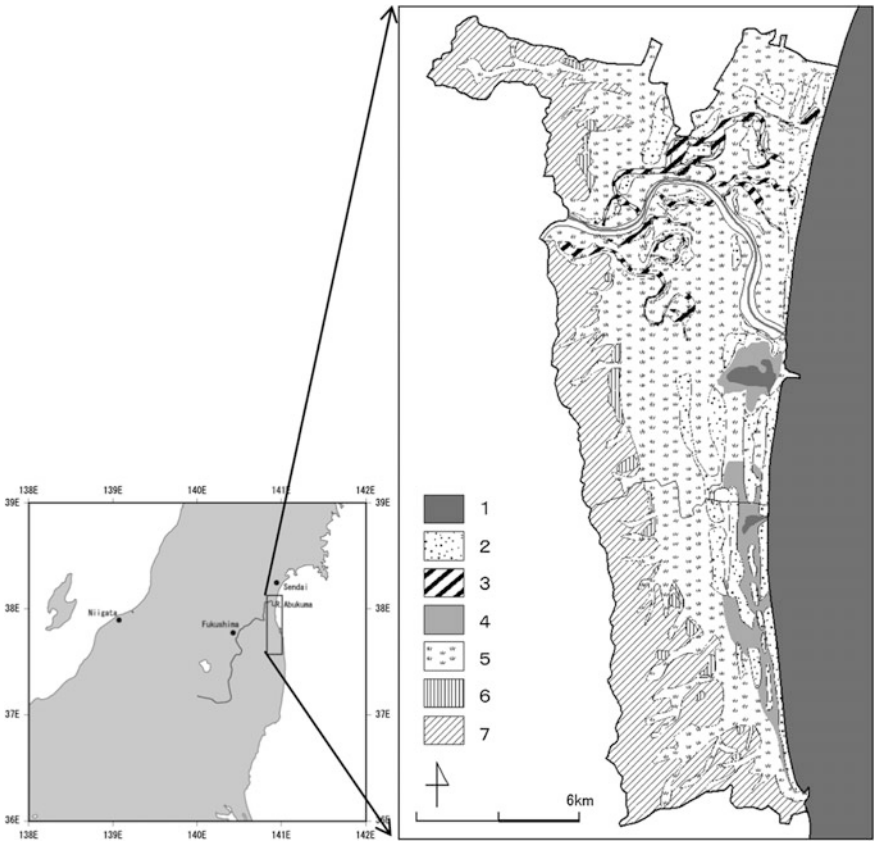

Fig. 1.1 Geomorphologic land classification map of the southern part of mouth of the Abukuma River basin (modified Taresawa and Haruyama 2013) *Explanatory note*: *1*. water surface, *2*. sand dune and sand ridge, *3*. former river course, *4*. former lagoon, *5*. flood plain including valley plain, *6*. terrace, *7*. hill and mountain

1.4 Social Response to the 2011 East Japan Earthquake and Tsunami

The study area that includes Iwanuma, Watari, and Yamamoto regions in former Sect. 1.3 showed differing responses to the 2011 tsunami intrusion (Figs. 1.1–1.3). Tsunami inundation affected 48.27 % of the area of Iwanuma, 48.63 % of Watari, and 37.53 % of Yamamoto regions, respectively. The ratios of damaged areas differed because of differences of coastal landforms in these towns located on such as sand ridges, sand dunes, valley plains, former lagoons, natural levees, former channels, delta, and marine terraces. In the Yamamoto region, several small fishing villages on sand ridges along the coastline suffered from severe damage. The coastal landform affected the tsunami damage to these towns. The inundation of

Photo 1.1 Araham located in the lowest part of the Abkuma River affected by 2011 tsunami (taken in 2012)

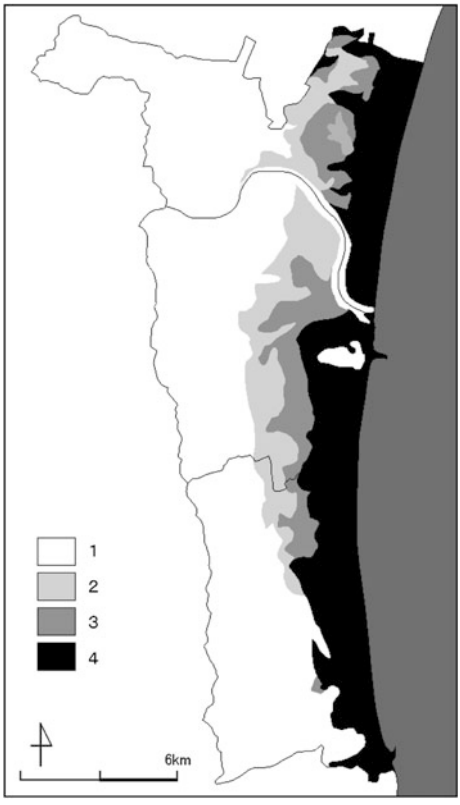

Fig. 1.2 Tsunami inundation map along the coastal area of the lower Abkuma River (after ground truth in 2012 and verify tsunami inundation map prepared by Fukkow Sien Research Team 2011) *Explanatory note*: *1*. non affection, *2*. inundation 0–2 m, *3*. inundation 2–3 m, *4*. inundation over 3 m

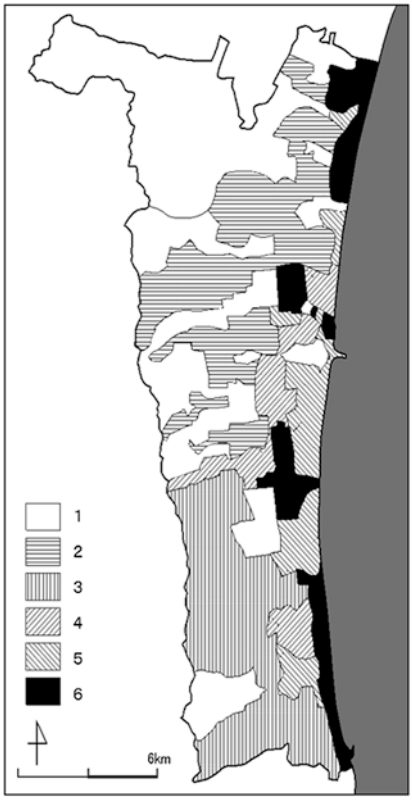

Fig. 1.3 Classification map of deceased by 3.11 tsunami along the coastal area in southern part of the mouth of the Abumuma in each local administration (damaged level was calculated in each local administration and tied up in damaged levels) *Explanatory note*: *1*. 0 % damage, *2*. below 1 % damage, *3*. 1–2.5 % damage, *4*. 2.5–5 % damage, *5*. 5–10 % damage, *6*. over 10 % damage

2 m depth threshold was confined to the coastal side of Yamamoto by the barrier formed by an inland sand ridge. Natural levees along the Abukuma River and its branches limited tsunami intrusion (Fig. 1.3), and sand ridges in Iwanuma region also served to obstruct the tsunami. The narrow, dissected valley plains on the flank of Mt. Abukuma in Yamamoto region were severely affected by the tsunami. The each landform along the coastline took different functions or made roles in the damage.

Land-use change is the other damage risk dimension and human-induced factor, in that rural and urban areas are known to have greater risk than agricultural areas in land-use changing (Haruyama and Yoshida 2014, Hlaing and Haruyama 2014; Haruyama et al. 2014). The field survey of land-use change compared with coastal landforms of the lower Abukuma River proved that the transformed vulnerability to natural disaster has been generated in this region. In the results of the questionnaire survey of damage, evacuation process and reconstruction process in these tsunami damaged areas (Tables 1.1 and 1.2) showed that the local community activities

Table 1.1 Land use in the Iwanuma, Watari, and Yamamoto regions in 2011

	Area (km^2)						
	Paddy field	Upland crop and orchard	Forest	Urban land use	Water surface	Wasteland and barren land	Total
Iwanuma	19	3	15	10	5	8	61
Watari	32	8	11	10	6	4	74
Yamamoto	19	12	21	6	1	4	64

Table 1.2 Landform and victims of the selected communities in the study area by using 2012 questionnaire survey

Community number	Population	Main landform	Flooded %	Deceased %
1	514	Beach ridges	100	8.17
2	273	Beach ridges	100	13.55
3	361	Beach ridges	100	5.26
4	167	Beach ridges	100	2.99
5	875	Terrace	0	0
6	1052	Former lagoon	100	12
7	370	Natural levee	100	6.76
8	185	Natural levee	100	0.54
9	681	Valley plain	0	0.59
10	1074	Former lagoon	100	13.04

were very important roles in protecting lives during the tsunami and rebuild region, in addition to the crucial role of geomorphology as documented in Table 1.2 and Fig. 1.4. Haruyama and Mizuno (2007) and Tujimura and Haruyama (2009) reported that the local community preparedness was instrumental in successful evacuations during the severe disaster, and the strong local community network with better risk communication brought the appropriate evacuation process with secureness in each local residence.

1.5 Geomorphologic Land Classification Maps and Disaster Risk

Because landform symbolizes the long-term results of repeated geologic processes that can cause natural disasters, geomorphic land classification maps are an important tool for analyzing the physical conditions that foster natural disasters and the historic or prehistoric background of disaster occurrence. Oya (1956) prepared the first hazard map of Nobi Plain in central Japan, in which he explicitly related the

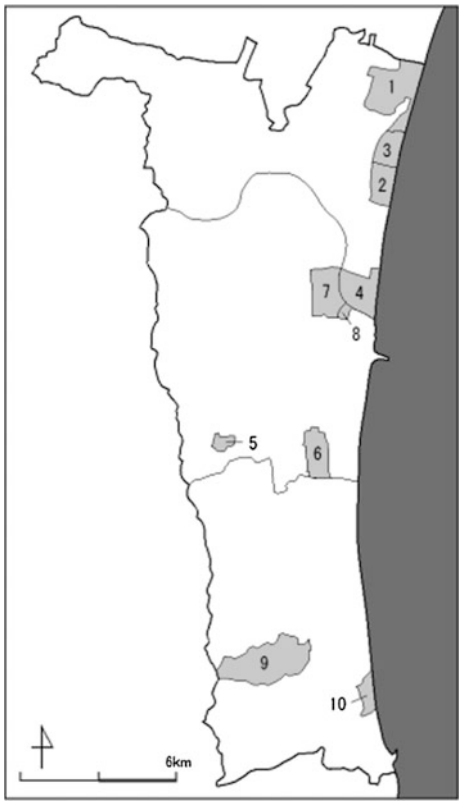

Fig. 1.4 Location map of each local community region (number is showing the same location number shown in Table 1.2)

geomorphologic land classifications map to flood-prone areas. Later, he explained the relationship between flooding tendencies and micro-geomorphologic features left by Great Ise Bay Typhoon in 1959 (Oya 1993). The repeated deposition of layers of sand, silt, and clay by floods creates a record of land modification by successive floods. Each of these sediment layers may be termed the memory of a past flood.

Verstappen (1983) discussed that the landform is one of the important functions of natural phenomena in environmental change process and revealed the full dimensions for natural disaster in his "Applied geomorphology" published in 1983. He showed the civilization with geomorphology, alluvial plain landform with flooding and debris flow, volcanic geomorphology, and engineering works for disaster mitigation with many examples of different river basins in the world, especially Asia region. From the beginning to the end, he mentioned that landform and sedimentation explain the geo-history of the river basin evolution with natural disaster and the misunderstanding of natural phenomena and natural process of the river basin guided the future huge geo-hazard again. Also, the active faults provide the examples of the effect of earthquakes and tectonism on surface landform. The resulting dynamic environmental changes of Holocene are recorded by

sedimentation of the fluvial and coastal plains in Japan. The flooding history preserved in and on landforms serves notice of future different unknown disaster risks, and geomorphologic land classification maps make visible basic geo-information needed to carry out local or regional mitigation measures after severe weather events.

Haruyama (1993) and Haruyama and Ramphin (2012) discussed that the important issue is understanding geomorphologic structure of the central plain of Thailand with its history of floodings related with disaster prevention works. The subversive 2011 flooding in the central plain of Thailand underscored the importance of geomorphology and appropriate land use in regional planning for future flood mitigation. The geomorphologic land classification map provided geo-space of landform and historical evidences of flooding in the fluvial plains, and sustainable development should be fully aware of geomorphologic condition. Haruyama and Hayashi (2013) evaluated the micro-landform in pocket beaches for tsunami intrusion risks and geomorphologic roles of vulnerability. Also, Haruyama and Yoshida (2014) reported that the lower Shonai River basin in central Japan has been more fragile in rapid urban sprawling and the demolition of the community network has brought the secondly disaster risk. Hlaing et al. (2014) tried to clarify the results of land-use change and the watershed transformation and pointed out that the anthoropogenic activities were affected by rapid land-use changes of Inle Lake and surrounding lake lowlands.

The decision-making policy-development challenge for disaster mitigation is an essential issue for the Pacific–Asia region and also for the whole world. Sound policies with respect to natural disaster mitigation, including land-use planning, should be informed by interdisciplinary scientific information if they are to promote sustainability and sustainable development. The research described here demonstrates that the geomorphology of coastal and fluvial plains affected the losses that followed the 2011 East Japan earthquake and tsunami.

1.6 Toward Societal Security and Sustainability

In January 2015, the International Tokyo Conference on Disaster Risk Reduction and Resilience was held at the University of Tokyo as a part of the preparatory process for the Third World Conference on Disaster Risk Reduction held in March 2015 at Sendai City in Japan. As anthropogenic factors for natural disaster losses, such as land-use change, urban sprawl, and unappropriate land-use pattern, population growth and aging, globalization and poverty increase, are also increasing in both developed and developing countries, and these topics were discussed at the conference. Natural disaster science should include human dimension for disaster mitigation in future continued research and appropriate discussion toward to secure social system should be needed into the structural factors affecting disasters and hazard risks, by science, literature and social sciencies.

Geographic conditions have caused Asia and Pacific regions to be plagued by natural disasters, especially flooding in fluvial and coastal plains. Being part of both regions, Japan has a long history of natural disasters and disaster preparedness as structure measures and non-structure measures, the most recent being the 2011 East Japan earthquake. In the process of strengthening social system in Japan against future disasters through improved land and river management, increasing the resilience of social systems is an important related task for future researchers. To reduce disaster risks, it is necessary to implement disaster preventive measures based on scientific findings at all levels of society. It is important for the future to establish a balance between sustainable development and disaster risk reduction in policy-making, planning, and all other phases of the disaster management cycle. The authors of this volume offer descriptions and analyses of the coastal geomorphology of northeastern Japan, with the desire to clarify the relationships between geomorphology and natural disasters and the hope of making meaningful contributions to future disaster reduction planning.

Acknowledgments I should express my thanks to local people in tsunami intrusion area for giving me important information to understand the relationship between Tsunami and landform in the study area. Also, I tender my thanks to Mr. Yuji Taresawa who studied the local community activities analysis under the 3.11 tsunami damage with his voluntary works for supporting to reconstruct and recover the damaged houses in the study area. His study was a fundamental issue of this introduction chapter in this book.

References

Fukkou-sien Research Team (2011) Fukkou-sien research Archive. http://fukkou.csis.u-tokyo.ac.jp/ (in Japanese)

Koarai M, Okatani T, Nakamori T, Kamiya I (2011) http://www.gsi.go.jp/common/000064460.pdf. (Japanese)

Haraguchi T, Iwamatsu A (2011) Detailed Maps of the Impacts of the 2011 Japan tsunami 2, Kokon-Shoin Publishers Ltd, Tokyo,Japan, 97 (in Japanese)

Haruyama S (1993) Geomorphology of the central plain of Thailand and its relationship with recent flood conditions. Geo-J 26(12):327–334

Haruyama S, Mizuno S (2007) The disaster feature and local prevention availability in 2014 Fukui flood. J of Nat Dis, 26(3): 307–322 (in Japanese)

Haruyama S, Ramphing S (2012) 2011 flooding of the central plain of Thailand in view of geomorphology. J of Nat Dis, 30(4): 463–476 (in Japanese)

Haruyama S, Hayashi K (2013) Tsunami 2004 Disaster impacted by Recent Land Use Change in Phuket, Thailand. In: Haruyama S (ed) Coastal geomorphology and vulnerability of disaster towards disaster risk reduction, TERRAPUB Publisher, Tokyo, Japan, 69–86

Haruyama S, Taresawa Y (2014) Local community activities for disaster reduction in regard to the 2011 Tsunami. Geographica Polonia 87(3):401–408

Hayashi K, Haruyama S, Miura M (2007) Coastal geomorphology and Tsunami varunerability of the Pocket beaches in Phuket Island, Thailand. J of Nat Dis, 26(1): 21–41 (Japanese)

Haruyama S, Yoshida A (2014) Flood risk under recent land use change in the lower Syonai River Basin. In: SLUAS (2014) Science report Towards Sustainable land use in Asia (V), JSPS Science Fund Basic Reseach (S) No.21222003,177–188

Hlaing KT, May SY, Haruyama S (2014) Recent Land Cover Changes of the Inle Watershed affected by Anthoropogenic Activities. In: SLUAS (2014) Science report Towards Sustainable land use in Asia (V), JSPS Science Fund Basic Reseach (S) No.21222003,85–100

Hlaing KT, Matsumoto M, Aye MM, Haruyama S (2013) GIS Analysis for tropical Cyclones and Coaslta Plain in Myanmar. In: Haruyama S, (ed) Coastal geomorphology and vulnerability of disaster towards disaster risk reduction, TERRAPUB Publisher, Tokyo, Japan, 139–154

Murooka M, Kuwahara Y, Haruyama S (2015) Mapping coastal erosion risk in the southern Red River Delta, Vietnam. In: Li J, Yang X (eds) Monitoring and Modeling of global changes: a geomatics perspective, Springer, 199–220

Oya M (1956) Geomorphologic Land classification map showing flood prown area in Nobi Plain. Minstory of Construction

Oya M (1993) Fluvial Geography. Kokon-Shoin Ltd Publisher, Tokyo, Japan, 253 (in Japanese)

Takahashi M (1996) Geo-environmental analysis of the Hanshin-Awaji Great Earthquake Disaster. Geograph Rev, 69A(7): 501–514 (in Japanese)

Taresawa Y, Haruyama S (2013) Coastal landform in the southern part of Miyagi prefecture and 2011 tsunami disaster. In: Haruyama (ed) Coastal geomorphology and vulnerability of disaster towards disaster risk reduction, TERRA PUB Ltd Publisher, Tokyo, Japan. 87–96

Tujimura A, Haruyama S (2009) The smallest unit for areal prevention activities-lesson from 2004 Toyooka flooding, E-Journal GEO.4(1):1–20 (in Japanese)

Umitsu M (2011) Tsunami direction in Sendai and Ishinomaki plain.In: Symposium of East Japan Mega Earthquake in a viewpoint of earthplanet and human sphere, 22–25 (in Japanese)

Umitsu M, Takahashi M (2007) Geo-environmental Features in the damages of the 2004 Indian Ocean Tsunami in/around Banda Aceh, Indonesia. E-journal GEO,2(3): 121–131 (in Japanese)

Verstappen HTH (1983) Applied Geomorphology- Geomorphological survey for environmental development. Elsevier 438

Chapter 2
Geomorphology and Tectonic Setting of the Sanriku Coast, Northeastern Japan, and Introduction of Recent Studies on the Formation of Alluvial Plains and Holocene Crustal Movements Along the Coast

Yuichi Niwa and Toshihiko Sugai

Abstract The 2011 Tohoku-Oki earthquake dramatically changed the coastal environment along the Pacific coast of northeastern Japan. In particular, coseismic subsidence of up to 1.3 m was recorded along the Sanriku Coast. However, well-preserved Middle to Late Pleistocene marine terraces along the northern Sanriku Coast have been interpreted to indicate uplift since the Late Quaternary. This discrepancy between long-term uplift and short-term subsidence has been attributed to coseismic uplift during an unidentified megathrust earthquake. To clarify the interplay of uplift and subsidence, we introduce the tectonic setting of the Sanriku Coast and recent studies on the geomorphology and geology along the coast, which focus on crustal movements during the Holocene along the southern Sanriku Coast. The results of recent studies indicate that, contrary to the previous view that the northern Sanriku Coast has experienced long-term uplift, the southern Sanriku Coast has been subsiding since the 10 ka (since the latest Pleistocene).

Keywords Alluvial plain · Coastal geomorphology · Holocene crustal movement · Pacific coast of northeastern Japan · Tectonic setting

Y. Niwa (✉)
International Research Institute of Disaster Science, Tohoku University,
Aza-Aoba 468-1, Aramaki, Aoba-ku, Sendai 980-0845, Japan
e-mail: niwa@irides.tohoku.ac.jp

T. Sugai
Graduate School of Frontier Sciences, The University of Tokyo, 5-1-5
Kashiwanoha, Kashiwa 277-8563, Japan

S. Haruyama and T. Sugai (eds.), *Natural Disaster and Coastal Geomorphology*, DOI 10.1007/978-3-319-33814-9_2

2.1 Introduction

Well-preserved Middle to Late Pleistocene marine terraces along the Sanriku Coast of northeastern Japan have generally been interpreted to indicate long-term uplift in the region, especially along the northern coast (Koike and Machida 2001). However, geodetic and tide gauge data show rapid subsidence in this area over the last several decades, including considerable subsidence during the 2011 Tohoku-Oki earthquake (*Mw* 9.0) (Kato and Tsumura 1979; Ozawa et al. 2011). This discrepancy between long-term uplift and short-term subsidence has been recognized by several researchers but has not yet been fully explained (e.g., Ikeda et al. 2012; Niwa et al. 2015). In this chapter, we summarize the tectonic setting and geomorphology of the Sanriku Coast, introduce recent studies on the processes that formed the alluvial plains along the coast, which consider the relationship of those processes to Holocene crustal movement on the southern Sanriku Coast.

2.2 Plate Tectonic Setting and Overview of Large-Scale Landforms in the Tohoku Region

There are four major tectonic plates in the region of the Japanese Islands: the Pacific, North America, Eurasia, and Philippine Sea plates (Fig. 2.1). The northeastern Japan arc lies on the southwestern extremity of the North America plate where it is separated from the Pacific plate to its east by the Japan Trench. The Pacific plate is currently subducting under the North America plate at about 10 cm/year (Koike 2005).

Basement in the Tohoku region consists mainly of Jurassic accretionary complex rocks (Taira 2001). North–south-trending reverse fault systems in the region indicate an east–west compressional stress regime. Three ranges of north–south-trending mountains are developed in the Tohoku region (Fig. 2.2). The O-u and Dewa mountains of the inner arc region have been uplifted by faulting and are separated by basins and lowlands (Koike 2005). The Kitakami and Abukuma mountain ranges of the outer arc region consist of Cretaceous granitic rocks intruded into older basement and are the result of upwarping (Okada and Ikeda 2012). North–south-trending lowlands separate the mountain ranges of the inner and outer arc regions.

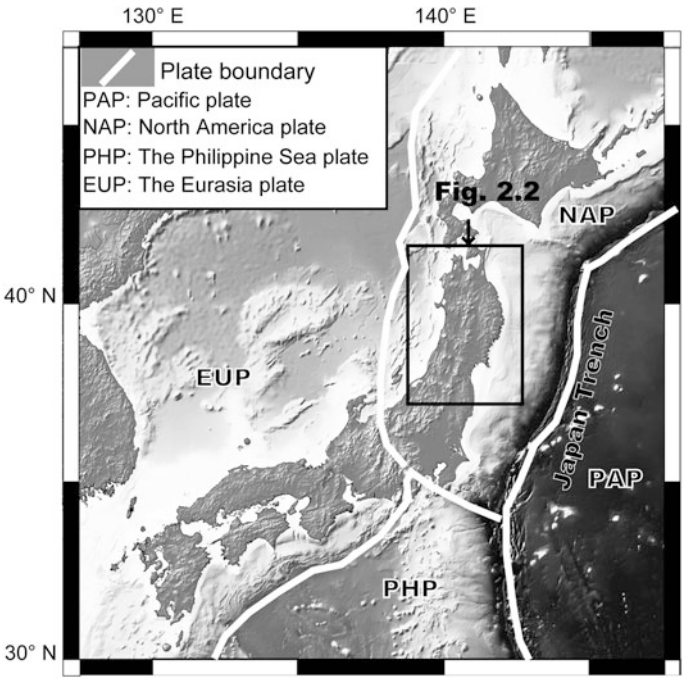

Fig. 2.1 Regional map showing distribution of major tectonic plates in the region of the Japanese Islands

2.3 Landforms of the Sanriku Coast and Distribution of Quaternary Marine Terraces

The Sanriku Coast lies east of the Kitakami Mountains and extends over a distance of about 600 km. Basement consists mainly of Mesozoic and Paleozoic sedimentary rocks (Fig. 2.3; Koike 2005). Sheer, rocky coastal cliffs are common along the northern Sanriku Coast, and indentation of the coastline there is uncommon. A marine terrace formed during the last interglacial (MIS 5e; 125 ka) stretches continuously from Hachinohe to Kuji, decreasing in elevation from 40 m at Hachinohe to 20 m at Kuji. There are six or seven levels of Middle Pleistocene marine terraces at elevations above the MIS 5e terrace; the oldest of these has been correlated with MIS 19 (ca. 800 ka) (Koike and Machida 2001). The elevation of this uppermost terrace is 280 m east of Kuji, and decreases to 140 m at Miyako, some 70 km to the south. The elevations of the younger of these terraces also decrease southward (Figs. 2.3c and 2.4; Yonekura 1966; Miyauchi 1985).

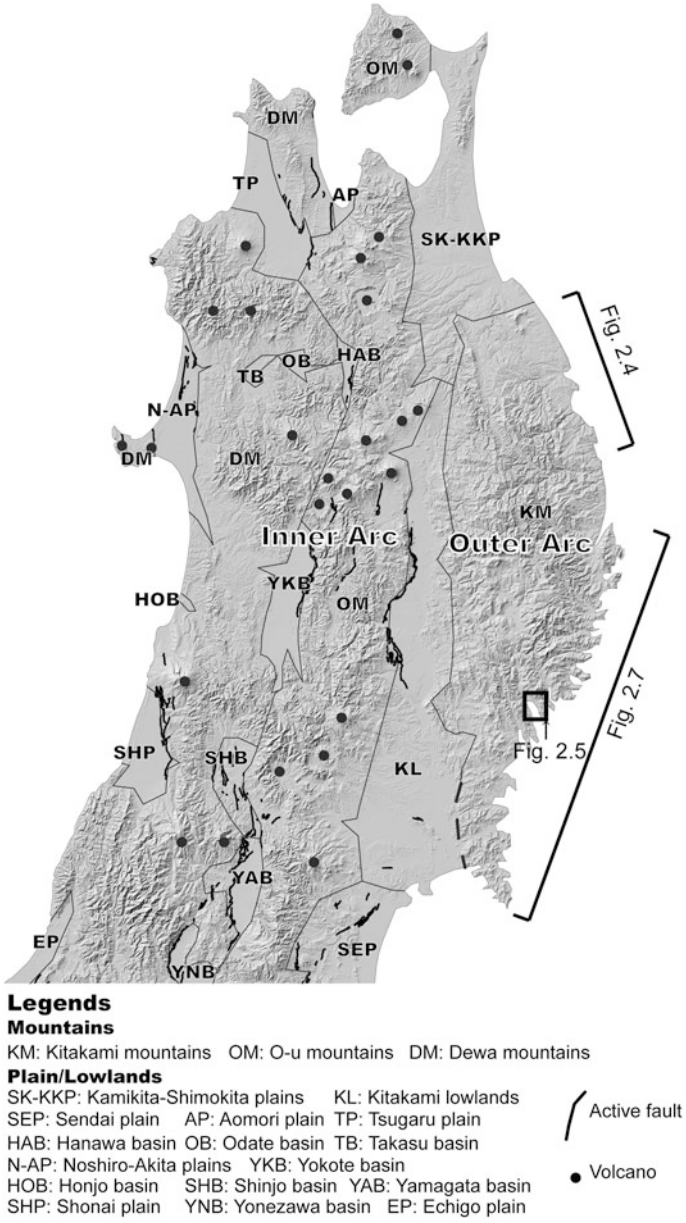

Fig. 2.2 Large-scale landform classification map of the Tohoku region. Landform classification is from Koike (2005). Distributions of active faults and volcanoes are from Nakata and Imaizumi (2001) and Imaizumi (1999), respectively

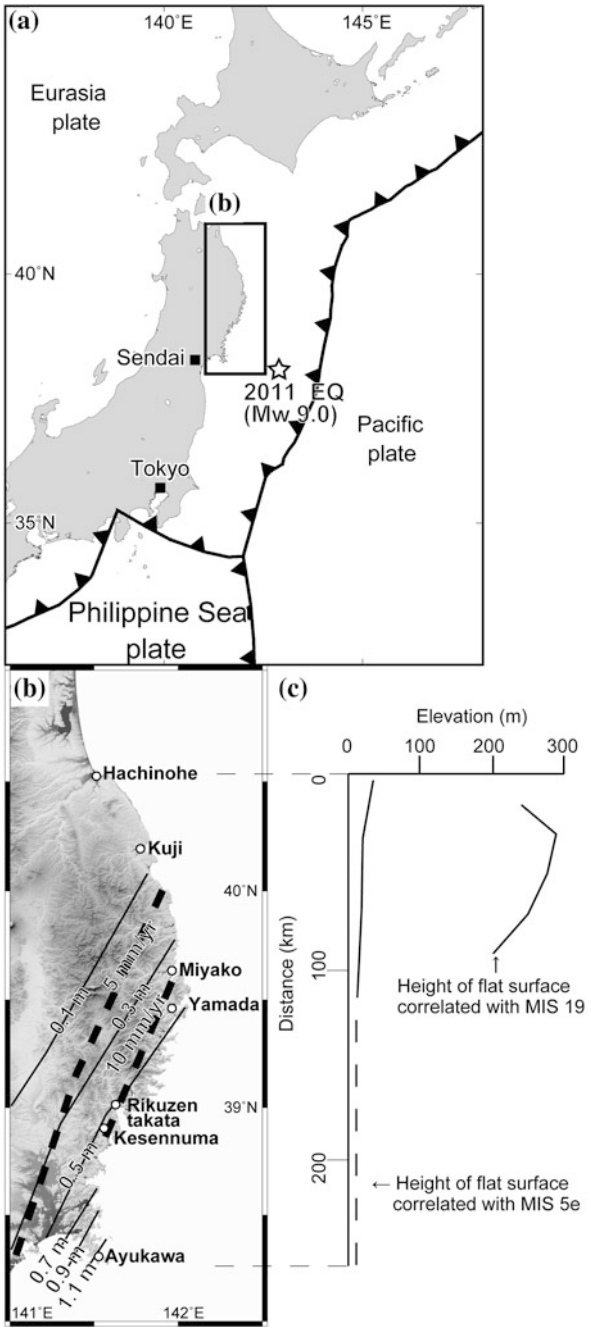

Fig. 2.3 **a** Epicenter of the 2011 Tohoku-Oki earthquake in relation to the Japanese Islands and major tectonic plates. **b** Amount of subsidence during the 2011 Tohoku-Oki earthquake (thin contours) and rate of subsidence (thick broken contours) over the last several decades. **c** Elevation profile of flat surfaces interpreted as Pleistocene marine terraces. **a** and **b** are modified from Niwa et al. (2015). **c** is modified from Miyauchi (2012)

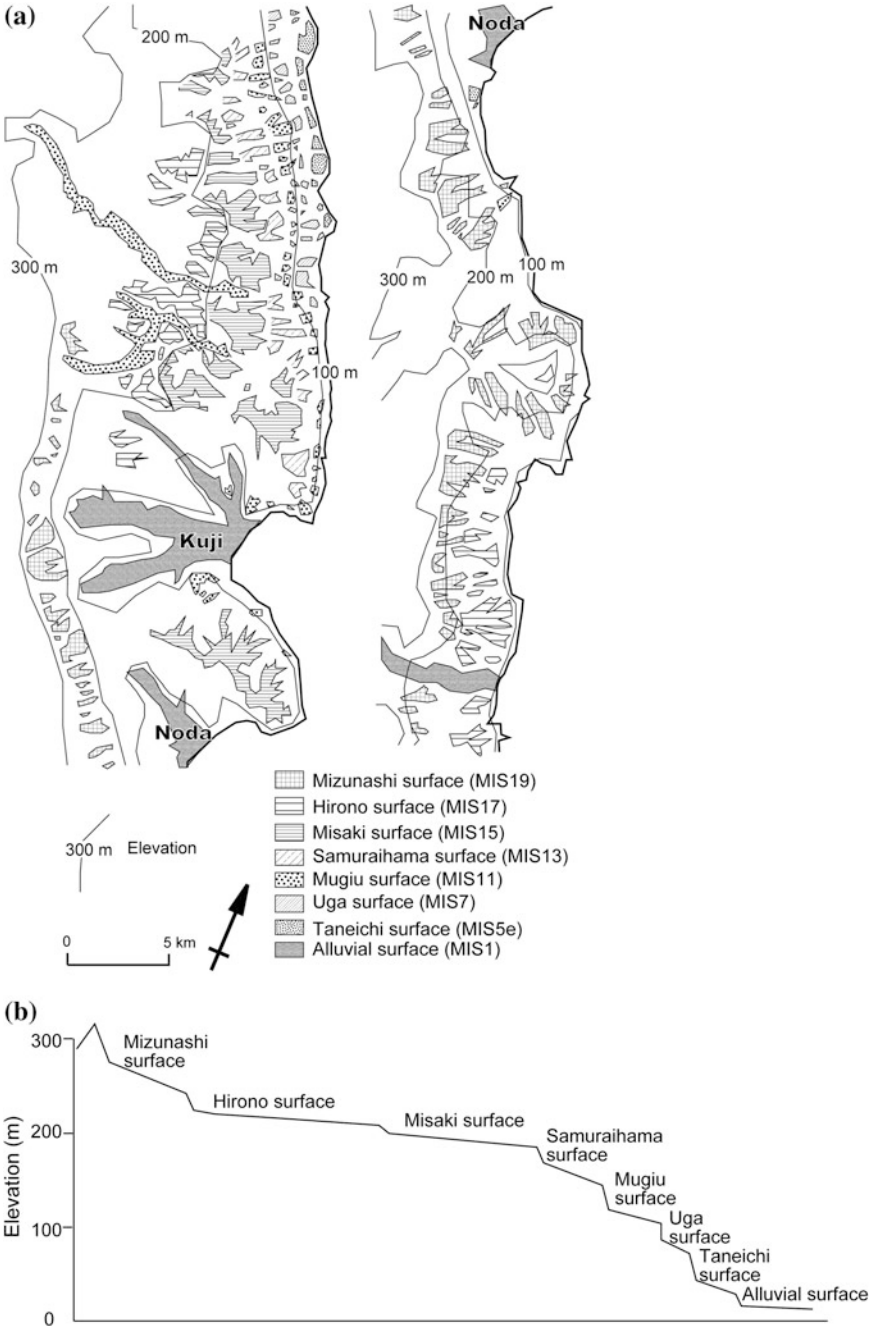

Fig. 2.4 **a** Distribution of marine terraces along the northern Sanriku Coast and **b** schematic geomorphic cross section (after Yonekura 1966). Correlation of ages of marine terraces with Marine Isotope Stage (MIS) is from Koike and Machida (2001). Location of map is shown in Fig. 2.2

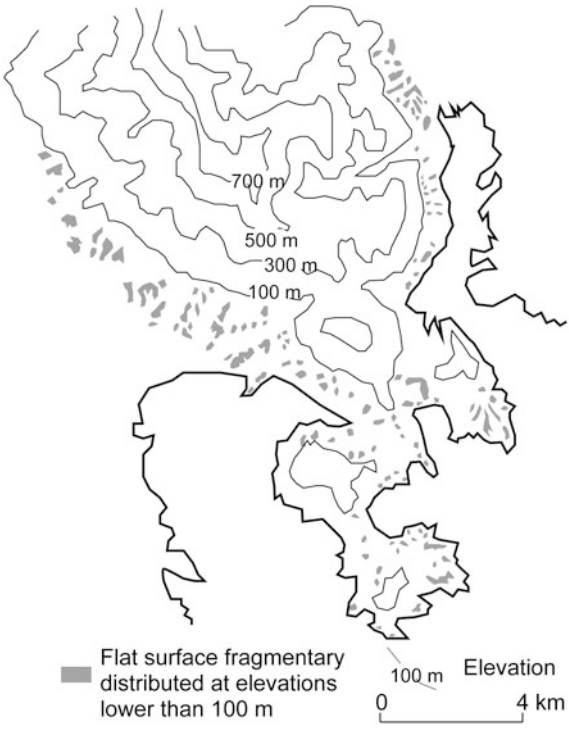

Fig. 2.5 Example of fragmentary distribution of flat surfaces along the southern Sanriku Coast (after Miura, 1968) that has been interpreted as Pleistocene marine terraces. Their distribution and lack of clear evidence of marine origin (e.g., shells, burrows) preclude confirmation that they represent marine terraces. Location of map is shown in Fig. 2.2

In contrast, the southern Sanriku Coast (south of Miyako; Fig. 2.3b) is a typical ria coast with many deep embayments and capes. Along this part of the coast, there are fragmentary flat surfaces at elevations from several tens of meters to 70 m (Fig. 2.5; Miura 1966, 1968; Yagi and Suzuki 2001). Gravel layers have been identified in outcrop on these surfaces (Miura 1966, 1968; Yagi and Suzuki 2001), but whether they are of marine or nonmarine origin is unclear, and a lack of tephra layers has precluded determination of the timing of terrace formation (Miura 1966, 1968; Yagi and Suzuki 2001). Thus, the processes of formation and the ages of these surfaces are unclear.

2.4 Crustal Movement on the Sanriku Coast During the 2011 Tohoku-Oki Earthquake

On 11 March 2011, the Tohoku-Oki earthquake (Mw 9.0) caused subsidence of up to 1.3 m along the entire Sanriku Coast (Fig. 2.3b; Ozawa et al. 2011). The source of the earthquake was in the Pacific Ocean off the Sanriku Coast (Fig. 2.3a) at a focal depth of about 24 km (Japan Meteorological Agency 2011), and the resultant tsunami flooded most of the coastal plain (Haraguchi and Iwamatsu, 2011). The

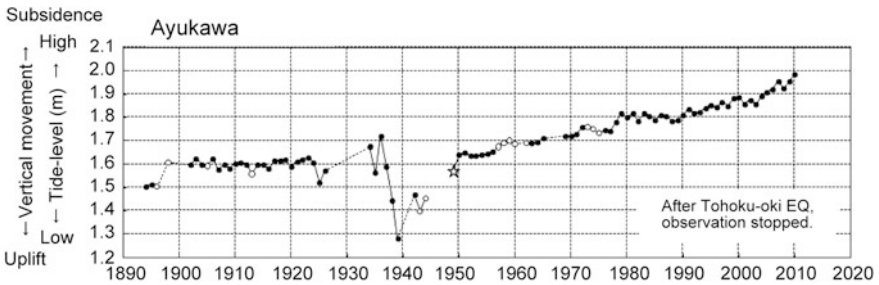

Fig. 2.6 Example of tide-gauge data suggesting continuous subsidence during the past several decades at Ayukawa on the southern Sanriku Coast (Coastal Movements Data Center 2015). Location of Ayukawa is shown in Fig. 2.3b

coseismic subsidence during the 2011 earthquake is consistent with the century-long subsidence trend of several to ten millimeters per year determined from geodetic and tide gauge data (Figs. 2.3b and 2.6; Kato and Tsumura 1979; Nishimura 2012). However, this subsidence is in conflict with the longer term (10^5 years) uplift suggested by the marine terraces along the northern Sanriku Coast.

2.5 Late Quaternary Crustal Movement Along the Sanriku Coast Before and After the 2011 Tohoku-Oki Earthquake

The well-preserved Middle to Late Pleistocene marine terraces along the northern Sanriku Coast have been interpreted to indicate uplift since the Late Quaternary. Interpretation of fragmentary flat surfaces along the southern Sanriku Coast as marine terraces also suggests Late Quaternary uplift (Yagi and Suzuki 2001). Thus, the trend of crustal movement since the Late Quaternary appears to be uplift along the entire Sanriku Coast. However, geodetic records show rapid subsidence at several to 10 mm per year over the past 100 years (Fig. 2.3b; Kato and Tsumura 1979; Nishimura 2012).

Ikeda (1996) explained the discrepancy between long-term uplift and short-term subsidence by inferring coseismic uplift caused by an unidentified past megathrust earthquake. Other hypotheses to explain the long-term uplift include uplift of the coastal area by a large earthquake with a different mechanism to that of the 2011 earthquake, or uplift due to afterslip of the 2011-type earthquake (Ikeda et al. 2012; Miyauchi 2012; Nishimura 2012). However, long-term crustal movements along the Sanriku Coast are not fully understood because of the fragmentary distribution of terrace surfaces and a lack of data to allow determination of their ages, especially along the southern Sanriku Coast. To clarify the uplift and subsidence history of the Sanriku Coast, estimates of long-term crustal movement based on geomorphologic and geologic data must become more accurate than those made to date.

2.6 Recent Studies Indicating Holocene Subsidence on the Southern Sanriku Coast

Because of the fragmentary distribution of flat surfaces (previously interpreted to be possible marine terraces) and lack of chronological data along the southern Sanriku Coast, an understanding of long-term crustal movements there must rely on analyses of other geomorphic and geologic features.

The small alluvial plains adjacent to the shores of embayments along the southern Sanriku Coast (Fig. 2.7; Chida et al. 1984) are composed of incised-valley-fill sequences that are typical of ria coastlines. Facies analyses and high-density radiocarbon dating of cores from those sequences can reveal changes of relative sea level (RSL), including the effect of tectonic crustal movements. The contribution of tectonic crustal movements can be determined from the difference of RSL curves estimated using core data from RSL curves modeled excluding tectonic movements (Fig. 2.8).

Here, we use paleo-geodetic data from recent studies on the southern Sanriku Coast to examine long-term crustal movements by considering the processes that formed two alluvial plains: the Rikuzentakata (Niwa et al. 2014) and Kesennuma Okawa (Niwa et al. 2015) plains.

2.6.1 Rikuzentakata Plain

2.6.1.1 Regional Setting and Sediment Core

The Rikuzentakata Plain is in a restricted-bay setting on the shore of Hirota Bay (Fig. 2.7); it extends about 2 km from north to south and about 2.5 km from east to west. Most of the plain is less than 5 m above sea level. The Kesen River, which flows through the plain, is about 50 km long with a catchment of about 540 km^2. The basement around the plain consists of Paleozoic sedimentary rocks in the upper reaches and Mesozoic granite in the middle and lower reaches (Chida et al. 1984). Paleo-channels are widely distributed on the plain (Fig. 2.9).

Before the 2011 Tohoku-Oki earthquake, there was a beach ridge along the shoreline with a lagoonal area (Furukawa Lake) landward of it. Most of this beach ridge was destroyed by the tsunami associated with the 2011 Tohoku-Oki earthquake, resulting in a marine incursion into Furukawa Lake. Sediment core RT1 was drilled on the back marsh about 500 m inland from the shoreline before the 2011 earthquake and tsunami. Niwa et al. (2014) conducted facies analyses and radiocarbon dating of 25 sediment samples from core RT1.

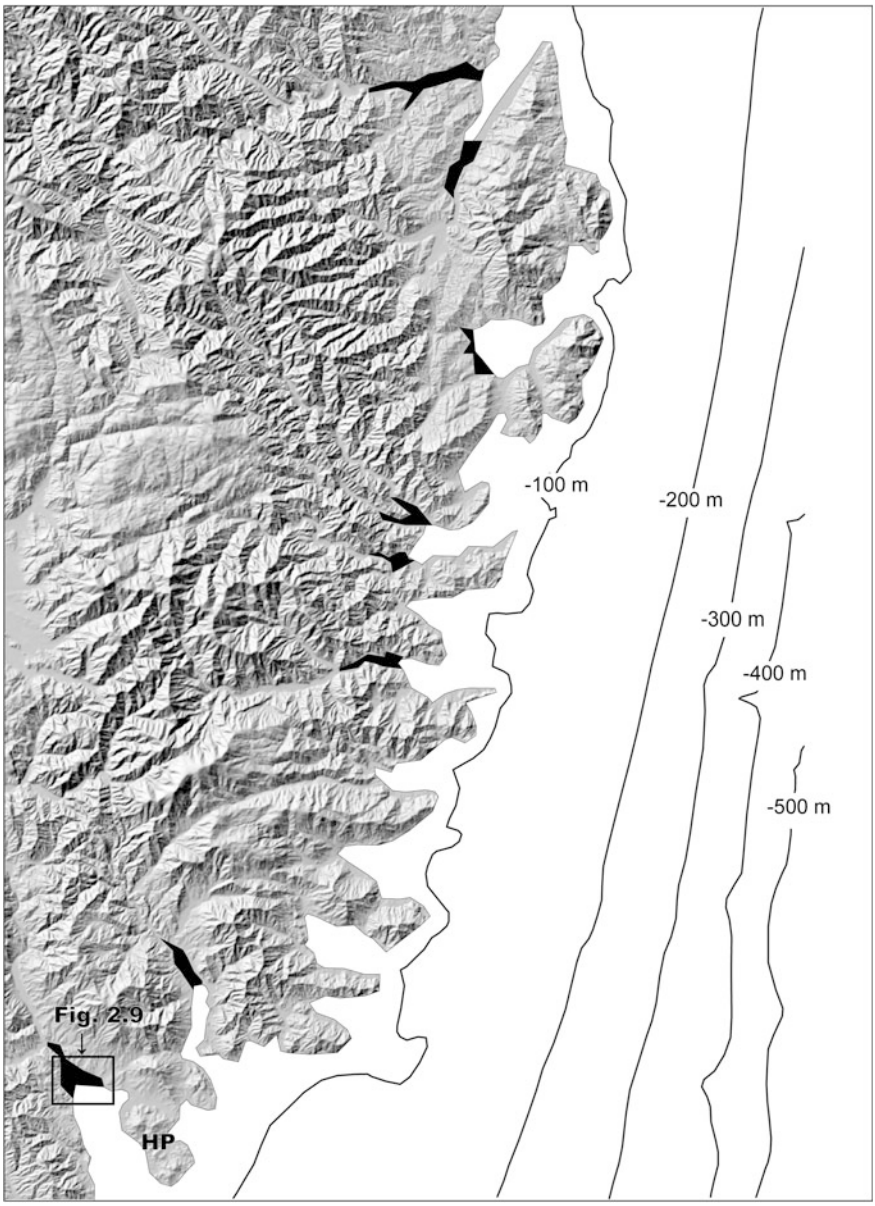

Fig. 2.7 Distribution of alluvial plains (*shaded black*) on the shores of embayments along the southern Sanriku Coast. Bathymetry from Cabinet Office, Government of Japan (2006)

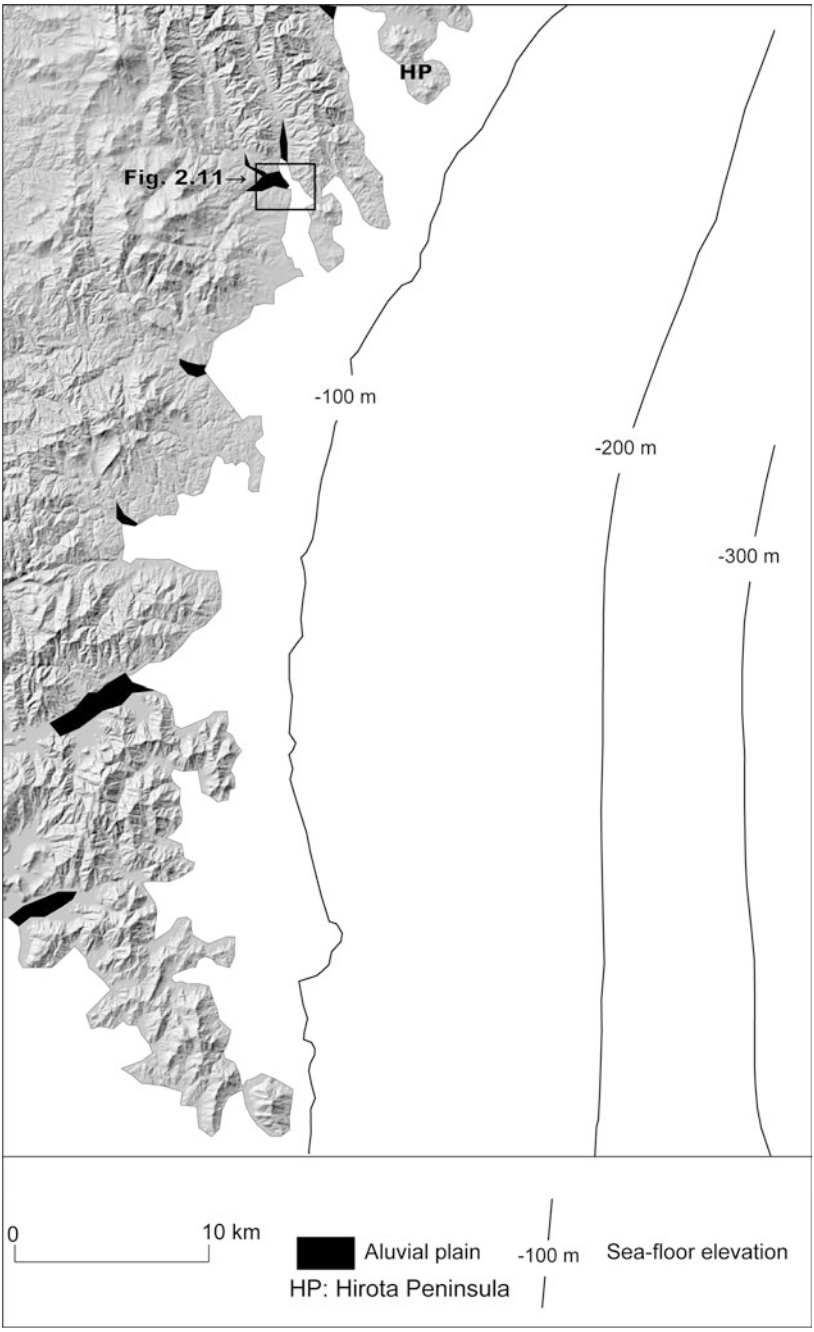

Fig. 2.7 (continued)

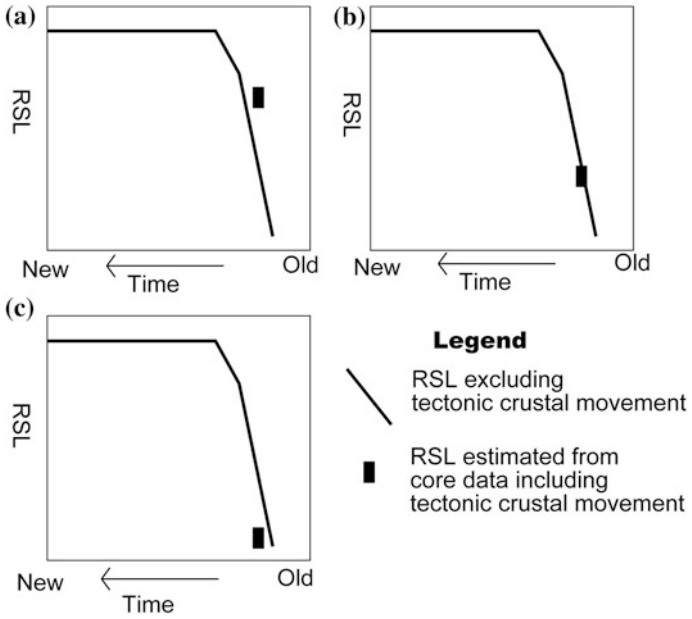

Fig. 2.8 Schematic diagrams showing the relationship between relative sea level (RSL) estimated from core data and a modeled RSL curve. **a** RSL estimated from core data higher than a modeled RSL curve excluding tectonic crustal movements, indicating an uplifting trend. **b** RSL estimated from core data similar to a modeled RSL curve, indicating tectonic stability. **c** Estimated RSL lower than a modeled RSL curve, indicating a subsiding trend

2.6.1.2 Holocene Sequence

Sediments in core RT1 were divided on the basis of lithofacies into depositional units 1–6, in ascending order (Fig. 2.10). Molluscan shells, and diatoms were identified in the core sediments (Niwa et al. 2014).

Unit 1 consists of sand and well-rounded gravel containing no shell fragments and was interpreted by Chida et al. (1984) to represent the basal gravel of the incised-valley-fill sequence, thus indicating deposition in a fluvial environment during the lowstand of the Last Glacial Maximum (Iseki 1975).

Unit 2 consists of alternating, thin laminated layers of silt and very fine sand, indicating deposition in a tidally influenced environment (Reineck and Singh 1980). The upper sequence of unit 2 fines upward, indicating an upward decrease of current velocity in a tidally influenced channel (Dalrymple 1992). Niwa et al. (2014) interpreted this unit to represent tidal river deposits.

Unit 3 consists of sandy silt to silty sand and includes thin laminated alternations of very fine sand and silt similar to those identified in unit 2. The presence of molluscan shells (e.g., *Macoma contabulata*, *Batillaria cumingii*) in the lower part of unit 3 indicates deposition in an intertidal environment. Thus, Niwa et al. (2014)

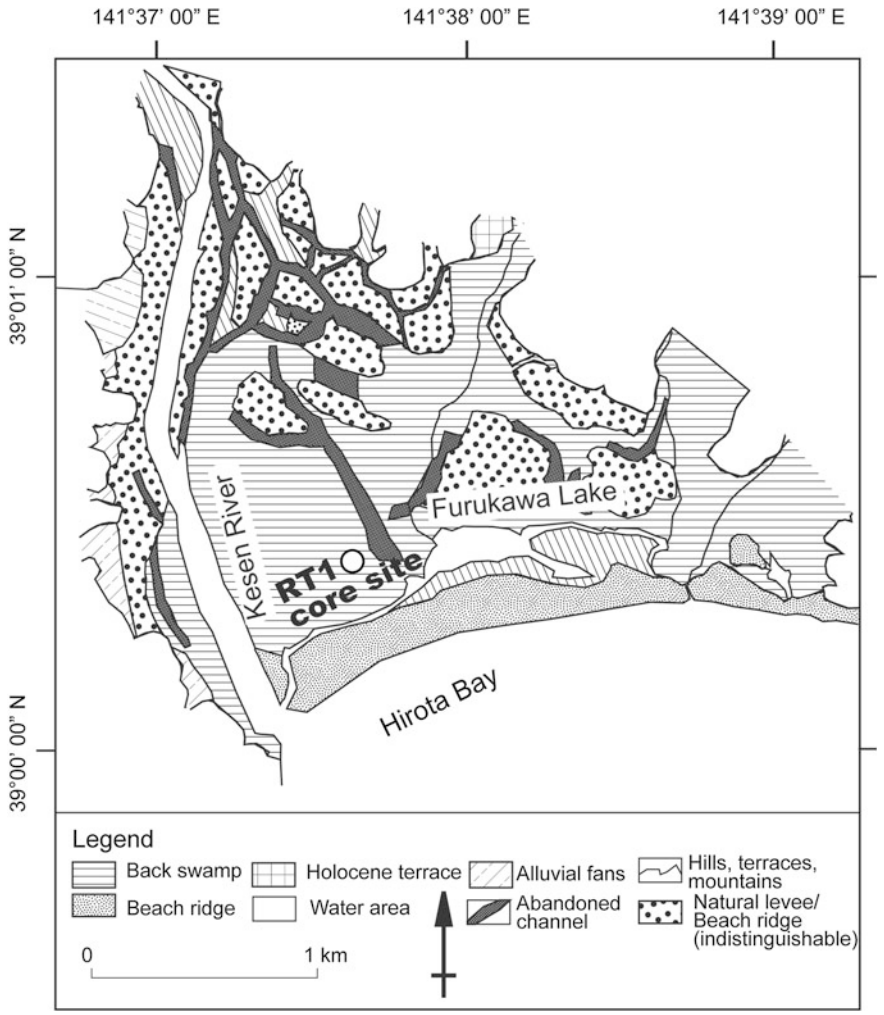

Fig. 2.9 Landform classification map of the Rikuzentakata Plain showing location of core RT1 (after Niwa et al. 2014)

interpreted this unit to be tidally influenced shallow-marine deposits (including tidal flat deposits).

Unit 4 is an upward coarsening sequence of sandy silt to fine sand. The lower part of the unit contains molluscan shells (e.g., *Dosinella penicillata*), indicating deposition in an inner bay subtidal environment. Plant fragments are more prevalent in the upper part of the unit. Thus, unit 4 represents prodelta to delta-front deposits, indicating the approach of the river mouth to the core site (Bhattacharya and Walker 1992).

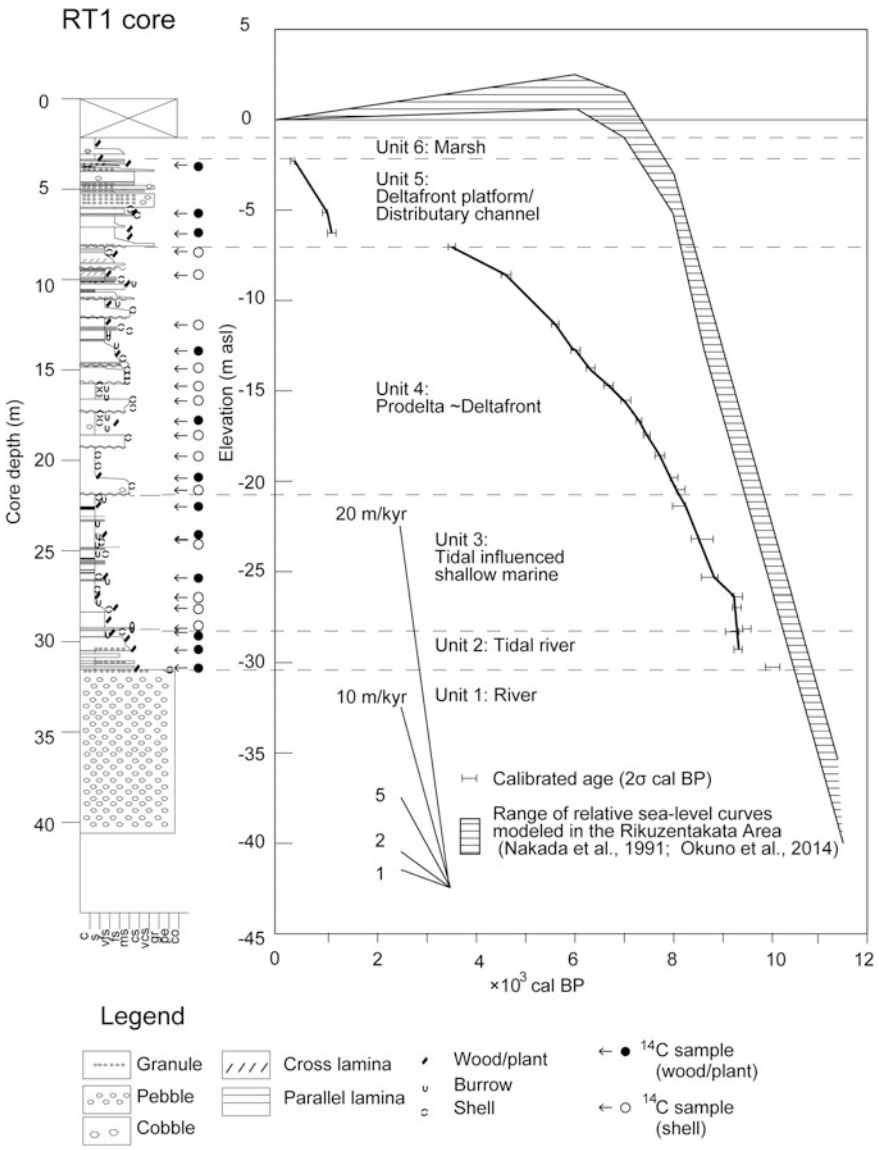

Fig. 2.10 Sedimentary column, sediment-accumulation curve from core RT1, and previously modeled RSL curves excluding tectonic crustal movements (after Niwa et al. 2014). The theoretical RSL calculated at Rikuzentakata is shown as in Niwa et al. (2014). Thus, the theoretical RSL is referred from Nakada et al. (1991) for 11,500 cal BP and Okuno et al. (2014) for the period after 8500 cal BP at the Rikuzentakata. Between 11,500 and 8500 cal BP, the RSL is interpolated from those at 11,500 and 8500 cal BP. The vertical range of the RSL at 11,500 cal BP is shown as difference between the RSL from ARC3 + ANT3B and viscosity model B and that from ARC3 + ANT3B and viscosity model C of Nakada et al. (1991). After 8500 cal BP, the vertical range represents the difference in RSLs based on ANUr model and ANU model of Okuno et al. (2014)

Unit 5 consists of sediment of fine sand to granule size. Some sand layers show cross-lamination. The boundary between units 5 and 4 is sharp. Unit 5 contains molluscan shells (e.g., *Dosinorbis japonicus*) indicative of deposition in an intertidal to subtidal environment. The unit 5 sequence is coarser than unit 4 and contains shallow-marine molluscan shells that indicate deposition in a delta-front platform environment (Yamaguchi et al. 2005) or in a distributary channel on a lower delta plain (Davis 1992).

Unit 6 consists mainly of silt and contains plant fragments and abundant freshwater diatom species, indicating that this unit represents terrestrial marsh deposits.

The sediment-accumulation curve we constructed based on 25 radiocarbon ages from core RT1 samples (Fig. 2.10) shows that accumulation rates were high (>20 mm/year) from 9500 to 9300 cal BP, low (2–7 mm/year) from 9300 to 3300 cal BP, and again high (5–10 mm/year) after 1200 cal BP. Niwa et al. (2014) interpreted the high accumulation rate from 9500 to 9300 cal BP to reflect large volumes of sediment supply due to increased accommodation space in response to sea-level rise during deglaciation. The decreased rate after 9300 cal BP probably reflects decreasing sediment supply due to expansion of the area of marine deposition and retreat of the river mouth as sea level rose. The high rate after 1200 cal BP reflects the close proximity of the river mouth to the RT1 core site at this time (Niwa et al. 2014).

2.6.1.3 Holocene Subsidence Inferred from Elevations and Ages of Intertidal Deposits

Niwa et al. (2014) estimated the trend of Holocene crustal movement by comparing the RSL curve we determined from core data with RSL curves derived from geophysical modeling in the Japan region by Nakada et al. (1991) and Okuno et al. (2014).

Because unit 2 (9500–9300 cal BP) represents tidal river deposits, RSL at the time of deposition was at or slightly higher than the elevation of the unit 2 depositional surface indicated by the sediment-accumulation curve (Fig. 2.10). The presence of molluscan shells in the lower part of unit 3 (9300–8600 cal BP) indicates an intertidal environment, so RSL at that time was at about the same elevation as the depositional surface indicated by the sediment-accumulation curve. Thus, core data indicate that RSL rose from about 30 m below present sea level at 9500 cal BP to about 23 m below present sea level at 8600 cal BP. However, the modeled RSL curves show a rise of RSL from about 20 m to about 15 m below present sea level (Fig. 2.10; Nakada et al. 1991; Okuno et al. 2014). Thus, the RSL determined from core data is lower than the modeled RSL, indicating that subsidence was predominant on the Rikuzentakata Plain during the Holocene, as has been the case over the last 100 years (Niwa et al. 2014).

2.6.2 *Kesennuma Okawa Plain*

2.6.2.1 Regional Setting and Sediment Core

The Kesennuma Okawa Plain on the western shore of Kesennuma Bay (Fig. 2.7) is a Holocene fluvial–coastal lowland on which a delta plain has been formed by sediments of the Kesennuma Okawa and Kamiyama rivers (Fig. 2.11). The Kesennuma Okawa and Kamiyama rivers are 23.9 and 6.9 km long, respectively, and drain a total catchment area of 168 km^2. The maximum spring tidal range in Kesennuma Bay is 1.3 m. The fluvial–coastal lowland extends 1.0 km from north to south and 3.0 km from east to west. Most of the plain is less than 5 m above sea level. Basement rocks under the catchment are Permian sedimentary rocks and Cretaceous granite, plutonic, volcanic, and sedimentary rocks (Geological Survey of Japan 2014).

Sediment core KO1 was drilled on reclaimed land in the lower reaches of the Kesennuma Okawa Plain. Niwa et al. (2015) conducted facies analyses and radiocarbon dating on 13 samples from this core.

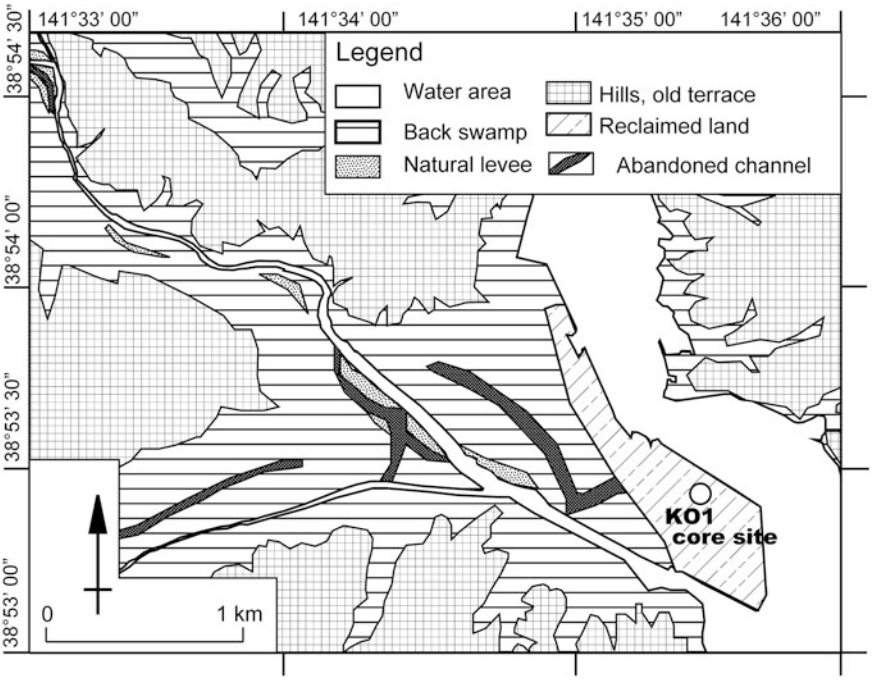

Fig. 2.11 Landform classification map of the Kesennuma Okawa Plain showing location of core KO1 (after Niwa et al. 2015)

2.6.2.2 Holocene Sequence

Sediments in core KO1 were divided into depositional units 1–5, in ascending order, on the basis of lithofacies and the molluscan shell species present (Fig. 2.12; Niwa et al. 2015).

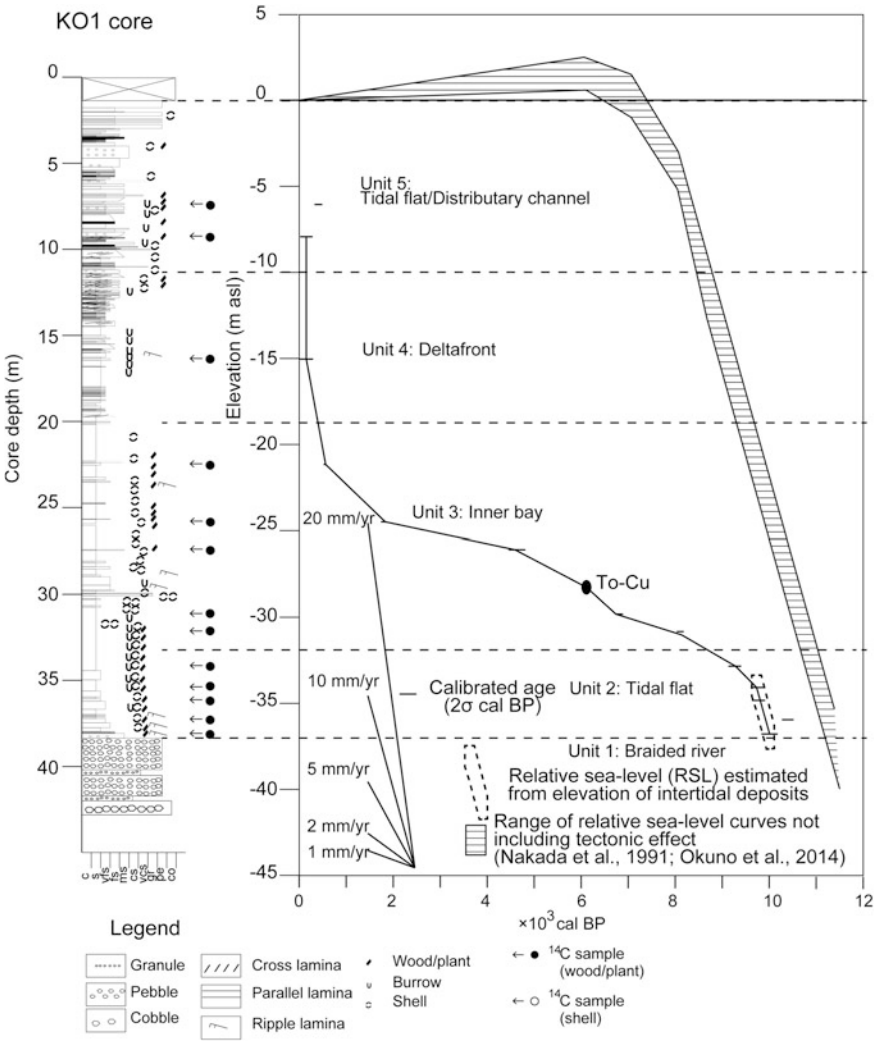

Fig. 2.12 Sedimentary column, sediment-accumulation curve of core KO1, and previously modeled RSL curves excluding tectonic crustal movements (after Niwa et al. 2015). The theoretical RSL calculated at Rikuzentakata, 15 km north of the study area, is shown as in Niwa et al. (2015). Thus, the theoretical RSL is referred from Nakada et al. (1991) for 11,500 cal BP and Okuno et al. (2014) for the period after 8500 cal BP at the Rikuzentakata. Between 11,500 and 8500 cal BP, the RSL is interpolated from those at 11,500 and 8500 cal BP. The vertical range of the RSL at 11,500 cal BP is shown as difference between the RSL from ARC3 + ANT3B and viscosity model B and that from ARC3 + ANT3B and viscosity model C of Nakada et al. (1991). After 8500 cal BP, the vertical range represents the difference in RSLs based on ANUr model and ANU model of Okuno et al. (2014)

Unit 1 consists of sand and well-rounded gravel and contains no shell fragments and is correlated with the basal gravel of the incised-valley-fill sequence of Chida et al. (1984), thus indicating deposition in a fluvial environment during the low-stand of the Last Glacial Maximum (Iseki 1975).

Unit 2 consists of silt and sand with thin laminated alternations of very fine sand and silt, suggesting deposition in a tidally influenced environment (Reineck and Singh 1980). The unit contains molluscan shells (e.g., *B. cumingii*) indicating an intertidal environment of deposition. Thus, Niwa et al. (2015) interpreted unit 2 to represent tidal flat deposits.

Unit 3 consists of massive silt to clay and contains molluscan shells (e.g., *Scapharca brouhtonii*, *Fulvia mutica*) indicative of a subtidal inner bay-floor environment of deposition. Thus, Niwa et al. (2015) interpreted unit 3 to represent inner bay deposits.

Unit 4 consists of sandy silt to fine sand in an upward coarsening succession, indicating deposition in a delta-front environment.

Unit 5 consists of sediments of silt to granule size and contains molluscan shells (e.g., *Batillaria multiformis*, *Nuttallia ezonis*) indicative of deposition in an intertidal or sandy-floored shallow-marine environment. Unit 5 is interpreted to represent tidal flat and/or distributary channel deposits (Niwa et al. 2015).

The sediment-accumulation curve we constructed based on 13 radiocarbon ages from core KO1 (Fig. 2.12) shows that accumulation rates were high (>10 mm/year) from 10,000 to 9700 cal BP, low (1–2 mm/year) from 9700 to 500 cal BP, and again high after 500 cal BP. Niwa et al. (2015) interpreted the high sediment-accumulation rate from 10,000 to 9700 cal BP to reflect large volumes of sediment supply in response to increased accommodation space as a result of sea-level rise during deglaciation. The decrease after 9700 cal BP probably reflects decreasing sediment supply in response to expansion of the area of marine deposition and river mouth retreat during sea-level rise. The high rate after 500 cal BP reflects the close proximity of the river mouth to the site of core KO1 at this time. These changes of sediment-accumulation rate are consistent with the sequence penetrated at the site of core KO1 representing a typical deltaic sequence (Niwa et al. 2015).

2.6.2.3 Holocene Subsidence Inferred from Elevations and Ages of Intertidal Deposits

The RSL rise from about 37 to 34 m below sea level determined from core data from 10,100 to 9600 cal BP (mainly unit 2) is almost equal to the elevation of the depositional surface because unit 2 is rich in intertidal molluscan shells (e.g., *B. multiformis*, *B. cumingii*) and therefore represents tidal flat deposits. However, the modeled RSL curves show a rise of sea level from about 17 to 11 m below present sea level (Fig. 2.12; Nakada et al. 1991; Okuno et al. 2014). Thus, the RSL curve derived from core data is lower than those of the two models and indicates that

Table 2.1 Summary of key geomorphic features and crustal movements on the Sanriku Coast

	Northern Sanriku Coast	Southern Sanriku Coast
Geomorphic features	Well-developed Pleistocene marine terraces	Fragmented flat surfaces; no definitive marine terraces Typical ria coastline
Long-term crustal movement	Marine terraces suggesting uplift since the Middle to Late Pleistocene	Lack of definitive marine terraces suggesting no uplift since the Late Pleistocene Sedimentary succession indicating possibility of long-term Holocene subsidence

subsidence was predominant in the Kesennuma Okawa Plain during the Holocene (Niwa et al. 2015).

2.6.3 Comparison of Subsidence Rate Through the Holocene with that During the Last Several Decades

The predominance of subsidence during the Holocene on the two alluvial plains described above (Table 2.1) suggests long-term subsidence of the southern Sanriku Coast (Niwa et al. 2015), contrary to the previous views that there has been long-term uplift in the region since the Late Quaternary. On the basis of radiocarbon ages and the differences between RSL derived from core data and modeled RSL curves, Holocene subsidence rates were 0.6–1.3 mm/year on the Rikuzentakata Plain (Niwa et al. 2014), and 0.9–1.8 mm/year on the Kesennuma Okawa Plain (Niwa et al. 2015). These rates are considerably lower than the rate of subsidence over the last several decades (5–10 mm/year; Kato and Tsumura 1979). Because the Early Holocene tidal deposits, used in calculation of subsidence rate, lies directory on the basement or gravel layer, the influence of compaction on the Holocene subsidence rate is likely to be negligible. Thus, one possibility is that we attribute this difference to the contribution of compaction to the subsidence rate over the last several decades. And, another possibility is that the Holocene subsidence rate includes contributions from undiscovered crustal movements (Niwa et al. 2015).

2.7 Summary and Conclusions

In this chapter, we described the geomorphology of the Sanriku Coast, introduce recent studies on the development of alluvial plains and reconstruction of Holocene crustal movement along the southern Sanriku Coast. The main points are summarized below.

1. The Sanriku Coast subsided dramatically by up to 1.3 m during the 2011 Tohoku-Oki earthquake. Geodetic and tide gauge data from the coastal region show rapid subsidence at several to ten millimeters per year over the last several decades.
2. The northern Sanriku Coast is characterized by well-developed Middle to Late Pleistocene marine terraces, which indicate a long-term trend of uplift since the Late Quaternary. On the southern Sanriku Coast, there are no definitive marine terraces, and the lack of information about terrace geomorphology precludes a clear understanding of long-term crustal movements there.
3. The southern Sanriku Coast has a typical ria coast line with many capes and deep embayments. Since the 2011 Tohoku-Oki earthquake, there have been several studies of small alluvial plains on the shores of embayments, which have focused on their development on the basis of facies analyses and high-density radiocarbon dating.
4. Recent studies of the alluvial plains along the southern Sanriku Coast have recognized sedimentary successions influenced by Holocene sea-level changes and identified a long-term trend of subsidence during the Holocene on the basis of the elevations and ages of intertidal deposits. The results of these studies suggest that, unlike the previous view that the southern Sanriku Coast has experienced long-term uplift since the Late Quaternary, subsidence has probably been predominant during Holocene.

More research is needed to further clarify the interplay of uplift and subsidence in the Late Quaternary history of the Sanriku Coast. Construction of RSL curves, including tectonic crustal movements, on the basis of the burial histories of incised-valley-fill sequences should be the first step, followed by reconstruction of Holocene crustal movements based on those RSL curves. Finally, there is a need to better understand the relationship of deformation during the 2011 Tohoku-Oki earthquake to long-term crustal movements and plate tectonics in the region.

Acknowledgments We thank Dr. Shinji Toda for providing guidance on the geomorphology and geology of the Sanriku coastal area, Dr. Yoshiaki Matsushima for assistance with the identification of paleo-environments of deposition based on the species of molluscan shells present in sediment cores, and Mr. Tsuyoshi Yamaichi for helping us to conduct sediment core analyses. This research was financially supported by a Grant of Research Project of International Research Institute of Disaster Science, Tohoku University, a Grant-in-aid from the Scientific Research Project (Nos. 26282078 and 26750106) of the Ministry of Education, Culture, Sports, Science and Technology of Japan, and a Research Grant of Japan Geographic Data Center. We thank the Japan Association of Quaternary Research for permitting reprint of Figs. 2.9 and 2.10, the Association of Japanese Geographers Figs. 2.4 and 2.5, and Tokyo Geographical Society Figs. 2.3, 2.11, and 2.12.

References

Bhattacharya JP, Walker RG (1992) Deltas. In: Walker RG, James NP (eds) Facies models: response to sea level change. Geological Association of Canada, pp 157–177

Cabinet Office, Government of Japan (2006) Survey report of ocean trench earthquake around Japan and Chishima Trench. Cabinet Office, Government of Japan, 51 p (in Japanese)

Chida N, Matsumoto H, Obara S (1984) Resent alluvial deposit and Holocene sea-level change on Rikuzentakata coastal plain. Ann Tohoku Geogr Assoc 36:232–239 (in Japanese with English abstract)
Coastal Movements Data Center (2015) Table of annual mean sea level along the Japanese coast. http://cais.gsi.go.jp/cmdc/center/annualgra.html (in Japanese; cited 18 May 2015)
Dalrymple RW (1992) Tidal depositional systems. In: Walker RG, James NP (eds) Facies models: response to sea level change. Geological Association of Canada, pp 195–218
Davis RA Jr (1992) Depositional systems: an introduction to sedimentology and stratigraphy, 2nd edn. Prentice-Hall, Upper Saddle River, 604 p
Geological Survey of Japan, AIST (ed) (2014) Seamless digital geological map of Japan 1: 200,000. Jan 14, 2014 version. Geological Survey of Japan, National Institute of Advanced Industrial Science and Technology
Haraguchi T, Iwamatsu, A (2011) Detailed Maps of the Impacts of the 2011 Japan Tsunami, Vol 1: Aomori, Iwate, and Miyagi Prefectures. Kokon Shoin, Tokyo, Japan. 167 p (in Japanese)
Ikeda Y (1996) Implications of active fault study for the present-day tectonics of the Japan arc. Active Fault Res 15:93–99 (in Japanese with English abstract)
Ikeda Y, Okada S, Tajikara M (2012) Long-term strain buildup in the Northeast Japan arc-trench system and its implications for gigantic strain release events. J Geol Soc Japan 118:294–312 (in Japanese with English abstract)
Imaizumi T (1999) Topographic relief in the northeast Japan and some question on the basis of distribution of active faults. Chikyu Monthly Symp 27:113–117 (in Japanese)
Iseki H (1975) On the basal gravel beds of the recent deposits. J Geogr 84:247–264 (in Japanese with English abstract)
Japan Meteorological Agency (2011) Monthly report on earthquakes and volcanoes in Japan March 2011. 324 p (in Japanese)
Kato T, Tsumura K (1979) Vertical land movement in Japan as deduced from tidal record (1951–1978). Bull Earthquake Res Inst 54:559–628 (in Japanese with English abstract)
Koike K (2005) Major landform and landform classification in the Tohoku Japan. In: Koike K (ed) Regional geomorphology of the Japanese islands, vol 3. Geomorphology of the Tohoku Region, pp 20–26 (in Japanese)
Koike K, Machida H (eds) (2001) Atlas of Quaternary marine terraces in the Japanese island, University of Tokyo Press, Tokyo ,105 p (in Japanese)
Miura O (1966) Coastal terraces and rias along the Kesennuma bay, Miyagi prefecture. Ann Tohoku Geogr Assoc 18:116–122 (in Japanese with English abstract)
Miura O (1968) Rias coast and coastal terraces of Sanriku, northeastern Japan. Geogr Rev Japan 41:732–747 (in Japanese with English abstract)
Miyauchi T (1985) Quaternary crustal movements estimated from deformed terraces and geologic structures of the Kamikita coastal plain, northeast Japan. Geogr Rev Japan, SerA 58:492–515 (in Japanese with English abstract)
Miyauchi T (2012) Dangerous offshore active faults and their possible seismotectonics in Japanese coastal areas. Sci J Kagaku 82:651–661 (in Japanese)
Nakada M, Yonekura N, Lambeck K (1991) Late Pleistocene and Holocene sea-level changes in Japan: Implications for tectonic histories and mantle rheology. Palaeogeogr Palaeoclimatol Palaeoecol 85:107–122
Nakata T, Imaizumi T (2001) Digital active fault map of Japan. University of Tokyo Press, Tokyo, 68 p (in Japanese with one map and two DVD)
Nishimura T (2012) Crustal deformation of northeastern Japan based on geodetic data for recent 120 years. J Geol Soc Japan 118:278–293 (in Japanese with English abstract)
Niwa Y, Toda S, Sugai T, Matsushima Y (2014) Holocene sedimentary facies, sediment accumulation rate and coastal subsidence estimated from a sediment core in the Rikuzentakata Plain, northeast Japan. Quat Res (Dai-Yonki Kenkyu), 53:311–322 (in Japanese with English abstract)

Niwa Y, Sugai T, Matsushima Y (2015) Holocene crustal movement in the Kesennuma Okawa Plain, southern Sanriku Coast, northeast Japan, estimated from coastal geology. J Geogr 124:545–560 (in Japanese with English abstract)

Okada S, Ikeda Y (2012) Quantifying crustal extension and shortening in the back-arc region of Northeast Japan. J Geophys Res 117(B1): B01404.1–B01404.28

Okuno J, Nakada M, Ishii M, Miura H (2014) Vertical tectonic crustal movements along the Japanese coastlines inferred from late quaternary and recent relative sea-level changes. Quat Sci Rev 91:42–61

Ozawa S, Nishimura T, Suito H, Kobayashi T, Tobita M, Imakiire T (2011) Coseismic and postseismic slip of the 2011 magnitude-9 Tohoku-oki earthquake. Nature 475:373–377

Reineck HE, Singh IB (1980) Depositional sedimentary environments. Springer, Berlin, 549 p

Taira A (2001) Tectonic evolution of the Japanese island arc system. Ann Rev Earth Planet Sci 29:109–134

Yagi H, Suzuki T (2001) Southern Sanriku coast and Joban area. In: Koike K, Machida H (eds) Atlas of quaternary marine terraces in the Japanese island. University of Tokyo Press, Tokyo, pp 29–32 (in Japanese)

Yamaguchi M, Sugai T, Fujiwara O, Ohmori H, Kamataki T, Sugiyama Y (2005) Depositional process and landform of the Kiso river delta, reconstructed from grain size distributions, and accumulation rate of sediment cores. Quat Res (Dai-Yonki Kenkyu), 44:37–44 (in Japanese with English abstract)

Yonekura N (1966) Geomorphic development of northern Rikuchu coastal region, north-eastern Japan. Geogr Rev Japan 39:311–323 (in Japanese with English abstract)

Chapter 3
Coastal Geomorphology and Tsunami Disaster by the 2011 off the Pacific Coast of Tohoku Earthquake

Tomoya Abe and Kazuaki Hori

Abstract This study investigated the tsunami deposits accumulated at the Pacific coast of Tohoku district by the tsunami associated with the 2011 off the Pacific coast of Tohoku Earthquake. Influence of coastal landforms on the tsunami deposits and run-up heights was also discussed. Pleistocene terraces, rias, strand plain, and valley plain surrounded by terraces or hills occur generally along the coast from north to south. Tsunami deposits up to several tens of centimeters in thickness accumulated broadly in strand plain and valley plain. Although thick tsunami deposits also formed at small bay-head deltas in rias, tsunami deposits were not clear and erosional landforms caused by tsunami backwash were common in a very small, steep valley plain along the ria coasts. Sandy deposits show landward-thinning trend at wide strand plain and valley plain. However, the similar trend was not clear at narrow strand plain. The difference is probably related to decrease in sediment transport capacity of the tsunami and sediment supply. Sediment distribution and run-up height are strongly influenced by onshore topography. In high-lying topography, run-up height may relate to onshore slope and shape of lowland. On the other hand, run-up height is possibly controlled mainly by the characteristics of incident wave (wave period and height) in low-lying topography. Further detailed investigation about submarine topography is also required in the near feature.

Keywords Tsunami deposit · Run-up height · Rias · Strand plain · Valley plain

T. Abe (✉)
Marine Geology Research Group, Institute of Geology and Geoinformation, Geological Survey of Japan, Tsukuba Central 7, 1-1-1 Higashi, Tsukuba, Ibaraki 305-8567, Japan
e-mail: tomoya-abe@aist.go.jp

K. Hori
Department of Geography, Graduate School of Environmental Studies, Nagoya University, D2-2 Furocho, Chikusa-ku, Nagoya Aichi 464-8601, Japan

S. Haruyama and T. Sugai (eds.), *Natural Disaster and Coastal Geomorphology*, DOI 10.1007/978-3-319-33814-9_3

3.1 Introduction

The 2011 off the Pacific coast of Tohoku Earthquake (*Mw* 9.0) occurred on March 11, 2011. The earthquake triggered huge tsunami (hereinafter called the 2011 Tohoku-oki tsunami), and the tsunami inundated and damaged to the wide range of the coastal areas facing the Pacific Ocean in the northeast Japan. In particular, coastal area in Iwate, Miyagi, and Fukushima prefectures was mostly damaged by huge tsunami.

Tsunami causes huge sediment transport near coastal area. Sediment formed by tsunami is called "tsunami deposit". Researches of tsunami deposits can provide useful information of past tsunamis to aid in the future assessment of the tsunami hazard (Goff et al. 2012). Tsunami deposits on coastal lowlands are useful for estimating recurrence intervals and magnitudes of ancient tsunami events. It enables us to expand our knowledge on the history of past tsunamis older than thousands of years ago. For example, maximum inland extent of tsunami deposits is assumed to represent a minimum of inundation distance (Jaffe and Gelfenbaum 2002; Koshimura et al. 2002; Nanayama et al. 2003).

Maximum landward extent of the sandy tsunami deposits can be regarded as the minimum inundation limit. Before the 2011 Tohoku-oki tsunami, recent post-tsunami field surveys along low-lying coastlines showed that sandy tsunami deposits commonly extend to approximately over 90 % of the actual inundation limit (MacInnes et al. 2009). On the other hand, after the 2011 Tohoku-oki tsunami, some researches of the 2011 tsunami pointed out that there was the significant gap (0.6–2.0 km) between the inundation limit and the maximum landward extent of the sandy tsunami deposit where the inundation distance was more than 2.5–3.0 km (Goto et al. 2011; Abe et al. 2012; Shishikura et al. 2012).

Case studies of recent tsunami impacts have proven to be extremely useful in understanding the geological processes involved in inundation and return flow, and refining the criteria to identify paleo-tsunami deposits in the geological record (Richmond et al. 2012). Many studies were conducted after recent tsunamis including 2004 Indian Ocean tsunami and the 2011 Tohoku-oki tsunami. In general, tsunami deposits thin and fine landward, although local microscopic topographic features give strong effects to the distribution trend of the deposits. Post-tsunami field surveys after the 2011 Tohoku-oki event revealed that the thickness and grain size varied significantly because of the small-scale undulations (Nakamura et al. 2012), redistribution of the vented sediments from liquefaction (Goto et al. 2012), and scouring at the lee side of engineering structures (Takashimizu et al. 2012).

Onshore tsunami behavior, mainly characterized by run-up height, inundation height, inundation distance, velocity, and direction, widely varied depending on coastal geomorphology. Several types of coastal geomorphology are distributed along the coasts of Iwate, Miyagi, and Fukushima prefectures. For example, central to southern parts of Iwate Prefecture to northern part of Miyagi Prefecture are well known to the development of rias, whereas strand plains are distributed at the southern parts of Miyagi Prefecture. Geomorphological approaches to deposition,

erosion, and flow characteristics of the tsunami were applied to ria coast (e.g., Komatsu et al. 2014; Hayakawa et al. 2015). However, difference of distribution pattern of the tsunami deposit and tsunami height among these coasts was poorly understood.

In this paper, we reported the characteristics of the tsunami deposits formed by the 2011 Tohoku-oki tsunami based on the field survey. We also discussed the influence of the onshore landform on the tsunami deposits and run-up heights.

3.2 Regional Setting

The study area belongs to non-volcanic outer arc in the northeast Japan. Most of the study area except for the northern end and central part is located at the east side of the Kitakami and Abukuma mountains characterized by gentle plateau-like topography. The Kitakami Mountain is underlain largely by Palaeozoic and Mesozoic sedimentary rocks and the Lower Cretaceous granitic rocks and has the elevation of 600–1300 m. The Abukuma Mountain consists mainly of the Cretaceous granitic rocks, metamorphic rocks, and Palaeozoic and Mesozoic sedimentary rocks. The mountain is bordered on the northeast by the Futaba Fault. Neogene sedimentary rocks are common along the coast on the east side of the mountain.

The coast faces the Pacific Ocean. Tidal range along the coast is around 1 m (National Astronomical Observatory of Japan 2013). Yearly average significant wave height ranges from 0.6 to 1.2 m at stations along the coast in 2013 (Kawaguchi et al. 2015). Maximum significant wave heights, 4.0–7.5 m, were associated with tropical cyclones and low pressures.

Coastal landforms can be roughly divided into four areas from north to south based on their characteristics. These areas are called conveniently as Kamikita Plain, Sanriku Coast, Sendai Plain, and Iwaki Coast (Fig. 3.1). Geomorphic studies about these coastal landforms were summarized by Koike et al. (2005).

Marine terraces occur widely at the Kamikita Plain. The terraces are dissected by rivers flowing into the Pacific Ocean and fluvial terraces formed by these rivers. The distribution of the marine and fluvial terraces combined with tephrostratigraphic studies suggests that the plain has uplifted since at least ca. 430–470 ka (Miyauchi 1987). Furthermore, the uplift rate along the coast is estimated to be 0.1–0.2 mm/year during the last 120 ka (Miyauchi 1987).

Coastal cliffs and smoothly shaped coastlines are common along the northern part of the Sanriku Coast. Middle to Late Pleistocene marine terraces also develop well at the coast like the Kamikita Plain (Yonekura 1966). Elevation of the highest terrace called “Mizunashi Surface” ranges from 80 to 280 m above sea level and is estimated to be built at marine isotope stage (MIS) 19, ca. 760 ka (Miyauchi 2001).

In contrast, indented coastlines characterize the middle and southern parts of the Sanriku Coast. Many rias with long and narrow inlets are distributed at river mouths originated from the Kitakami Mountain. Water depth at each bay entrance is usually

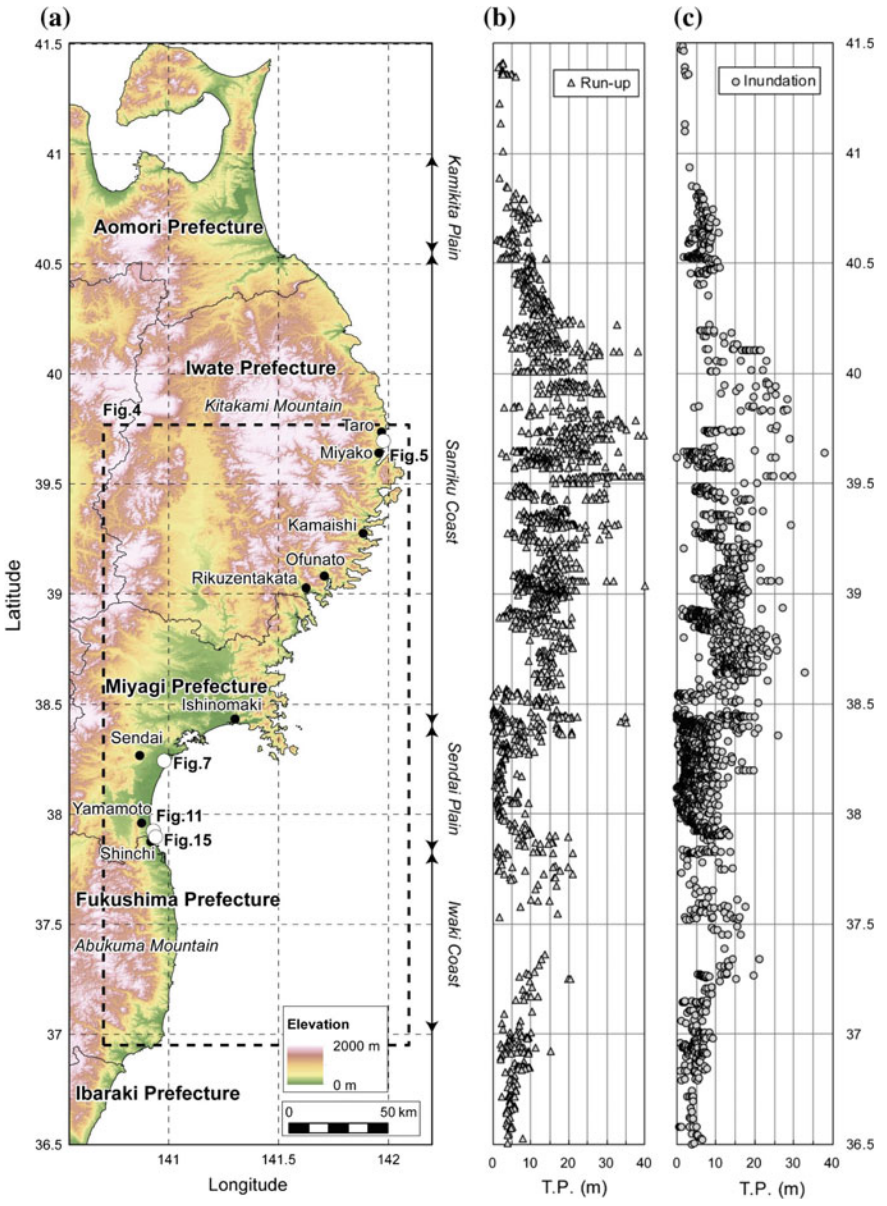

Fig. 3.1 **a** Elevation map of study area using 10 m mesh digital elevation model (DEM) provided by the Geospatial Information Authority of Japan (GSI), location of survey sites and main cities, **b** run-up height above Tokyo Peil (TP), **c** inundation height above TP provided by the 2011 Tohoku Earthquake Tsunami Joint Survey Group (TETJSG) (2011)

around 100 m. Thus, the bay reduces water depth rapidly landward. The original shape of the rias was probably formed around the latest Neogne to the earliest Pleistocene, ~2 Ma due to the submergence of valleys cutting into the Kitakami Mountain (Yoshikawa 1964, 1997; Miura 1968), though no absolute ages have been obtained. Marine terraces occur fragmentally along the valley wall of the rias and the present coast (Yoshikawa 1964; Miura 1966, 1968). For example, the formation age of the highest terrace distributed around Kesennuma may be correlated with MIS 11, 400 ka (Yagi and Suzuki 2001), though tephrochronology could not have been available for the terrace. The presence of the terraces implies that the middle and southern parts of the Sanriku Coast have uplifted. The rias have been generally less sedimentary filling. As the rivers through the Kitakami Mountain are small in length and cut the Palaeozoic to Mesozoic hard sedimentary rocks, fluvial sediment supply to the rias has been small. However, relatively minor coastal lowlands (e.g., bay-head delta) can be found at the head of some rias. For example, thick sedimentary sequence (i.e., incised-valley fill) accumulated during deglaciated sea-level rise and highstand following low sea-level phase at the Last Glacial Maximum was reported from the Rikuzentakata coastal plain built by the Kesen River (Chida et al. 1984). Several cities such as Miyako, Kamaishi, Ofunato, Rikuzentakata, and Kesennuma with estimated population of ca. 19,000–65,000 are distributed at these lowlands.

Sendai Plain extends between the southern end of Kitakami and the northern end of Abukuma mountains. There are two widespread strand plains under wave-dominated condition. The northeastern part usually called as Ishinomaki coastal plain with 20 km in length and 9 km in maximum width has been formed at the lower reach of the Kitakami, Eai, and Naruse rivers (Matsumoto 1981b; Ito 1999). The southwestern part called as Sendai coastal plain with 50 km in length and 10–15 km in maximum width has been built at the lower reach of the Nanakita, Natori, and Abukuma rivers (Matsumoto 1981a). Elevation of both plains is generally less than 5 m. Several beach ridges almost parallel to the present shoreline develop well at both plains. They have been formed during the sea-level highstand since the mid-Holocene (Matsumoto 1984). Back marsh underlain by organic-rich mud occurs widely landward and between the beach ridges. Relative elevation between back marsh and beach ridge is approximately 0.5–1.5 m. Natural levees and the former river channels are also developed along the rivers.

Late Pleistocene to Holocene sediment thickness reaches approximately 60 m under the present coast (Matsumoto 1981b). Incised valleys were formed in response to sea-level lowering and were filled by fluvial and marine deposits during the subsequent sea-level change. In particular, the Holocene succession, <30 m thick, overlies latest Pleistocene to Early Holocene non-marine deposits in the Sendai coastal plain (Tamura and Masuda 2005). It is composed of ravinement, inner shelf, and shoreface to coastal plain deposits (Tamura and Masuda 2005).

Valley plain, fluvial and marine terraces, and hills occur repeatedly from north to south along the smoothly shaped Iwaki Coast. Rivers from the Abukuma Mountain into the Pacific Ocean and each landform generally extend east–west direction. In particular, the terraces become to cover a larger area toward south. Elevation of the

terraces formed at MIS 5e suggest that uplift rate along the coast is 0.2 mm/year in the north and 0.5 mm/year in the south (Suzuki 1989). Shore erosion has retreated coastal cliffs composed of Neogene soft sedimentary rocks rapidly and has resulted in the formation of widespread abrasion platform. Valley plains are surrounded by the terraces and hills to the north and south. Lagoons are often found along the coast where sedimentary filling by the rivers has been not enough. Land reclamation has changed some of these lagoons into paddy field.

Sea-level change during the Holocene was estimated from Rikuzentakata coastal plain and Sendai coastal plain based on age–depth plots of peat, wood piece, and molluscan shells (Chida et al. 1984; Matsumoto 1981a). According to these studies, sea level has reached close to the present level around 5 ka. Sea level has been almost stabilized since the mid-Holocene, though small fluctuations, $\sim$1–2 m, have been estimated.

3.3 Method

We conducted field survey in four areas having different topographic features (Fig. 3.2). Landform types are very small, steep gradient valley plain along the north end of ria coasts (Matsutsuki, Iwate Prefecture), wide strand plain (Sendai, Miyagi Prefecture), narrow strand plain (Yamamoto, Miyagi Prefecture), and valley plain surrounded by hills (Shinchi, Fukushima Prefecture). We observed tsunami deposit formed by the 2011 tsunami in Sendai, Yamamoto, and Shinchi areas. On the other hand, geological survey of the tsunami deposit was not conducted in Matsutsuki area, because erosional features were dominant and we hardly found the tsunami deposit.

Three shore-normal transects were established to determine the inundation limit of the Tohoku-oki tsunami in Sendai, Yamamoto, and Shinchi areas (Fig. 3.1). The inundation limit, run-up heights, and inundation heights and depths (Fig. 3.3) along each transect were identified based on the tsunami-deposited debris, watermarks, and eyewitness accounts of local people during our field survey from April to June, 2011. The topography (elevation) from the coastline to the inundation limit was measured along each transect using RTK GPS instruments (Promark 3; Ashtech). We adopted the inundation heights and run-up heights measured by the Tohoku Earthquake Tsunami Joint Survey Group (TETJSG) (2011) near the transects. Trench surveys of the tsunami deposit were conducted at 86 sites spaced about 30–100 m apart on average along each transect. Thickness of the tsunami deposit was documented at each site, and erosional features of the tsunami were observed at each area.

We use run-up height database of TETJSG (2011) in order to examine relationship between average onshore slope from the shoreline to inundation limit and run-up height at inundation limit in various types of coastal landform from the middle part of Sanriku to Iwaki coasts. TETJSG database totally includes run-up data at 1962 points in the coasts shown in Fig. 3.1 (N41.5°–N36.5°). We selected

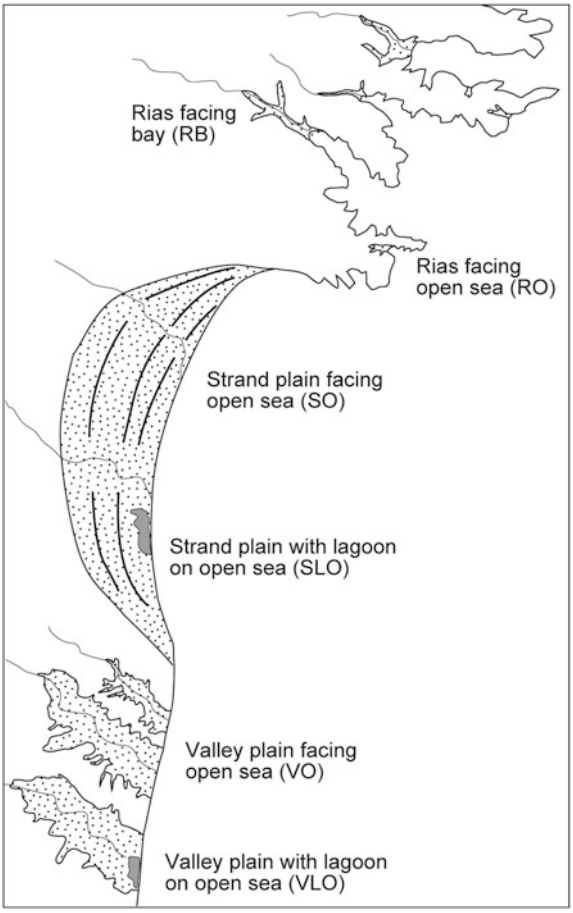

Fig. 3.2 Topographic types in study area

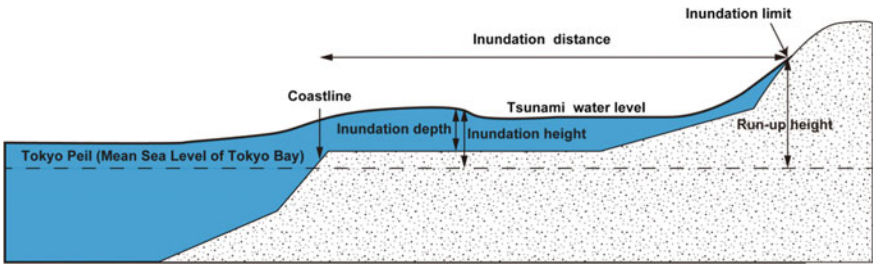

Fig. 3.3 Definition of inundation distance, inundation height, inundation depth, inundation limit, and run-up height in this study

the data based on some geomorphological criteria. Firstly, we removed the data obtained at terrace cliff, because onshore slope may not be associated with run-up height at terrace cliff. Secondly, we excluded the data within the rivers and channels on the ground that rivers have highly potentially extend inundation distance and height irrespective of onshore slope. We also excluded the data where high seawall or gate for tsunami protection, for example, Taro-cho, Fudai-mura, and Kamaishi-city in Iwate Prefecture, was constructed. These structures may decrease the run-up height. Finally, we chose 117 points (Fig. 3.4) from various types of coastal landform under the standards described above. Landforms at these points are classified into six types. Here, we conveniently call them as rias facing open sea (RO), rias facing bay (RB), valley plain facing open sea (VO), valley plain with lagoon on open sea (VLO), strand plain on open sea (SO), and strand plain with lagoon on open sea (SLO) (Fig. 3.2).

3.4 Results

3.4.1 Small, Steep Valley Plain Along the Ria Coasts

This valley is located at Matsutsuki between Taro-cho and Miyako city, Iwate Prefecture (Fig. 3.1), north end of ria coasts. The valley extends east–west to southeast–northwest direction (Fig. 3.5a) and is surrounded by hills with over 50 m height (Fig. 3.5b). The width of the main valley is only 100–200 m. The coastline faces directly the open ocean and is covered with sandy and gravelly sediments.

The run-up height is 27–30 m above from the Tokyo Peil (TP) near the shoreline. Inundation area mostly covered main valley and branch valleys (Fig. 3.5a). Tsunami inundated up to 1.20 km inland from the shoreline and 29.3 m above TP (TETJSG 2011). Run-up flow stopped due to steep slope (Fig. 3.6a). The gradient between the inundation limit and the shoreline was 24.10 ‰ on average.

Erosional features were dominant in this valley. Trees and grasses at the lower part (less than about 30 m above TP) of the valley wall were lost by the tsunami (Fig. 3.6a). Backwash flow formed narrow channel with 100 m long, 5 m width, and 1–2 m depth (Fig. 3.6b) and mostly discharged paddy soil distributed before the tsunami into the sea. Since it is difficult to observe the deposition by the tsunami, we did not conduct geological survey of the tsunami deposit.

3.4.2 Wide Strand Plain

We set the 4.02-km-long transect from the shoreline to inundation limit in the northern part of the Sendai coastal plain located at Sendai City in middle part of Miyagi Prefecture (Fig. 3.1). The transect is almost parallel to the present Nanakita

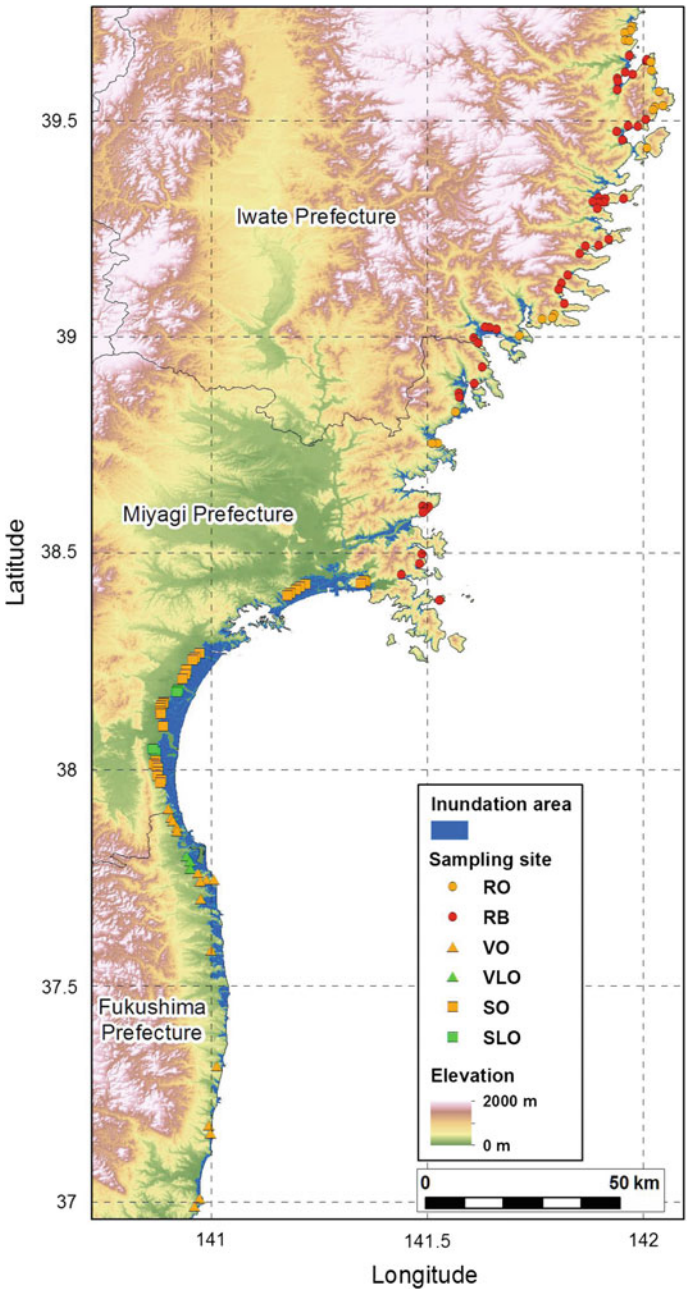

Fig. 3.4 Elevation map using 10 m mesh DEM of study area, inundation area provided by Ministry of Land, Infrastructure, Transport and Tourism, and location of analyzed run-up height data provided by TETJSG (2011)

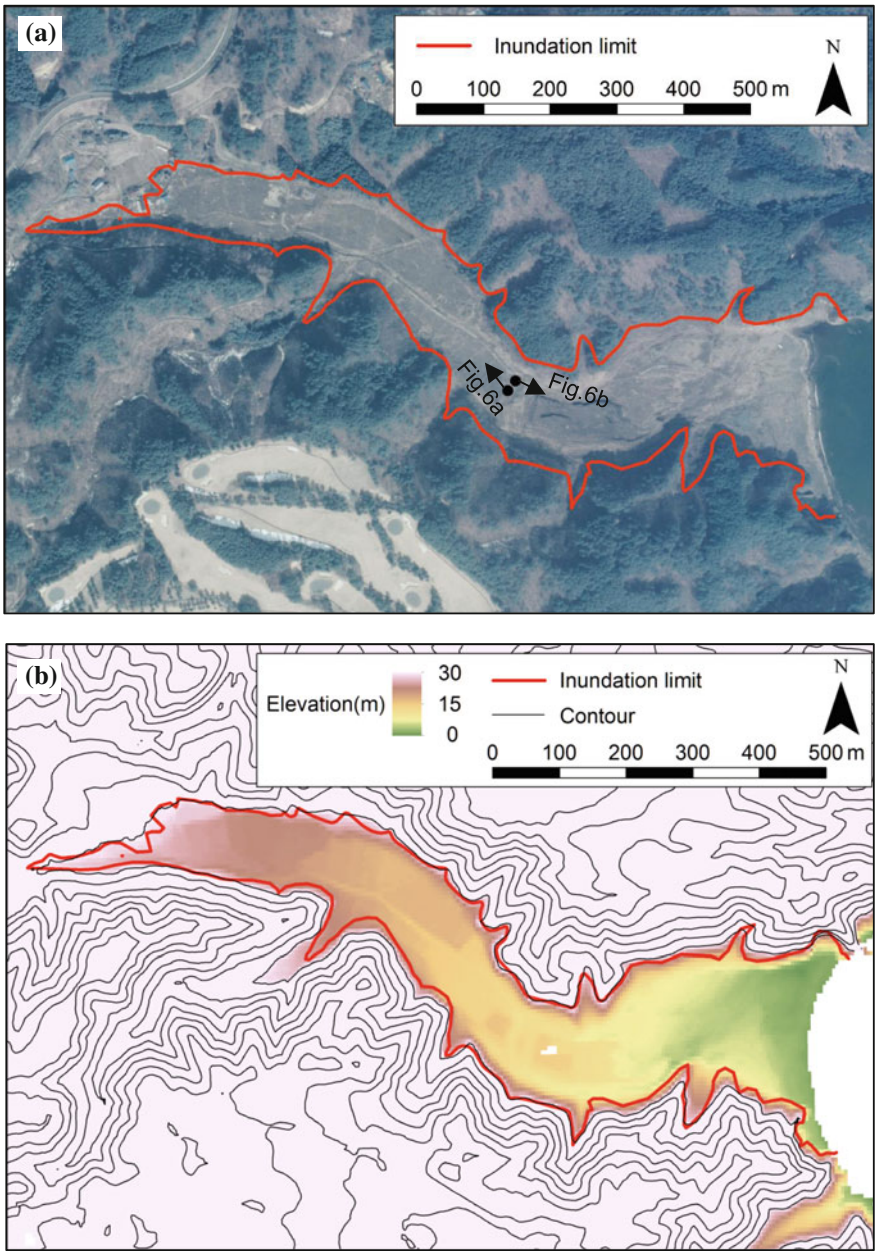

Fig. 3.5 **a** Aerial photograph (March, 2011) provided by GSI, inundation area, shooting locations and direction of photographs in Fig. 3.6, **b** elevation map using 5 m mesh DEM provided by GSI, 10 m interval contour line (except for less than 20 m above T.P.), and inundation area in rias at Matsutsuki. The location is shown in Fig. 3.1

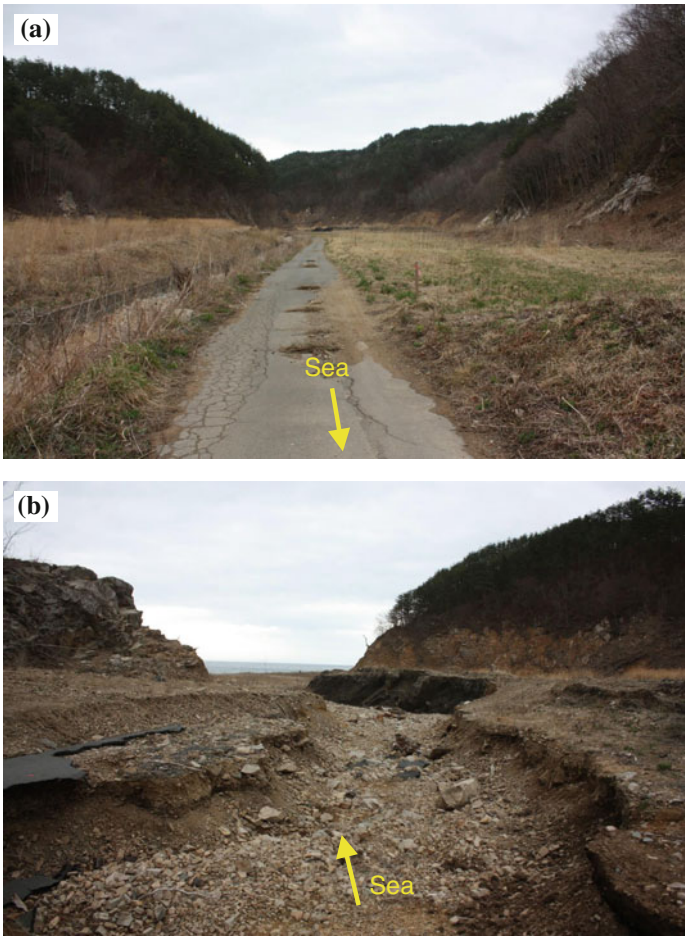

Fig. 3.6 Photographs of (**a**) steep gradient topography and (**b**) channel formed by the tsunami backwash in rias at Matsutsuki. Shooting locations and direction of photographs are shown in Fig. 3.5a

River flowing along the northern side of the transect. The survey area mainly covered the following topographies and structures landward: (a) 0.13-km-wide sandy beach, (b) 6.2-m-high onshore seawall, (c) 2–3-m-high sand dune, (d) 0.62-km-wide coastal forest planted pine tree behind the beach, and (e) low-lying rice paddy field that extends from 0.75 to 3.93 km from the coastline (Fig. 3.7a). Local subsidence of 0.2 m occurred by the 2011 earthquake according to real-time observation of the GSI electronic reference point near this transect.

The tsunami inundated up to 4.02 km inland from the shoreline and 3.1 m above TP at a maximum (TETJSG 2011) (Fig. 3.7b) due to flat topography (Fig. 3.8a). Tsunami eroded sand beach and dune with 2 m depth at a maximum (Fig. 3.8b) and

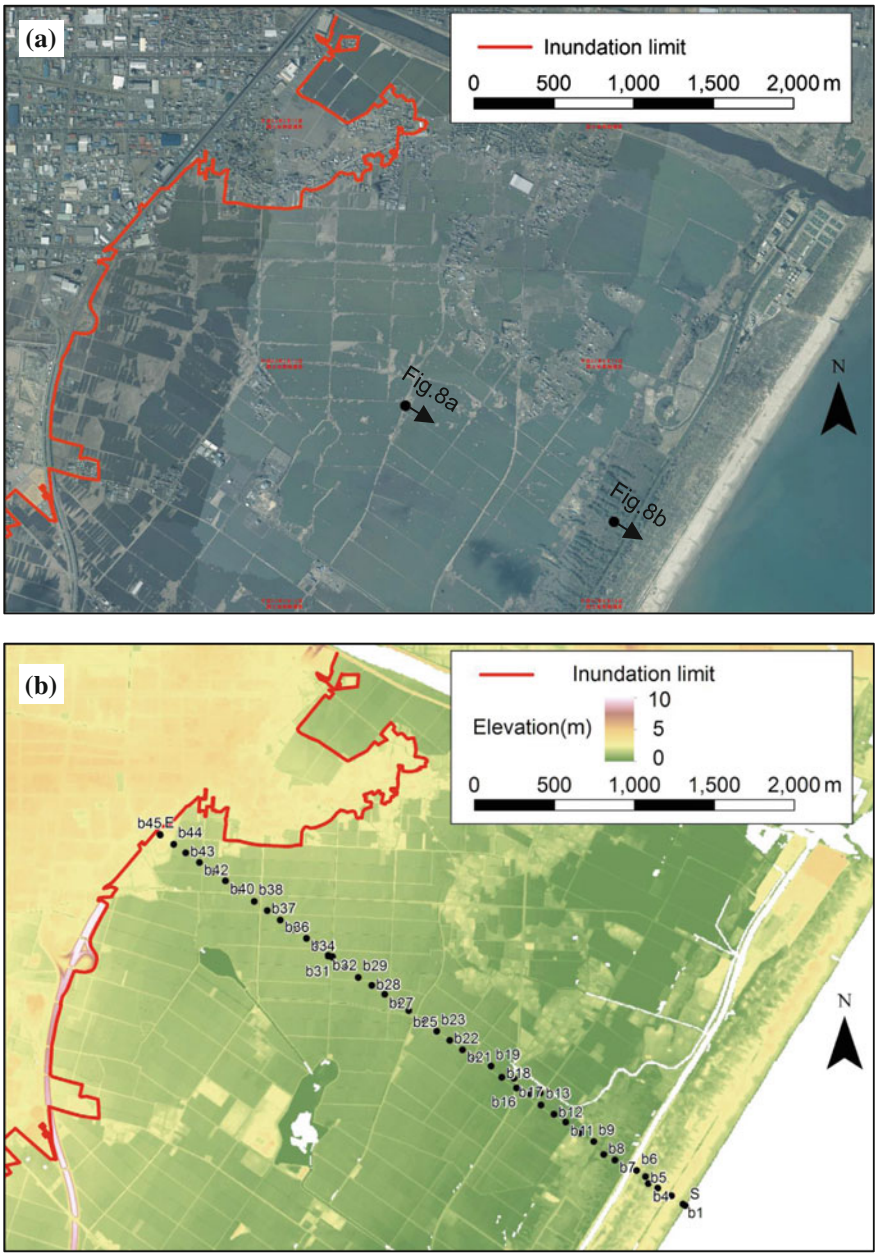

Fig. 3.7 **a** Aerial photograph (March, 2011) provided by GSI, inundation area, shooting location and direction of photograph in Fig. 3.8, **b** elevation map using 5 m mesh DEM, inundation area, and observation sites of the tsunami deposit in wide strand plain at Sendai City. The location is shown in Fig. 3.1

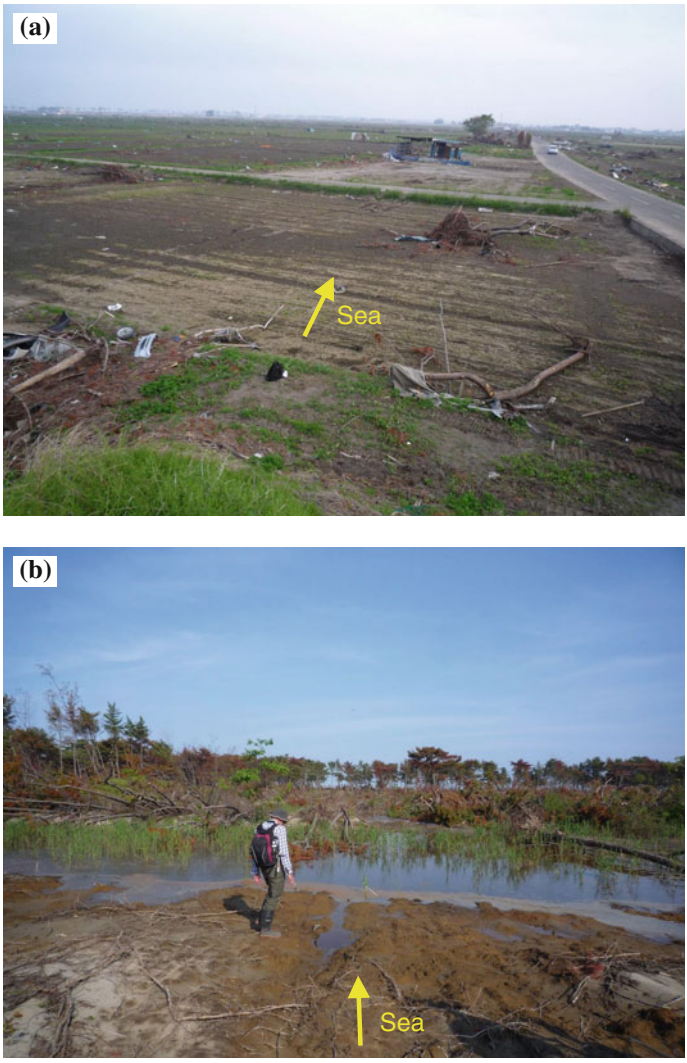

Fig. 3.8 Photographs of (**a**) flat topography and coastal trees transported by the run-up flow and **b** erosion in sand dune in wide strand plain at Sendai City. Shooting locations and direction of photographs are shown in Fig. 3.7a

transported inland huge amount of beach and dune sand, and many pine trees planted on sand dune (Fig. 3.8b) with a long distance (Fig. 3.8a). Additionally, paddy soil landward of the road was eroded with several tens of centimeters depth. Inundation heights were 6.3 m above TP landward of the coastal forest and decreased inland (Fig. 3.9a). Inundation depths were 3 m at 1.6 km from the

shoreline and decreased inland. The average gradient between the inundation limit and the shoreline was 0.77 ‰.

The tsunami deposit was described every 50–100 m at 45 sites (b1-b45) shown in Fig. 3.7b. The tsunami sand layer and mud layer were composed of 0.1–34-cm-thick fine-to-medium sand and 0.1–3-cm-thick silt, respectively (Figs. 3.9b and 3.10). Generally, sand thickness thinned landward, and mud thickness gently became thicker landward. However, the sand and mud thickness fluctuated in associated with local topography. Up to a distance of 0.1 km from the shoreline, tsunami deposit was not observed and erosion was dominant in sand beach. Between 0.1 and 1.2 km from the shoreline, the deposit was composed of 1–34-cm-thick, medium-grained sand layer. Between 1.2 and 3.0 km inland, the

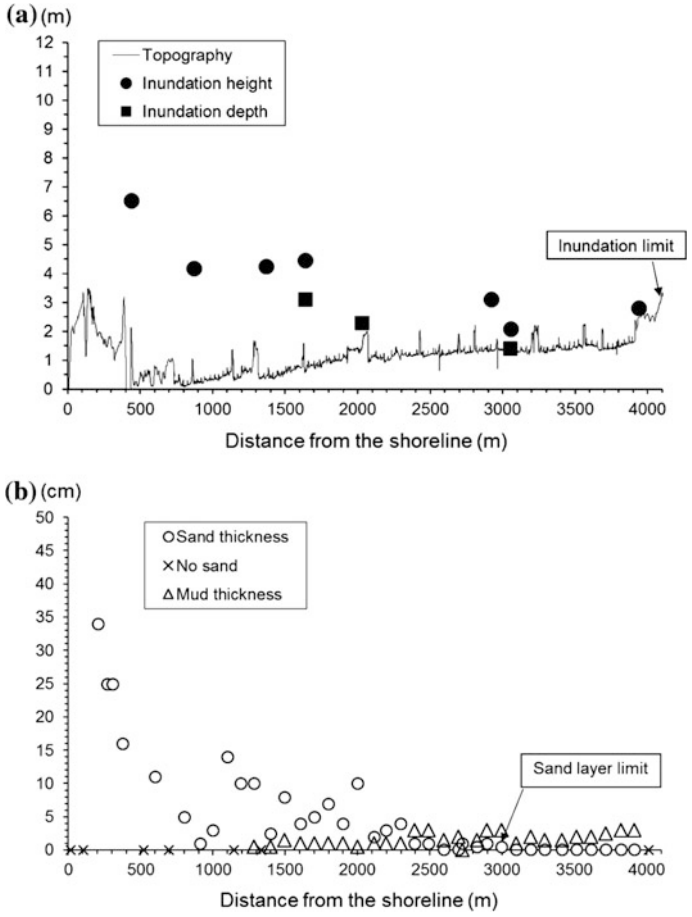

Fig. 3.9 **a** Elevation (m), inundation height (m) above TP, inundation depth (m), and inundation limit, **b** sand thickness (cm) and mud thickness (cm) along the transect in wide strand plain at Sendai City

Fig. 3.10 11-cm-thick sand layer at 0.6 km from the shoreline (site b8 in Fig. 3.7b) in wide strand plain at Sendai City

tsunami deposit was sand-dominated and was composed of 0.5–10-cm-thick fine- to medium-grained sand layer with a mud cap in 0.1–3 cm thickness. Further inland (3.0–4.0 km), the deposit became mud-dominated and was composed of 1–3-cm-thick mud overlying a patchy thin layer of massive fine- to medium-grained sand (0.1–0.3 cm thick).

The tsunami sand layer thicker than 0.5 cm was found up to approximately 3.0 km inland, which corresponds to 74.5 % of the inundation distance. The sub-millimeter (sub-mm) tsunami sand layer and the mud layer were found up to approximately 3.9 km inland, which is equal to 97.3 % of the inundation distance.

3.4.3 Narrow Strand Plain

We set the 0.60-km-long transect in narrow strand plain located at Yamamoto Town in southern part of Miyagi Prefecture (Fig. 3.1). This plain included in the Sendai coastal plain is located about 40 km south of Sendai City. The survey area covered (a) 0.03-km-wide sandy beach, (b) 6.2-m-high onshore seawall, (c) 2–3-m-high sand dune, (d) 0.14-km-wide coastal forest planted pine trees behind the beach, and (e) low-lying rice paddy field and dry field planted vegetables before the tsunami that extend from 0.17 to 0.60 km from the coastline. Local subsidence of 0.26 m occurred by the 2011 earthquake according to real-time observation of the GSI electronic reference point near this transect.

Tsunami inundated up to 0.60 km inland (Fig. 3.11a). Inundation area was limited by the occurrence of high terraces (over 15 m height) (Figs. 3.11b and 3.12a). Tsunami eroded the sandy beach and dune and formed a small "Tsunami Bay" landward side of the seawall (Fig. 3.12b). Inundation heights were 11.3 m above TP near the beach and slightly decreased landward (Fig. 3.13a) (TETJSG 2011). Run-up flow stopped at terrace cliff.

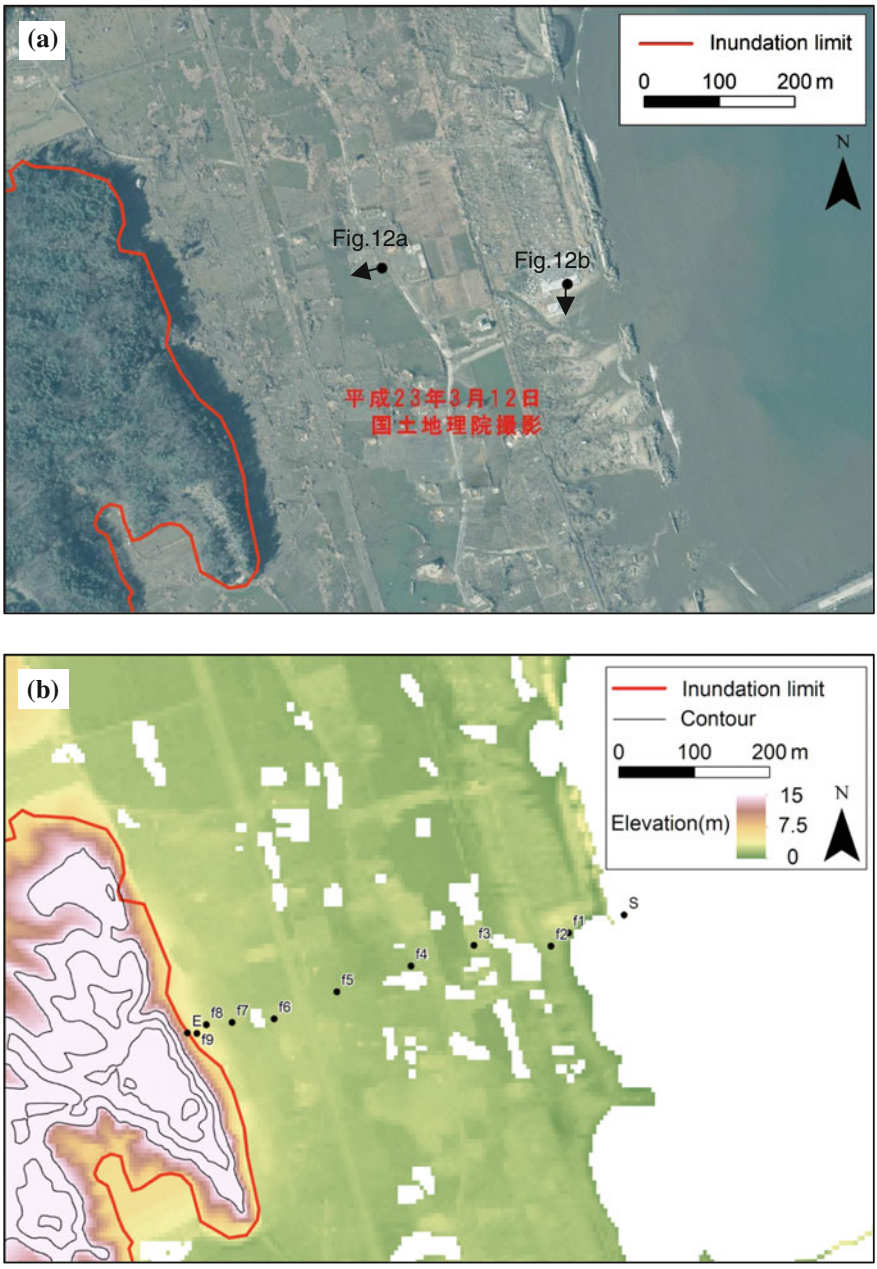

Fig. 3.11 **a** Aerial photograph (March, 2011) provided by GSI, inundation area, shooting location and direction of photograph in Fig. 3.12, **b** elevation map using 5 m mesh DEM, 5 m interval contour line (except for less than 10 m above TP), inundation area, and observation sites of the tsunami deposit in narrow strand plain at Yamamoto Town. The location is shown in Fig. 3.1

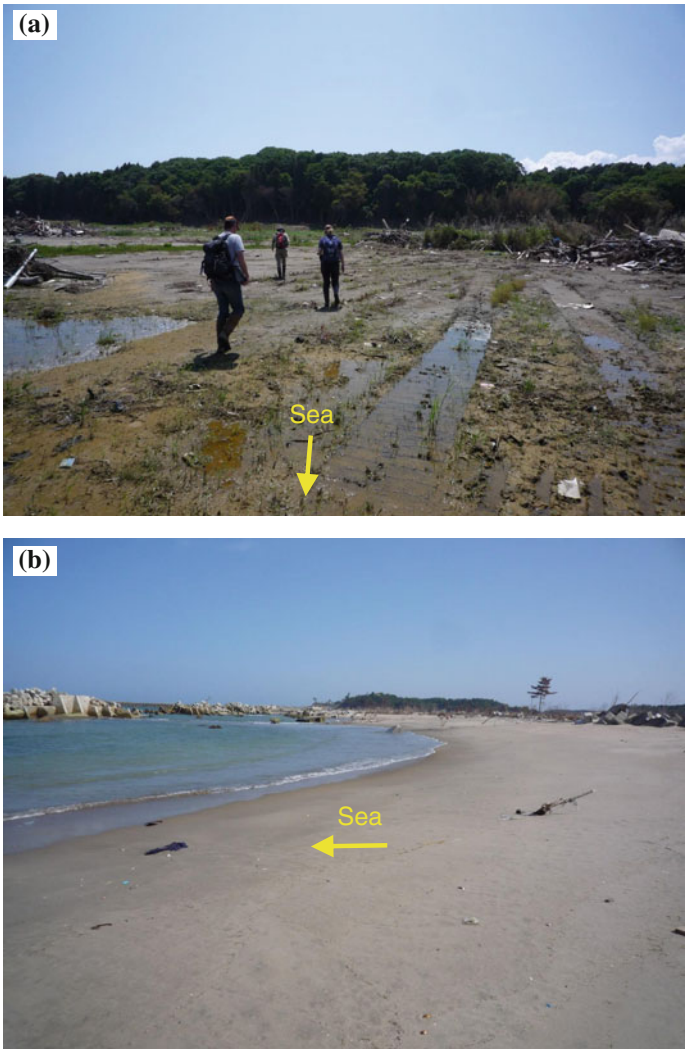

Fig. 3.12 Photographs of **a** lowland and terraces and **b** erosion in sand beach and dune in narrow strand plain at Yamamoto Town. Shooting locations and direction of photographs are shown in Fig. 3.11a

The tsunami deposit was described every 30–100 m at 9 sites (f1–f9) in Fig. 3.10b. Sand layer was composed of 4–12.5-cm-thick fine- to medium-grained sand (Figs. 3.13b and 3.14). Generally, sand thickness did not clearly thin landward. No sand was observed up to a distance of 0.25 km from the coastline, because erosion was dominant. Between 0.25 and 0.59 km inland from the shoreline, the deposit was mainly composed of 4–12.5-cm-thick, fine-to-medium sands overlain by thin mud (0.2–0.5 cm thick). Mud thickness was generally very thin than other areas. At the maximum extent of the tsunami deposits, the sand unit

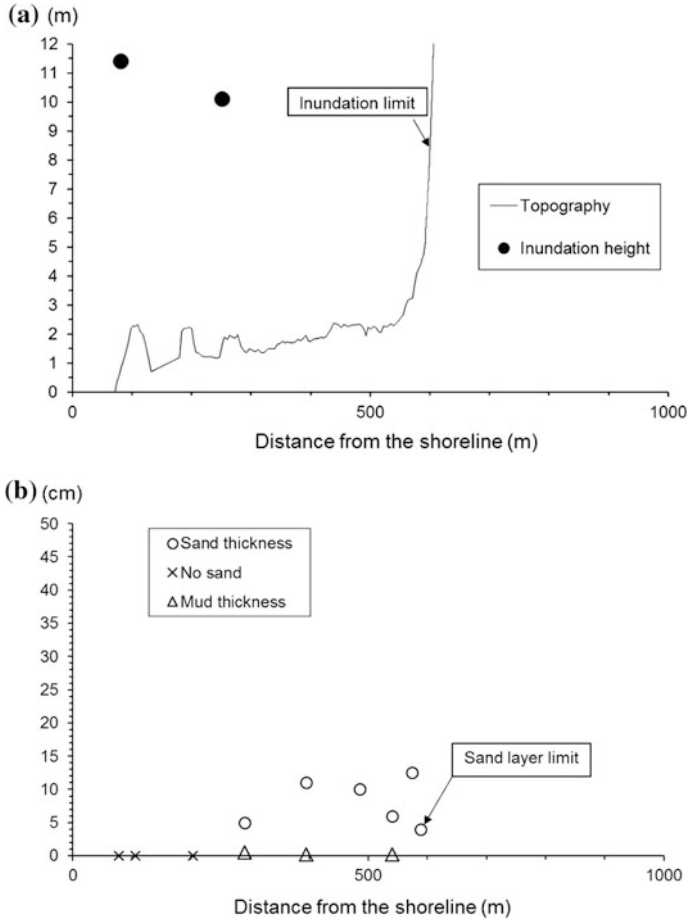

Fig. 3.13 **a** Elevation, inundation height above TP, and inundation limit, **b** sand and mud thickness in narrow strand plain at Yamamoto Town

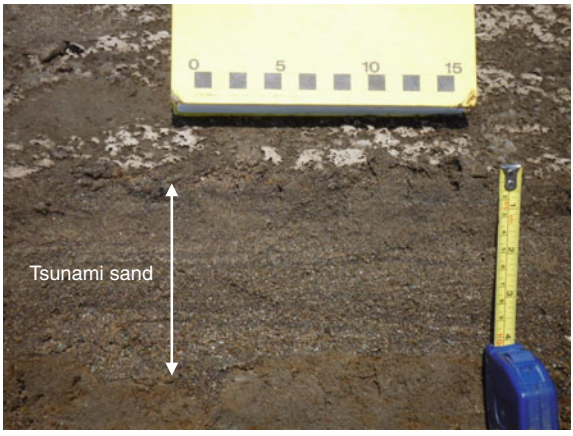

Fig. 3.14 10-cm-thick sand layer at 0.4 km from the shoreline (site f8 in Fig. 3.11b) in narrow strand plain at Yamamoto Town

had 4 cm in thickness. Sections of the tsunami deposit with a submillimeter and over 0.5-cm-thick sand layer were found up to approximately 0.59 km inland (98.2 % of the inundation distance).

3.4.4 Valley Plain

We surveyed a valley plain developed at Shinchi Town in northern part of the Fukushima Prefecture (Fig. 3.1). This valley plain is located on a coastal lowland, about 42 km south of Sendai City. The valley extends east–west direction (Fig. 3.15a) and is surrounded by hills with over 15–30 m height (Fig. 3.15b). The survey area covered (a) 0.04-km-wide sandy beach, (b) 6.2-m-high onshore seawall, (c) 3-m-high sand dune, (d) 0.16-km-wide coastal forest planted pine trees behind the beach, and (e) the rice paddy field that extends from 0.23 to 2.23 km from the coastline. The site was subsided locally with 0.31 m by the 2011 earthquake according to real-time observation of the GSI electronic reference point near this transect.

The tsunami inundated up to 2.23 km inland and 6.9 m above TP (Fig. 3.15b). Run-up flow would be forcibly stopped probably due to steep slope (Fig. 3.16a). Tsunami eroded sandy beach and dune and formed "Tsunami Bay" (Fig. 3.16b). Inundation height near the coast was approximately 8.5 m above TP and decreased landward (TETJSG 2011) (Fig. 3.17a). The average gradient between the inundation limit and the shoreline was 3.09 ‰.

The tsunami deposit was surveyed every 30–100 m at 32 sites (m1-m32) in Fig. 3.15b. The tsunami sand layer and mud layer were composed of 0.5–28-cm-thick fine-to-medium sand and 0.1–5.5-cm-thick silt, respectively (Figs. 3.17b and 3.18). Sand thickness generally thinned landward and fluctuated in associated with local duration. Mud thickness gradually became thicker inland. Erosion was dominant up to 0.2 km from the coastline (Fig. 3.17b). Between 0.2 and 0.45 km inland from the shoreline, sandy deposit was dominant and 5–28-cm-thick fine- to very coarse-grained sand layer was formed. Further inland (0.45–2.05 km), the tsunami deposit was sand-dominated and was composed of a 0.5–12-cm-thick fine-to-very coarse sand with a mud cap in 0.5–3 cm thickness. Sections of the tsunami deposit with submillimeter and over 0.5-cm-thick sand layers overlying mud layers were found up to approximately 2.05 km inland (92.0 % of the inundation distance).

3.4.5 Run-up Height and Onshore Slope

Inundation heights and run-up heights (Fig. 3.3) generally range from 0 to 40 m above TP in coastal areas from Aomori Prefecture to northern part of Ibaraki Prefecture (Figs. 3.1b and 3.1c). Both of them showed the highest values in middle

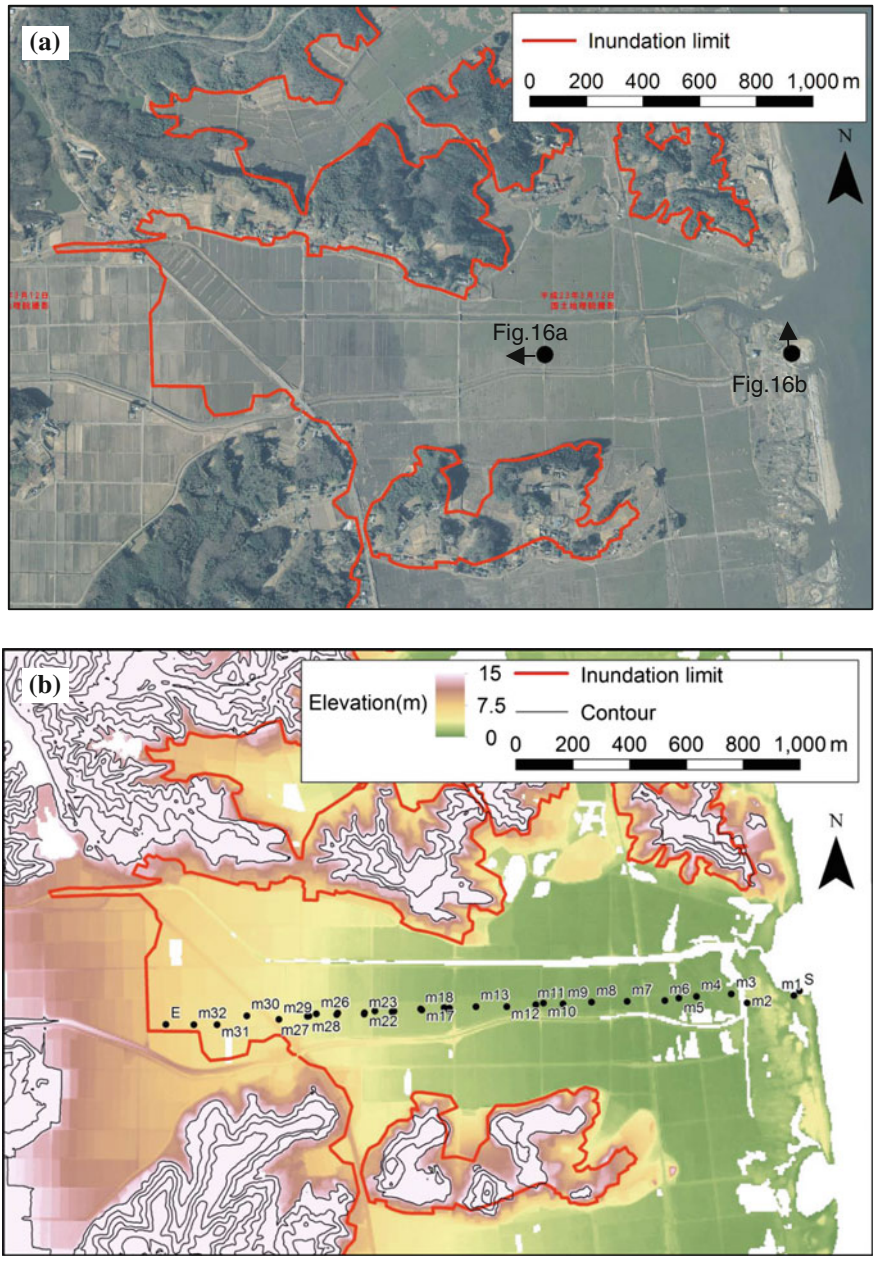

Fig. 3.15 **a** Aerial photograph (March, 2011) provided by GSI, inundation area, shooting location and direction of photograph in Fig. 3.16, **b** elevation map using 5 m mesh DEM, 5 m interval contour line (except for less than 10 m above TP), inundation area, and observation sites of the tsunami deposit in valley plain at Shinchi Town

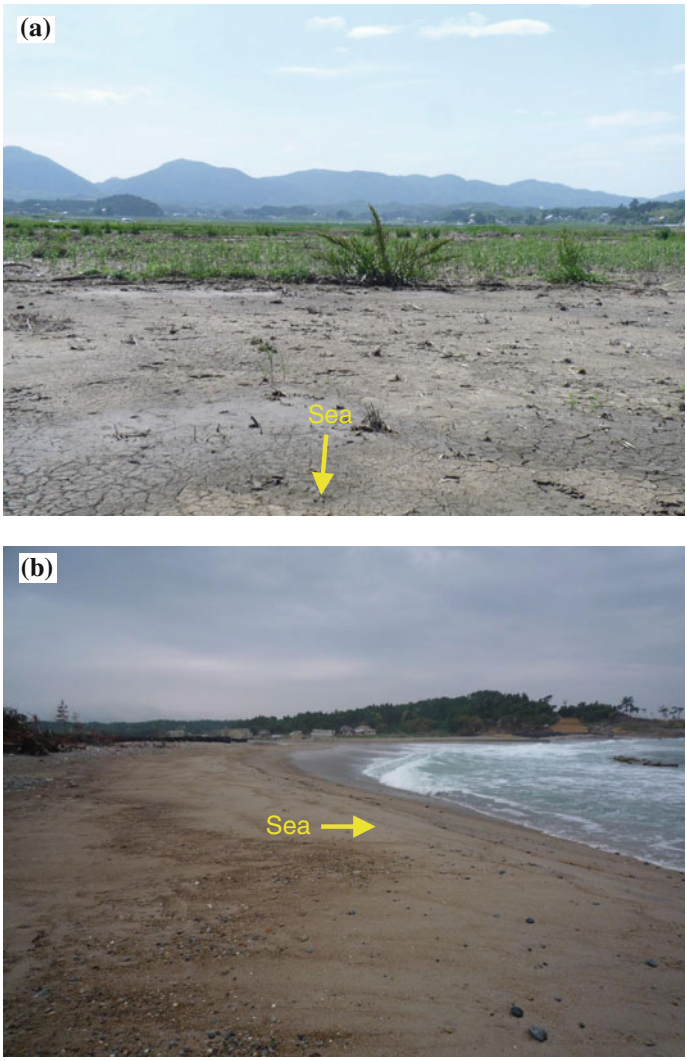

Fig. 3.16 Photographs of **a** erosion in sand beach and dune, **b** topography with steep longitudinal gradient in valley plain at Shinchi Town. Shooting locations and direction of photographs are shown in Fig. 3.15a

part of Sanriku Coast where indented coastlines characterized by rias are common. The values are mostly lower than 10 m above TP in Kamikita Plain and southern part of Iwaki Coast. Differences between inundation heights and run-up heights are not considerable at Kamikita Plain, Sanriku Coast, and Iwaki Coast. On the other hands, inundation heights are much higher than run-up heights in Sendai Plain.

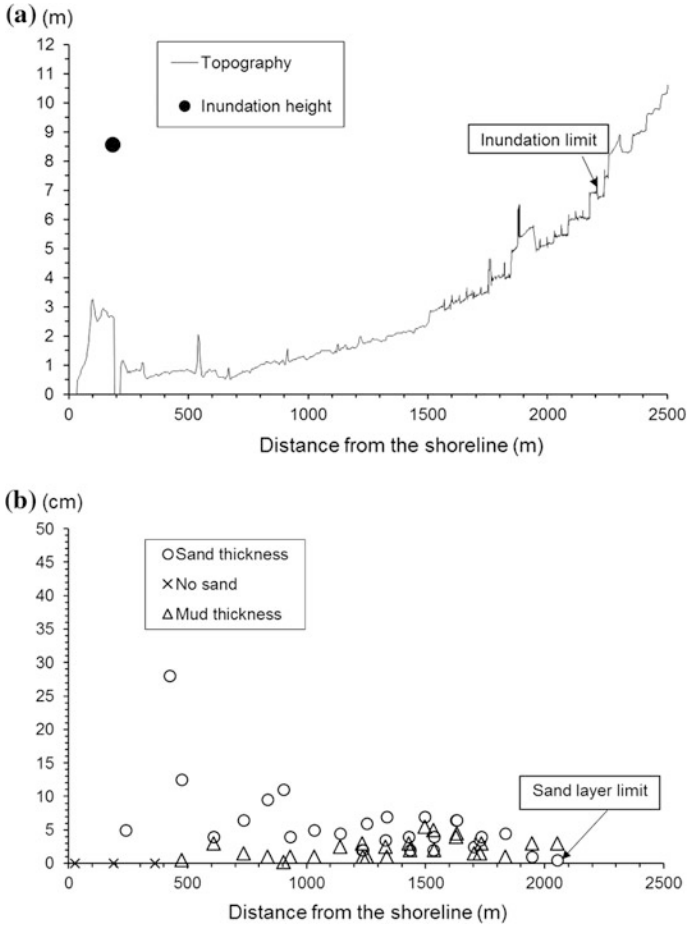

Fig. 3.17 **a** Elevation, inundation height above TP, and inundation limit, **b** sand and mud thickness in a valley plain at Shinchi Town

Maximum run-up height almost reached 40 m above TP (Fig. 3.19). The run-up height ranged from 6.8 to 39.4 m (TP) in RO type, from 5.7 to 30.1 m (TP) in RB type, and from 1.8 to 17.6 m (TP) in VO types (Table 3.1). The standard deviation of these coasts is large (3.6–7.8 m). In contrast, the heights are less than 3.3 m in VLO, SO, and SLO types. Furthermore, the standard deviation is also small (0.1–0.5 m).

Onshore slope from the shoreline to the tsunami run-up limit is less than 110 ‰. The slopes of RO, RB, and VO types are much larger than those of VLO, SO, and SLO types.

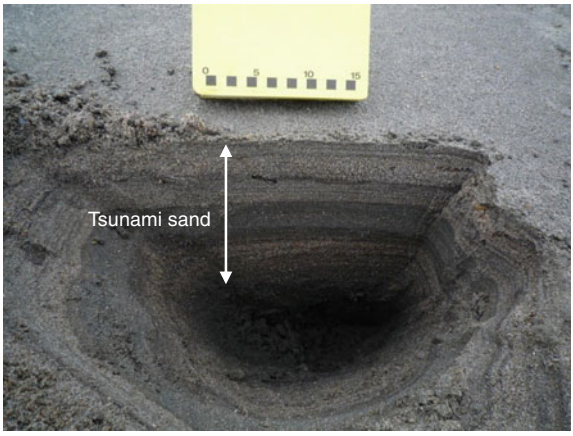

Fig. 3.18 28-cm-thick sand layer at 0.4 km from the shoreline (site m5 in Fig. 3.15b) in a valley plain at Shinchi Town

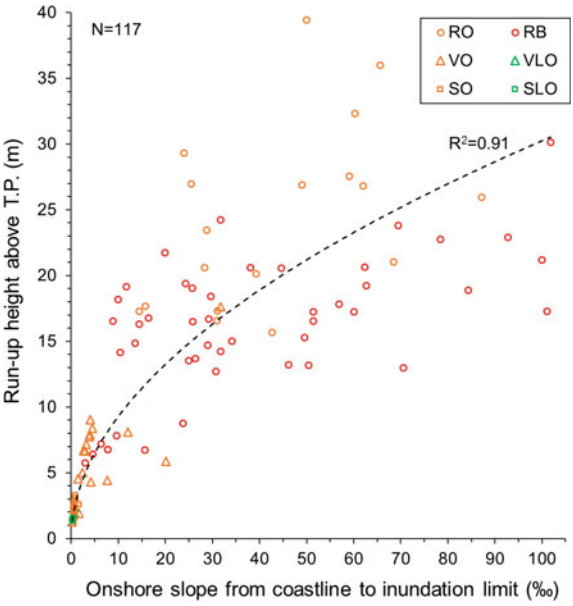

Fig. 3.19 Relationship between run-up height above TP and onshore slope from the coastline to inundation limit. Landforms are illustrated schematically in Fig. 3.2. The locations of the sampling points are shown in Fig. 3.4. Data are summarized in Table 3.1

Run-up heights roughly increase with onshore slope (Fig. 3.19). The coefficient of correlation value (R^2) between them is 0.76 using power function. Both of the onshore slope and run-up heights in RO and RB types were much larger than those in VLO, SO, and SLO types. Onshore slope and run-up heights significantly varied in VO type. Differences of onshore slope and run-up heights between rias on open sea (RO) and rias facing bay (RB) were unclear.

Table 3.1 Run-up height and onshore slope in various types of coastal landforms

		RO	RB	VO	VLO	SO	SLO
Number of data		19	46	16	3	29	4
Run-up height (m)	Max	39.4	30.1	17.6	2.4	3.3	1.6
	Min	6.8	5.7	1.8	2.0	1.1	1.3
	Ave	23.6	16.2	6.7	2.2	2.1	1.4
	SD	7.8	5.2	3.6	0.2	0.5	0.1
Slope (‰)	Max	87.2	101.8	31.7	0.7	1.6	0.4
	Min	7.8	2.9	0.5	0.6	0.2	0.3
	Ave	41.6	38.9	6.7	0.7	0.6	0.3
	SD	21.4	28.1	8.3	0.1	0.3	0.1

3.5 Discussion

3.5.1 Tsunami Deposit

Tsunami sand widely deposited and reached hundreds of meters to a few kilometers inland in wide strand plain, narrow strand plain, and valley plain. Tsunami deposits were not clear, and erosional landforms due to backwash were common in a very minor, steep narrow valley plain along the ria coasts. However, Naruse et al. (2012) reported the formation of thick, sandy tsunami deposits at Rikuzentakata City where bay-head delta occurs at the head of rias (Fig. 3.1). A wave-dominated spit formed by the reworking of sediment supplied from the Kesen River extends along the coasts. Thus, beach sand was one of the major sources of the tsunami deposits.

Limited sand supply from beach and sand dune decreases sand deposition area (Nakamura et al. 2012). Grain size of beach and dune sand also controls the sand deposition area. Coastline is covered with fine- to medium-grained sand building beach and dune at the three transects, and sand erosion in beach and dune was observed.

The onshore tsunami deposit was mainly sourced from land (beach, sand dune, and paddy soil) around Sendai Plain. Numerical modeling of sediment transport on the Sendai Plain (Sugawara et al. 2014) suggested that bathymetry especially steep bathymetric profile of the shoreface limited erosion in seafloor. The slope in Sendai Bay is 1/50 to 1/100 from the shoreline to 5 m depth, 1/100 to 1/200 between 5 and 15 m depth, and less than 2/1000 deeper than 15 m depth (Udo et al. 2013). In contrast, Naruse et al. (2012) showed that tsunami deposits were transported from the seafloor of Hirota Bay or more pelagic region as well as beach in Rikuzentakata based on paleontological analysis and estimation of the total volume of the tsunami deposits. Offshore seafloor slope is almost constant, approximately 7/1000, from the shoreline to 80 m depth in Hirota Bay (Shimamura 2011). Furthermore, width of the bay mouth of Hirota Bay, ca. 6 km, characterized by ria coast is much narrower than that of Sendai Bay, ca. 77 km. The difference of bathymetry in these bays possibly influences the location of source area of the tsunami deposits.

We found landward-thinning trend of the sand thickness in wide strand plain and valley plain. Landward thinning of the sand is a typical feature for the tsunami deposit (Goff et al. 2012). It may relate to landward decrease in sediment supply and flow velocity and depth. However, this feature was not clear in narrow strand plain. It is possible that high flow velocity and depth and a large amount of sediment supply maintained near the inundation limit and run-up were forcibly stopped by high terraces in narrow strand plain. Distribution pattern of tsunami deposit was critically dependent on landform types.

Tsunami mud deposition in broad area is distinctive feature of the tsunami in Sendai coastal plain. Diatom assemblage showed that mud is originated from paddy soil in Sendai coastal plain (Szczuciński et al. 2012). As Sendai coastal plain is known for one of the largest cultivation area of rice, rice paddy field covered a considerable area of the lowland. Mud thickness slightly became thicker landward in wide strand plain and valley plain. It probably results from increase in rice paddy area eroded by tsunami with progression of inundation.

Sand thickness largely varied in a zone up to 1.0–1.5 km inland. The thickness of tsunami sand was likely to be sensitive to the local undulation of topography (Nishimura and Miyaji 1995). Yamada and Fujino (2013) pointed out that the thicknesses of the tsunami deposits near the shore were more variable than the deposits left inland, and it may have resulted from complex tsunami behavior due to the existence of protection forest and other artificial structures around the shore. Therefore, micro-topography may have affected thickness variation.

3.5.2 Run-up Height and Onshore Topography

Run-up heights varied significantly in this area (Figs. 3.1b and 3.19). Maximum wave heights offshore in 137–204 m depth from Sanriku Coast to northern Iwaki Coast were higher than those of Kamikita Plain and southern Iwaki Coast based on GPS buoys (Japan Meteorological Agency 2013; Kawai et al. 2013). Differences of the maximum wave heights were not clear between Sanriku Coast and northern Iwaki Coast. Therefore, variety of run-up heights observed at the study area (Fig. 3.19) might relate to the shape of local and regional onshore topography.

Our analysis showed that onshore slope from coastline to inundation limit was positively correlated with run-up height in general (Fig. 3.19). However, the relationship between run-up height and onshore slope was quite variable in RO, RB, and VO types rather than the other three types. For example, the run-up heights in valley plains with narrow valley floor and steep valley wall were higher than valley plains with wide valley floor and gentle valley wall. It is possible that the shape of valley also controls the run-up height in RO, RB, and VO types. On the other hand, run-up height is less than 3.3 m and a positive correlation between run-up height and onshore slope is unclear in SO, SLO, and VLO types, most of which face the Sendai Bay.

3.6 Conclusions

We showed the differences of distribution pattern of the tsunami deposit and run-up height in various types of coastal landform, such as rias, strand plain, and valley plain. Our main results were summarized below.

(1) Distribution pattern of tsunami deposit was critically dependent on landform types when large amount of sediment was supplied from the coasts.
(2) Balance between deposition and erosion might depend on onshore slope in coastal areas.
(3) Micro-topography may locally control thickness variation of the tsunami deposit.
(4) Run-up height generally relates to onshore slope from coastline to tsunami inundation limit, though morphology of the inundated lowlands such as valley floor and valley wall also influences run-up height.

It is necessary to consider the effect of seafloor bathymetry on run-up height in the future. In addition, relationship between onshore tsunami behavior and topography should be further discussed by combining field observation, numerical simulation, and flume experiment.

Acknowledgment This study is financially supported by a research grant from Tohoku University for an emergency field survey following the 2011 Tohoku-oki tsunami and JSPS KAKENHI Grant Numbers 22241042, 24240114. We would like to acknowledge Dr. Masatomo Umitsu, Dr. Kazuhisa Goto, Dr. Daisuke Sugawara for their support during the field survey.

References

Abe T, Goto K, Sugawara D (2012) Relationship between the maximum extent of tsunami sand and the inundation limit of the 2011 Tohoku-oki tsunami on the Sendai Plain, Japan. Sed Geol 282:142–150

Chida N, Matsumoto H, Obara S (1984) Recent alluvial deposit and Holocene sea-level change on Rikuzentakata coastal plain, northeast Japan. Ann Tohoku Geogr Assoc 36(4):232–239 (in Japanese with English abstract)

Goff J, Chagué-Goff C, Nichol S, Jaffe B, Dominey-Howes D (2012) Progress in palaeotsunami research. Sed Geol 243–244:70–88

Goto K, Chagué-Goff C, Fujino S, Goff J, Jaffe B, Nishimura Y, Richmond B, Sugawara D, Szczuciński W, Tappin DR, Witter RC, Yulianto E (2011) New insights of tsunami hazard from the 2011 Tohoku-oki event. Mar Geol 290:46–50

Goto K, Sugawara D, Abe T, Haraguchi T, Fujino S (2012) Liquefaction as an important source of the A.D. 2011 Tohoku-oki tsunami deposits at Sendai Plain, Japan. Geology 40:887–890

Hayakawa YS, Oguchi T, Saito H, Kobayashi A, Baker RV, Pelletier DJ, McGuire L, Komatsu G, Goto K (2015) Geomorphic imprints of repeated tsunami waves in a coastal valley in northeastern Japan. Geomorphology 242:3–10

Ito A (1999) Holocene geomorphic development of the Kitakami River lowland, northeastern Japan. Kikan Chirigaku 51(1):1–18 (in Japanese with English abstract)

Jaffe BE, Gelfenbaum G (2002) Using tsunami deposits to improve assessment of tsunami risk. In: Solutions to coastal disasters '02, ASCE, pp 836–847

Kawaguchi K, Inomata T, Seki K, Fujiki T (2015) Annual report on nationwide ocean wave information network for ports and harbors (NOWPHAS 2013). Technical Note of the Port and Airport Research Institute, No. 1305

Kawai H, Satoh M, Kawaguchi K, Seki K (2013) Characteristics of the 2011 Tohoku tsunami waveform acquired around Japan by NOWPHAS equipment. Coast Eng J 55:1350008

Koike K, Tamura T, Chinzei K, Miyagi T (eds) (2005) Regional geomorphology of the Japanese Islands, vol. 3 geomorphology of Tohoku region. University of Tokyo Press, Tokyo

Komatsu G, Goto K, Baker VR, Oguchi T, Hayakawa YS, Saito H, Pelletier JD, McGuire L, Iijima Y, (2014) Effects of tsunami wave erosion on natural landscapes: examples from the 2011 Tohoku-oki Tsunami. In: Kontar Y, Santiago-Fandino V, Takahashi T (eds) Tsunami events and lessons learned: ecological and societal significance. Advances in natural and technological hazards research, vol 35. Springer, Berlin, pp 243–253

Koshimura S, Mofjeld HO, González FI, Moore AL (2002) Modeling the 1100 bp paleo tsunami in Puget Sound, Washington. Geophys Res Lett 29(20):1948

MacInnes BT, Bourgeois J, Pinegina TK, Kravchunovskaya EA (2009) Tsunami geomorphology: Erosion and deposition from the 15 November 2006 Kuril Island tsunami. Geology 37:995–998

Matsumoto H (1981a) Sea-level changes during the Holocene and geomorphic developments of the Sendai coastal plain, northeast Japan. Geogr Rev Japan 54(2):72–85 (in Japanese with English abstract)

Matsumoto H (1981b) Developmental process of alluvial plain related to the Holocene sea-level change. Sci Rep Tohoku Univ 7th Ser Geogr 31:151–171

Matsumoto H (1984) Beach ridge ranges on Holocene coastal plains in northeast Japan. Geogr Rev Japan, Ser A 57(10):720–738 (in Japanese with English abstract)

Miura O (1966) Coastal terraces and rias along the Kesennuma Bay, Miyagi Prefecture. Ann Tohoku Geogr Assoc 18(3):116–122 (in Japanese with English abstract)

Miura O (1968) Rias coast and coastal terraces of Sanriku, northeastern Japan. Geogr Rev Japan 41(12):732–747 (in Japanese with English abstract)

Miyauchi T (1987) Quaternary tectonic movements of the Kamikita Coastal Plain, Northeast Japan. Geogr Rev Japan, Ser. B 60(1):1–19

Miyauchi T (2001) Kamikita Plain. In: Koike K, Machida H (eds) Atlas of Quaternary marine terraces in the Japanese Islands. University of Tokyo Press, Tokyo, pp 27–29 (in Japanese)

Nakamura Y, Nishimura Y, Putra PS (2012) Local variation of inundation, sedimentary characteristics, and mineral assemblages of the 2011 Tohoku-oki tsunami on the Misawa coast, Aomori, Japan. Sed Geol 282:216–227

Nanayama F, Satake K, Furukawa R, Shimokawa K, Atwater BF, Shigeno K, Yamaki S (2003) Unusually large earthquakes inferred from tsunami deposits along the Kuril trench. Nature 424:660–663

Naruse H, Arai K, Matsumoto D, Takahashi H, Yamashita S, Tanaka G, Murayama M (2012) Sedimentary features observed in the tsunami deposits at Rikuzentakata City. Sed Geol 282:199–215

National Astronomical Observatory of Japan (ed) (2013) Chronological scientific tables 2014. Maruzen, Tokyo

Nishimura Y, Miyaji N (1995) Tsunami deposits from the 1993 Southwest Hokkaido earthquake and the 1640 Hokkaido Komagatake eruption, northern Japan. Pure and Applied Geophysics 144:719–733

Richmond BM, Szczuciński W, Chagué-Goff C, Goto K, Sugawara D, Witter R, Tappin DR, Jaffe BE, Fujino S, Nishimura Y, Goff J (2012) Erosion, deposition and landscape change on the Sendai coastal plain, Japan, resulting from the March 11, 2011 Tohoku-oki tsunami. Sed Geol 282:27–39

Shimamura K (2011) The relationship between the topographic features of bay and the tsunami-height-topographic study on the tsunami-height in the 2011 off the Pacific coast of

Tohoku earthquake of bay and the tsunami-height. Bull School Ind Eng Tokai Univ 4:1–8 (in Japanese with English abstract)
Shishikura M, Fujiwara O, Sawai Y, Namegaya Y, Tanigawa K (2012) Inland-limit of the tsunami deposit associated with the 2011 off-Tohoku earthquake in the Sendai and Ishinomaki Plains, Northeastern Japan. Ann Rep Active Fault Paleo Earthq Res 12:45–61 (in Japanese with English abstract)
Sugawara D, Takahashi T, Imamura F (2014) Sediment transport due to the 2011 Tohoku-oki tsunami at Sendai: results from numerical modeling. Mar Geol 358:18–37
Suzuki T (1989) Late Quaternary crustal movements deduced from marine terraces and active faults, Joban coastal region, northeast Japan. Geogr Rep Tokyo Metrop Univ 24:31–42
Szczuciński W, Kokociński M, Rzeszewski M, Chagué-Goff C, Cachão M, Goto K, Sugawara D (2012) Sediment sources and sedimentation processes of 2011 Tohoku-oki tsunami deposits on the Sendai plain, Japan-Insights from diatoms, nannoliths and grain size distribution. Sed Geol 282:40–56
Takashimizu Y, Urabe A, Suzuki K, Sato Y (2012) Deposition by the 2011 Tohoku-oki tsunami on coastal lowland controlled by beach ridges near Sendai, Japan. Sed Geol 282:124–141
Tamura T, Masuda F (2005) Bed thickness characteristics of inner-shelf storm deposits associated with a transgressive to regressive Holocene wave-dominated shelf, Sendai coastal plain, Japan. Sedimentology 52:1375–1395
The 2011 Tohoku Earthquake Tsunami Joint Survey Group (2011) The 2011 off the Pacific coast of Tohoku earthquake tsunami information. http://www.coastal.jp/ttjt/
The Japan Meteorological Agency (2013) The report on the 2011 off the Pacific coast of Tohoku Earthquake. Technical report of the Japan Meteorological Agency 133
Udo K, Tanaka H, Mano A, Takeda Y (2013) Beach morphology change of southern Sendai coast due to 2011 Tohoku earthquake Tsunami. J JSCE, Ser B2 (Coastal Engineering) 69:1391–1395 (in Japanese with English abstract)
Yagi H, Suzuki T (2001) Sanriku-nanbu to Joban. In: Koike K, Machida H (eds) Atlas of Quaternary marine terraces in the Japanese Islands. University of Tokyo Press, Tokyo, pp 29–32 (in Japanese)
Yamada M, Fujino S (2013) Sedimentary characteristics of the onshore tsunami deposits formed by the 2011 Tohoku-oki tsunami in coastal lowlands, Ibaraki and Chiba prefectures. J Sedimentol Soc Japan 72(1):13–25 (in Japanese with English abstract)
Yonekura N (1966) Geomorphic development of northern Rikuchu coastal region, north-eastern Japan. Geogr Rev Japan 39(5):311–323 (in Japanese with English abstract)
Yoshikawa T (1964) On the geomorphic development of Ria coasts in the Japanese Islands. Quat Res (Daiyonki-kenkyu) 3:290–296 (in Japanese with English abstract)
Yoshikawa T (1997) Continental shelf. Kokon Shoin, Tokyo (in Japanese)

Chapter 4
Relationships Between Coastal and Fluvial Geomorphology and Inundation Processes of the Tsunami Flow Caused by the 2011 off the Pacific Coast of Tohoku Earthquake

Hiroshi Shimazu

Abstract Spatial characteristics of tsunami flow caused by the 2011 off the Pacific coast of Tohoku Earthquake were described focusing the relationships between tsunami inundation processes and coastal and fluvial geomorphology in the northern and middle coast of the Tohoku district. Different tsunami inundation processes were recognized in the four types of areas having different geomorphological characteristics, the Miyako City area in the valley bottom plain of the Hei River, Otsuchi area of small coastal lowland with small rivers, the Aneyoshi area of a tiny cove with a small and steep slope stream, and the Natori River, and surroundings in the Sendai Plain largest plain in Tohoku district. The megatsunami got over the seawalls to inundate coastal lowlands and valley bottom plain, and it also ascended banked rivers. The tsunami flow ascending the banked river reached upstream area faster than the inundated flow in the habitation side of the floodplain. The tsunami flow in the river got over the river embankments to flood the habitation side. In the coastal area, the deep tsunami flow directly inundated landward is less affected by geomorphological characteristics and it caused geomorphological processes by erosion and sedimentation on land. The tsunami flow ascending the steep slope and small valley reached high elevation area whose elevation was double of the tsunami height in the coast. In the coastal and valley bottom plains, depth of the tsunami flow got shallower landward. In the landward area, the extent of the shallower tsunami flow was strongly affected not only by geomorphological characteristics but also by artificial constructions. In the area near the landward limit of tsunami inundation, micro-landforms, such as former river courses, affected tsunami inundation processes and spatial characteristics of the tsunami flow.

H. Shimazu (✉)
Department of Geography Faculty of Geo-Environmental Science,
Rissho University, Tokyo, Japan
e-mail: shimazu@ris.ac.jp

S. Haruyama and T. Sugai (eds.), *Natural Disaster and Coastal Geomorphology*, DOI 10.1007/978-3-319-33814-9_4

Keywords Tsunami inundation process · Coastal geomorphology · Fluvial geomorphology · Banked river · The 2011 off the Pacific coast of Tohoku Earthquake

4.1 Introduction

The megatsunami disaster was caused by the 2011 off the Pacific coast of Tohoku Earthquake. The megatsunami reached the coast of the Pacific side of eastern Japan and flooded ashore in broad areas (Fig. 4.1). Although high and strong seawalls were constructed on the coasts of the northern Tohoku district based on the experiences of the former megatsunami disasters which occurred in recent 120 years, the 2011 megatsunami destroyed and/or flowed over many seawalls and flooded lowlands widely.

The northern Pacific coast of the Tohoku district has rias characteristics. The mountains and hills face the Pacific Ocean and tiny coves, and small bays with small alluvial lowlands and valleys are formed along the coast. The alluvial lowlands and the small valleys have wide varieties of geomorphological characteristics, such as extent and shape of lowlands, and width and slope of the valleys. The elevation and distance from the coast of an extent of the tsunami flood area and degree of damages were affected by not only the height of attacked tsunami but also geomorphological characteristics. The 2004 tsunami disaster occurred in Banda Aceh, Indonesia, the micro-landforms affected on distribution and spatial characteristics of the tsunami flow and deposits (Umitsu et al. 2006) and the spatial differentiation in local damages (Umitsu and Takahashi 2007). Inundation processes of the flooded megatsunami were strongly affected by geomorphological characteristics of coastal lowlands and valley floors.

The tsunami also ascended river channels. Because high embankments were constructed in the lower reaches of the most Japanese rivers, the tsunami flood showed different inundation processes between the habitation side and the riverside of the embankments. The tsunami ascending along the river also damaged some areas several kilometers from the coast.

This chapter describes spatial characteristics of tsunami flow of the 2011 tsunami disaster event focusing the relationships between tsunami inundation processes and coastal and fluvial geomorphology in the northern and middle coast of the Tohoku district where more than 10 m high tsunami attacked. Four areas having different geomorphological characteristics were selected to discuss the relationships (Fig. 4.1). First three areas are located in the rias area. The first area is a city located at the river mouth. The tsunami inundated the city center on a valley floor. The second area is a town on small lowland with small rivers. In these areas, embanked rivers played important roles in a flood process and disaster. The third area is characterized by a tiny cove connecting a small and steep slope stream. This geomorphological characteristics cause the higher flood height. The last area is the

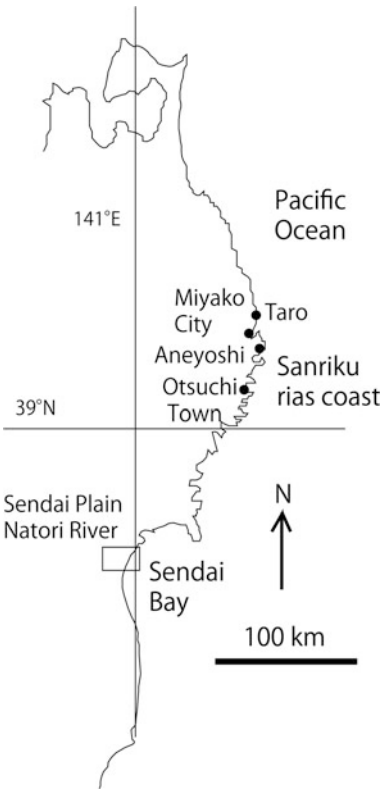

Fig. 4.1 The coast of the tsunami affected area in Tohoku district and study areas

alluvial plain which is the largest plain in the tsunami disaster area. Geomorphological effects on the tsunami flow, which ascended a gentle slope-wide embanked river, were recognized in this area.

4.2 MegaTsunami Characteristics in the Northern and Middle Coast of the Tohoku District

The earthquake occurred at 14:46 on March 11, 2011. The first wave of the tsunami reached the coast of this area in 30 min after the earthquake. Observed maximum height of the tsunami in this area was more than 8.6 m (Japan Meteorological Agency 2011). The flood height of the tsunami near the coastline was highest in the northern and middle coast of the Tohoku district. Maximum flood height was more than 25 m (Haraguchi and Iwamatsu 2013).

This area experienced tsunami disasters three times in recent 120 years, which were occurred in 1896 and 1933 whose epicenter was off this coast, and the tsunami in 1960 was caused by earthquake in Chile. Seawalls were constructed along the

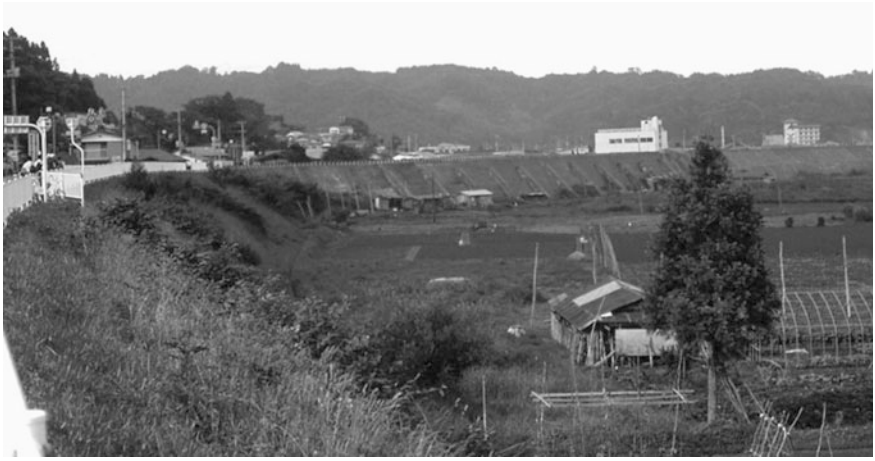

Fig. 4.2 The mega seawalls constructed along the coast of the Taro town before the 2011 tsunami event

coast of many bays of this area as they would prevent the next similar tsunami disaster. Because this tsunami exceeded the height of the seawalls and/or destroyed the seawalls, the tsunami flooded most coastal lowland.

A small town, Taro, Iwate prefecture (Fig. 4.1), was protected by the biggest seawalls in Japan whose height was over 10 m in elevation (Fig. 4.2). Because the tsunami got over one of the seawalls and destroyed the other seawalls (Fig. 4.3), the

Fig. 4.3 The destroyed mega seawalls of Taro. The upper right seawall was totally washed out. The lower left seawall was quite strong, so that this survived the tsunami overflow

town became under water 8–10 m deep. Most houses in lowland were washed out (Association Japanese Geographers (AJG) 2011). Because the inhabitants of this town had too much confidence in the seawalls, many people failed to get out from the flooded area in time and lost 140 people's lives (Tani 2012).

Tsunami inundation processes on the land in the four types of different geomorphological characteristic areas discussed in the following sections are the Miyako City area in the valley of the Hei River, the largest river in this area, the Otsuchi area of small coastal lowland with small rivers, the Aneyoshi area of a tiny cove with a small and steep slope stream in the northern coast of Tohoku district and the Natori River, and surroundings in the Sendai Plain, the largest coastal alluvial plain in the Pacific coast of Tohoku district (Fig. 4.1).

The height and inundation processes of the tsunami are strongly affected by a tide and river regime. There had little rain in 10 days before the tsunami event in this area. The low tide was recorded about 2 h before the tsunami first attack. Therefore, the water level of every river in this area was low at that time.

4.3 Geomorphological Effects of Tsunami Inundation Processes in Coastal Lowlands and Valleys

4.3.1 Coastal Valley Bottom Plain and Moderate Slope River

The Hei River is a mountain river of 86 km long and a gravel bed river. Gravel sediments are transported to the river mouth (Shimazu 1990, 1996). This river flows into the Miyako Bay, a part of Sanriku rias coast. The Miyako City is located in the valley bottom plain of the Hei River (Fig. 4.4). The valley bottom plain is about 1 km wide between hillside slopes. The bay is open to the north. The direction of the Hei River is west–east, which is a right angel to the direction of the bay.

The first sea level change after the earthquake occurred at the coast of the Miyako City at 15:01 (JST) (Japan Meteorological Agency 2011). The maximum depth of the tsunami flood along the coast was about 9 m (Haraguchi and Iwamatsu 2013). The inundation processes were recorded by a video camera by a city official from the fifth floor of the city hall, located 1 km from the river mouth (Iwafune 2012). Based on the movie, after the first wave of the tsunami went up to southward, the water level of the Hei River began to rise gradually. After that, a small wave began to ascend the Hei River against the river flow. The velocity of the first wave head was relatively slow, about 3 m/s, from the analysis of the movie. The water level of the bay and the river continued to rise next 15 min. Because of the moderate river channel slope, major floodwater ascended the Hei River rapidly, so that the water level quickly rose. When the water level exceeded the seawall of the coast, the tsunami began to flood the coastal area. This inundation occurred 6 min after the tsunami front in the river passed upward in front of the city hall.

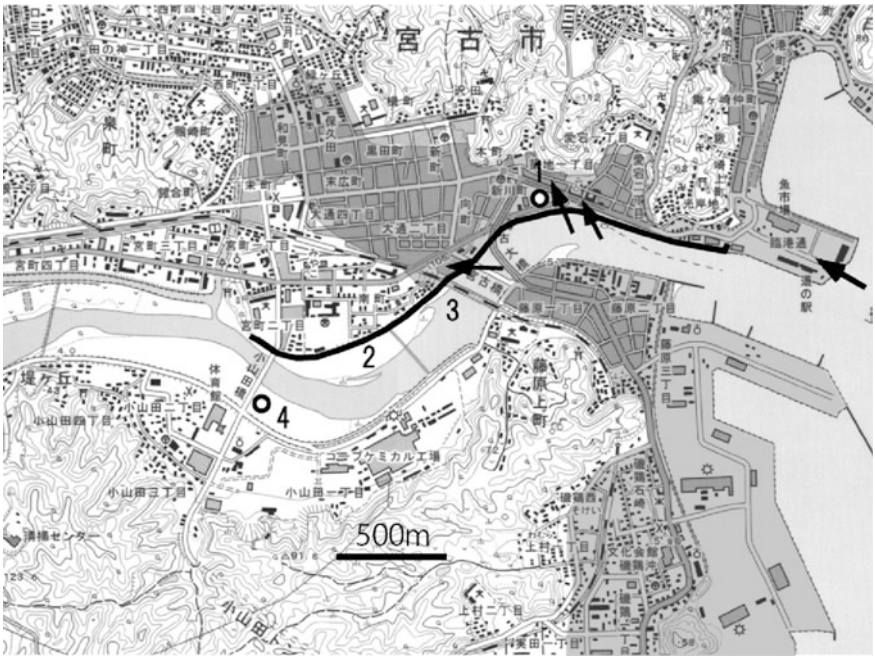

Fig. 4.4 The Miyako City and the tsunami inundation area. *Shaded areas* show the tsunami inundation area in the habitation side of the valley bottom plain and coastal lowland modified after Haragichi and Iwamatsu (2013). *Arrows* show the tsunami overflow points. *1* City hall, *2*embankment of the left bank, *3* railway bridge, *4* bended steel fence. *Base map* Geospatial Information Service of Japan (GSI) 1:25,000 Topographic map

The concrete embankment of about 3.5 m high had been constructed along the lowest course of the Hei River (Fig. 4.5). The water level in the embanked river reached the top of the embankment of the left side beside the city hall 3 min after beginning of the inundation in the coastal area. Before the floodwater from the coastal area reached the city hall, the water began to overflow into the city hall area. In 5 min, the depth of the flood got to 3.7 m, which was same as the level of the river water (Fig. 4.5). The floodwater extended upstream joining the water from the coastal area and overbank flow from the river. Many houses and cars floated upward. The movie recorded this situation from the city hall (Iwafune 2012). The tsunami floodwater ascended not the habitation side of the floodplain but the river. Because the high elevated river embankment hid the high water level caused by the tsunami, residents could not recognize the tsunami flood. Getting over the embankment the tsunami floodwater caused sudden increase of the flood depth in the habitation side. As a result, many people failed to be evacuate. 32 people of 416 residents died in this area.

The tsunami inundation area extended upward to 2.5 km from the river mouth where it was 4 m in elevation (AJG 2011, Fig. 4.2). The spatial characteristic of tsunami flow was affected not only by landform but also by artificial constructions.

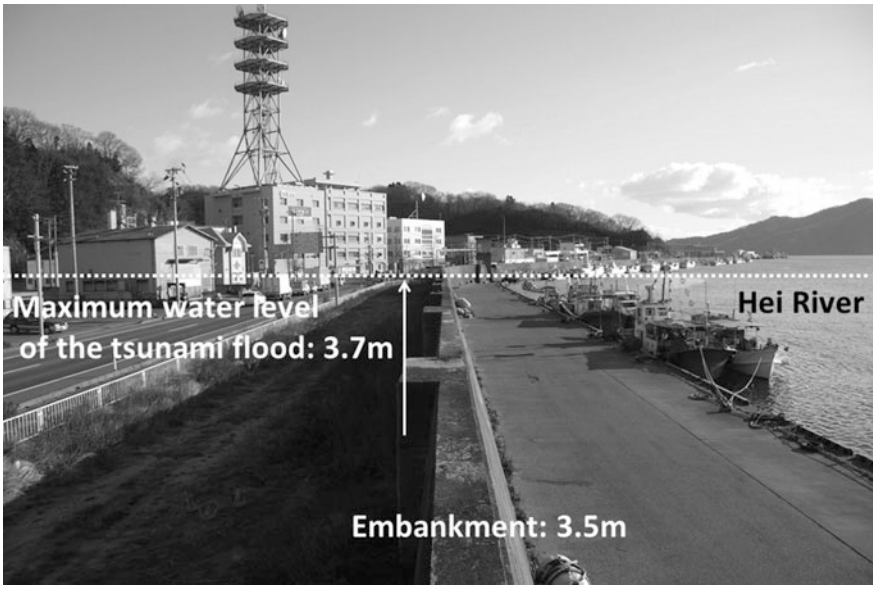

Fig. 4.5 A concrete embankment along the lower Hei River beside the city hall in the Miyako City and the maximum water level of the tsunami flood

A causeway of a railway playing the role of embankments restricted the extent of the tsunami inundation area.

A railway bridge which was washed out by the tsunami flood flow was just upstream of the overflow point (Fig. 4.6). The bridge dammed up the tsunami flow ascending the river piling up debris of transported broken houses, ships, and so on from the downstream. Because the height of the embankment of the upper side of the railway bridge was several tens of centimeters higher than that of the lower side and the water level in the upper section was lowered by the dam-up effect of the railway bridge, the upper city area could be free from the tsunami inundation.

The distribution of the tsunami flow was different between the river channel side of the embankment and the habitation side. Although the tsunami floodwater in the riverside of the embankments reached inland, more than 5 km from the river mouth and more than 5 m in elevation, the inundation area in the habitation side was restrictive. At 2.5 km from the mouth, the steel fence on the playground on the river side floodplain was bended upward by very strong power (Fig. 4.7).

The tsunami ran up to not only valley bottom plain but also embanked river course. The tsunami flow which rapidly ascended the embanked river course and which got over the embankment increased damages on the habitation side of the valley bottom plain. Extent of the inundation area was affected by artificial constructions in the valley bottom plain. Koarai et al. (2015) mentioned smaller artificial constructions affected by the margin of the distribution of the tsunami flow in

Fig. 4.6 The washed-out railway bridge crossing the Hei River in the Miyako City

Fig. 4.7 Bended steel fence in the river side floodplain

the 2011 tsunami disaster in the Sendai Plain and Ishinomaki Plain. To evaluate the risk of tsunami disaster estimating a tsunami overflow from a river and distribution of artificial constructions is very important.

4.3.2 Small Coastal Lowland with Small Rivers

Otsuchi town is located in the small coastal lowland formed at the confluence of two small rivers, the Otsuchi River and Kozuchi River (Fig. 4.8). The lowland extends 1 km along the coast and 1.5 km landward. The elevation of the lowland is lower than 2 m. The town center, such as town hall, railway station, stores, and houses, is located on the center of the lowland. Although the 6-m-high seawall had been constructed along the coast, the seawall was destroyed and the tsunami flooded lowland. The maximum tsunami flood depth at the coast was 13 m. The tsunami also ascended the Otsuchi River and the Kozuchi River.

The average of tsunami inundation depth in the lowland was about 10 m. The most houses were washed out, and the third floor of higher buildings, such as the

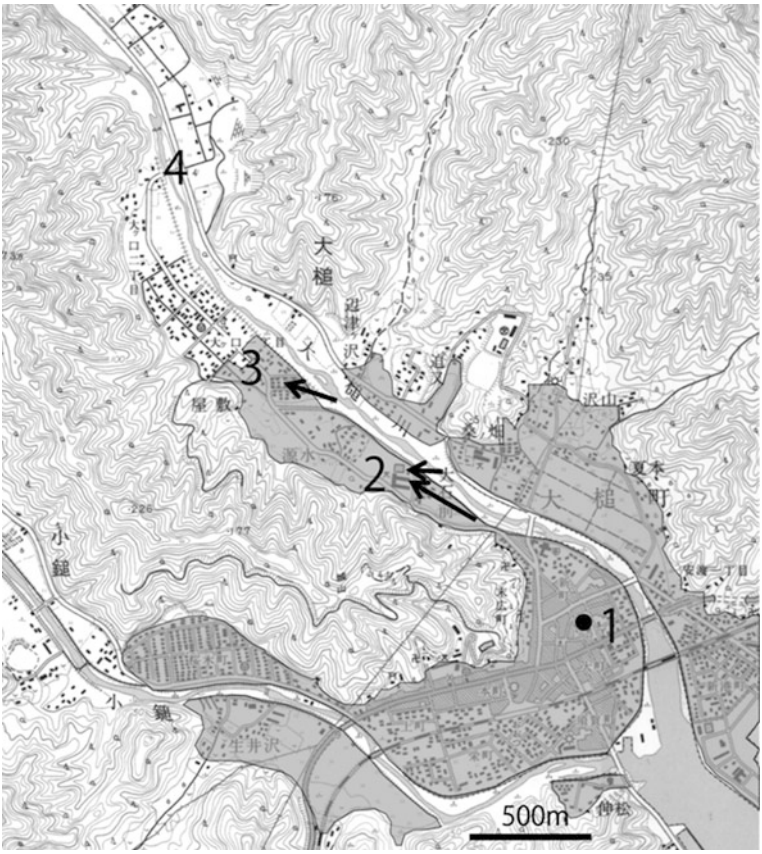

Fig. 4.8 The Otsuchi town and the tsunami inundation area. *Shaded areas* show the tsunami inundation areas in habitation side of the floodplain and coastal lowland modified after AJG (2011) and Haragichi and Iwamatsu (2013). *1* Destroyed town hall, *2* destroyed junior high school buildings by the tsunami came from embanked river and lowland, *3* destroyed settlement by the tsunami overflowed from the river, *4* fired house passed under the bridge. *Base map* GSI 1:25,000 Topographic map

Fig. 4.9 Destroyed town hall building in Otsuchi town

town hall and a hospital, were under water (Fig. 4.9). About 700 people of 4500 died in the town center area (Otsuchi Town 2011).

The Otsuchi River, a gravel bed mountain river, is 30 km long, and the basin area is 118 km^2. Gravels are transported to the river mouth (Shimazu 1990, 1996). The middle reaches of the river flow down on the valley bottom plain which is 400 m wide surrounded hillside slopes. The lowest 1.5 km section of the river flows down in the lowland. The both sides of the river are separated from the valley bottom plain and the lowland by the 3–m-high embankments. The tsunami, flooded on the lowland, separately ran up in the embanked river course and in the settled floodplain. Firstly, the floodwater ran up in the embanked river course. Flowing over the embankment, floodwater attacked houses on the floodplain of the habitation side. The tsunami ran up both in the river course and on the settled floodplain. Water though the river course overbanked at several points. One was the point of 2 km from the mouth. At this point, the ran-up tsunami destroyed embankment and flowed into settled floodplain. It joined another flow through the settled floodplain to attack the buildings of the junior high school (Fig. 4.10). The other point was the upstream area from there. Overbank flow of the tsunami flood over the embankment damaged an upstream settlement (Fig. 4.11). The uppermost inundation area in the habitation side of the floodplain was located at 2.5 km from the mouth at the elevation of 6.5 m. From an interview to a resident in the upper course of 3.5 km from the mouth, a fired house floated up the river. The tsunami running up in the Otsuchi River reached 4 km from the mouth and at the elevation of 8 m.

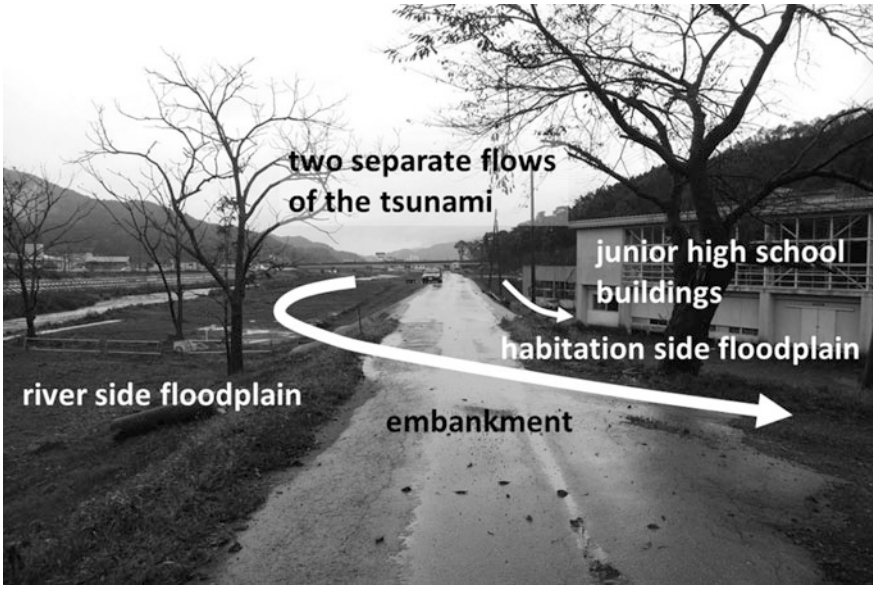

Fig. 4.10 Damages of junior high school buildings caused by attacked floodwater from two routes

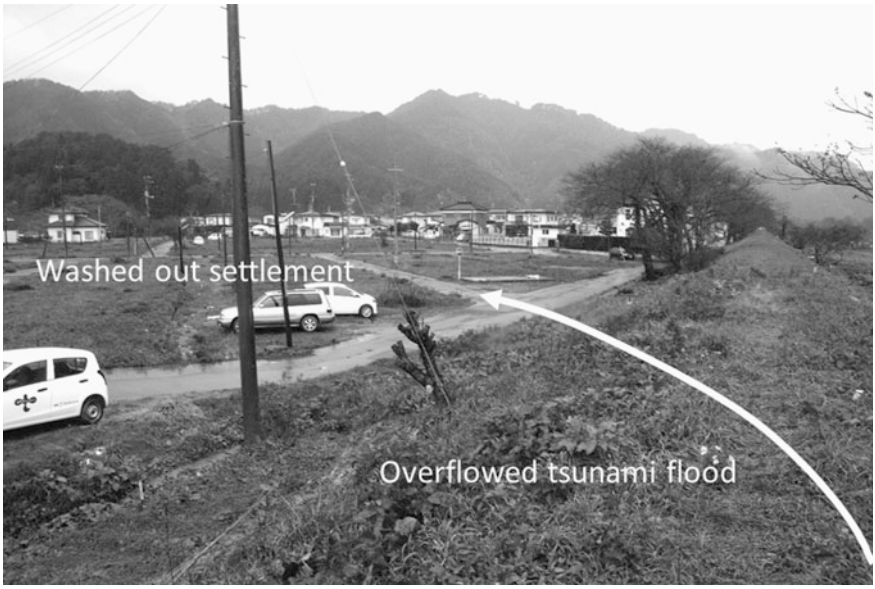

Fig. 4.11 Damaged area caused by overbank tsunami flood flow

The tsunami ran up in the small lowland without diminishing depth, and the whole central part of the town in the lowland was severely damaged. Although the depth and strength of the floodwater suddenly decreased at the mouth of the valley, tsunami flow which ran up in the river course flooded over the embankment and caused severe damages in the habitation side of the floodplain in the upstream area. In the river course, the tsunami could reach upper area of higher elevation through the river.

4.3.3 A Small and Steep Slope Valley

Aneyoshi, a tiny cove, directly facing the Pacific Ocean, is located in Omoe Peninsula, where the eastern fringe of the Honshu Island is located. A small and steep stream flows into the cove (Fig. 4.12). The stream is a bedrock channel with a narrow valley floor, less than 10 m wide and in steep hillslopes (Fig. 4.13). Here was the one of the largest points of the tsunami height at the coast. The height was to 28 m (Haraguchi and Iwamatsu 2013).

The tsunami ran up in the steep slope river and reached 36.7 m in elevation at 0.5 km from the river mouth (Konno et al. 2011, as shown Fig. 4.14). That

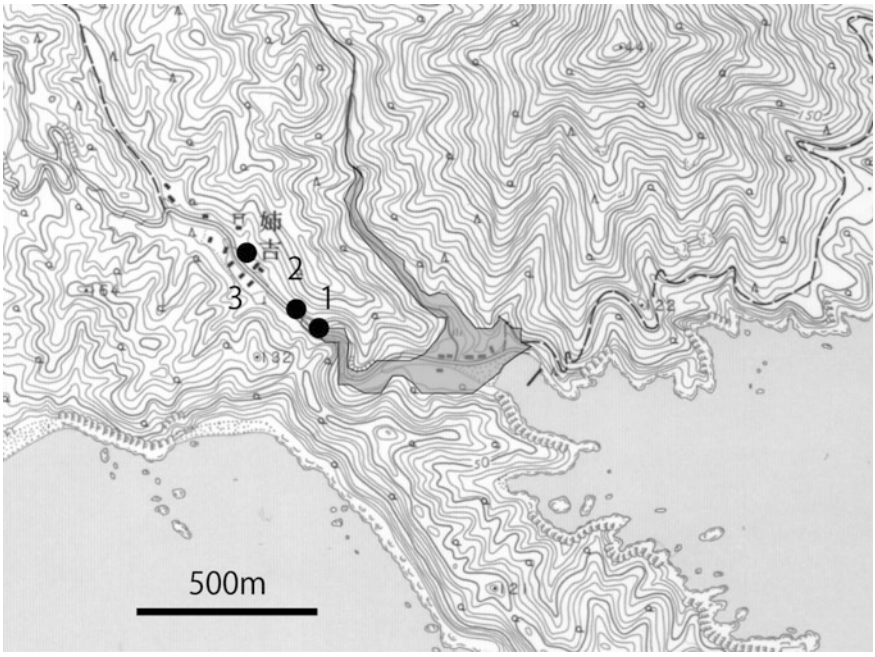

Fig. 4.12 Aneyoshi area and the tsunami ascended course. A *shaded area* shows the tsunami ascended course of the valleys modified after Haragichi and Iwamatsu (2013). *1* The monument of the 2011 tsunami ascending limit, *2* the monument of the former maximum tsunami ascending point, *3* Aneyoshi settlement

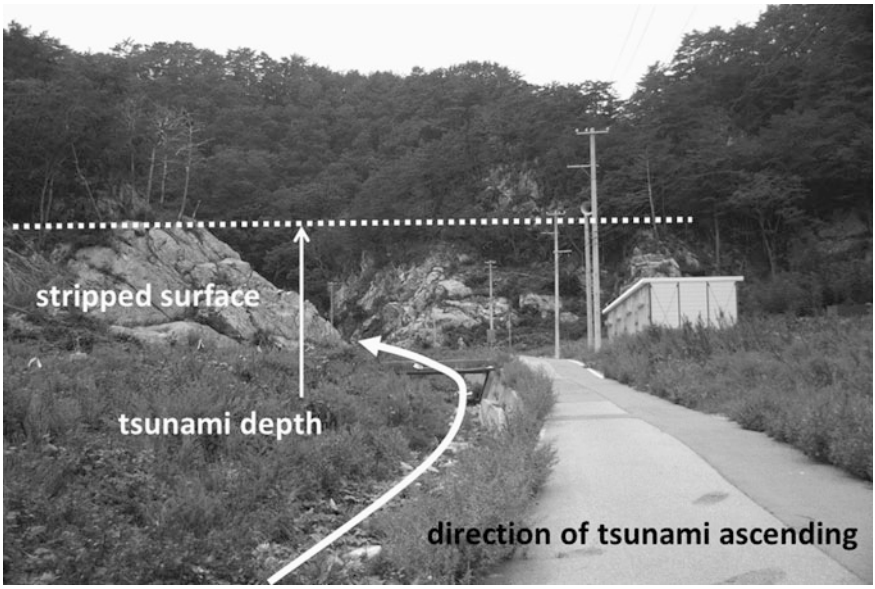

Fig. 4.13 Small and steep slope valley in Aneyoshi area

Fig. 4.14 The monument of the 2011s tsunami ascending limit in the valley of Aneyoshi

Fig. 4.15 The monument showing the upper inundated limit of the former maximum tsunami. The message of "the people in this settlement must not build own house below this point" was engraved on this monument

elevation was one of the highest points on this tsunami event. Seawater was concentrated in tiny cove and small stream, so that the tsunami ran up to higher elevation in the valley than at the coast. The surface soil was stripped 5 m high from the valley bottom, and trees on the slopes were washed out to. Because a small fisherman's village, Aneyoshi, was located in the narrow valley floor which is more than 50 m in elevation, this village was not damaged. The 1896 tsunami and the 1933 tsunami attacked a village on the coast of the cove. Some people who survived the tsunami events had decided to move to higher area than former maximum tsunami attacked area, which was 45 m in elevation (Fig. 4.15). Because they continue to live in this area, all houses could survive this tsunami event.

4.4 Geomorphological Effect on Tsunami Run-up in the Sendai Plain

4.4.1 Landforms and Inundation Processes of the Tsunami in the Sendai Plain

The Sendai Plain had the most widespread inundation area in this tsunami event. This is an alluvial plain surrounded by the Neogene hill, and the east side of this plain faces the Sendai Bay and the Pacific Ocean. The extent of the plain is 10–20 km long in the east–west direction and 50 km long in the north–south direction. The Nanakita River, the Natori River and its tributary, Hirose River, and the Abukuma River flow down in the northern part, the central part, and the southern part of the plain, respectively. This section discusses the tsunami inundation processes in the central part of the plain and along the Natori River.

The western half of the central part of the plain is the alluvial fan of the Hirose River, which descends eastward from 15 to 5 m in elevation. The city center of the Sendai is located on the alluvial fan. The eastern half of the plain is lowland with floodplain of the Natori River, backmarsh, and three rows of beach ridge ranges, paralleling the coastline (Matsumoto 1981, 1984, Fig. 4.16).

The tsunami attacked the coast in rectangular direction of the coastline. The maximum height of the tsunami along the coast near the Natori river mouth was

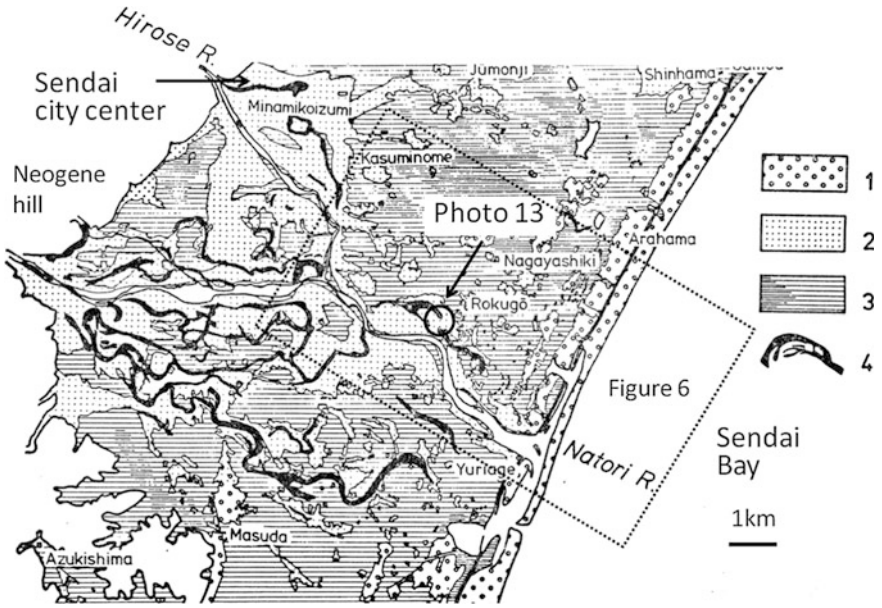

Fig. 4.16 Geomorphological map of the Sendai Plain (modified after Matsumoto 1981). *1* Beach ridge ranges, *2* natural levee and alluvial fan, *3* back swamp, *4* former river course

Fig. 4.17 Tsunami dammed up by the elevated motorway. Much debris was deposited along the road

from 9 to 11 m (Haraguchi and Iwamatsu 2013). Because there was no seawall along the coast, the tsunami came ashore directly. As the tsunami ran up 1 km into the floodplain and backmarsh, the maximum height of it diminished to 5 m in elevation (Haraguchi and Iwamatsu 2013). This was caused by going over the beach ridge ranges, which is about 2 m in elevation (Matsumoto 1981, 1984). An elevated motorway had been constructed 2 km ashore and parallel to the coastline. The tsunami was dammed up by this road (Fig. 4.17). The elevation of the maximum height of the tsunami was from 3 to 5 m in the coast side of the road and about 2.5 m in the land side (Fig. 4.18). The floodwater, going through underpasses and under the bridges of the motorway, inundated upward to about 3 m in elevation, where it was 3 km from the coast.

In the land side of the motorway, shallowed floodwater was affected by micro-landforms. There are former river courses and natural levees whose relative height is less than 1 m. The floodwater with broken debris ascended only in the former river course. Old settlement on the natural levee was not or little damaged (Figs. 4.16, 4.18 and 4.19).

Live images taken by Japan Coast Guard, NHK (broadcasting), and Japanese Forces showed the velocity of the front of the ascending tsunami was from 10 to 12 m/s. The courses of them were affected by the micro-landforms. The front selectively ran up through geomorphologically lower parts, such as backswamp, former river courses, and breaks of the beach ridge ranges. The difference in arrival time of the flood front between courses, which might be several tens of seconds, was very important role to evacuate people.

Fig. 4.18 Little damaged old settlement on a natural levee and debris deposited former river course. Many debris including cars and containers were deposited in a former river course

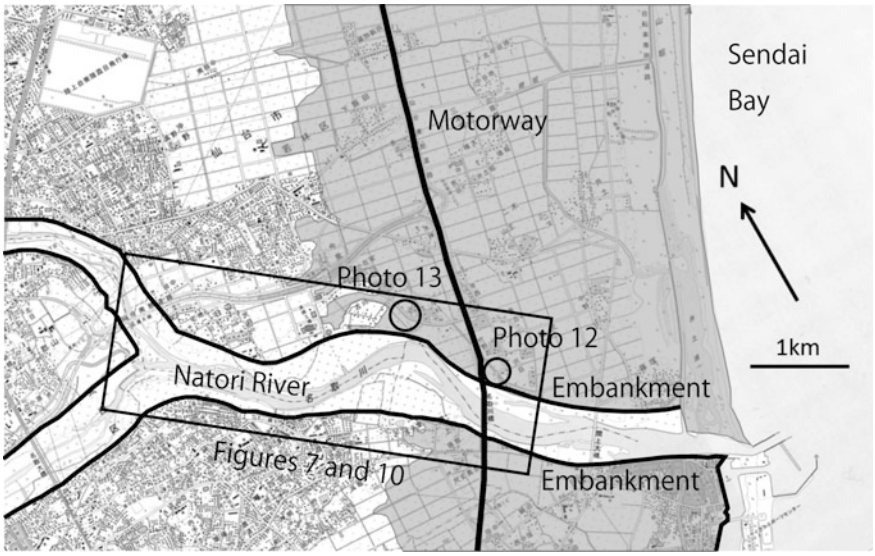

Fig. 4.19 Sendai Plain and the tsunami inundation area. *Shaded areas* show the tsunami inundation area modified after Haragichi and Iwamatsu (2013)

4.4.2 Tsunami Inundation Processes Along the Natori River

The Natori River is divided by both sides of high and strong embankments from the floodplain mentioned above. The height of the embankments is about 5 m. The tsunami firstly ran up to the channel because of little obstacle barriers, such as houses, roads, trees, and ridge-like landforms. The live images showed that the first front of the tsunami run-up reached the point of 5 km from the river mouth at 16:01 in the river channel. On the river side floodplain, the front was still 1.5 km lower at the same time. On the habitation side of the floodplain, the front reached only 2.5 km from the coast at 16:02. This shows the velocity of the front of the tsunami in the channel was, about 25 m/s, more than double in the habitation side of the floodplain.

Broad riverside floodplain of Japanese rivers is buffer space for the severe river flood. Although the river side floodplain of the most Japanese rivers is used for playground and/or athletic ground artificially planed, along the Natori River, it is used for vegetable field continuously before the construction of the embankments, so that only little artificial landform change had been performed on the surface of the floodplain and original micro-landforms were well preserved on the riverside floodplain. As a result, tsunami run-up processes on the floodplain were affected by micro-landforms. Figure 4.10 shows the micro-landforms of the riverside floodplain of the Natori River. The map was derived from elevation data, the images of Google Earth just after the tsunami disaster, cross-sectional surveying (Fig. 4.21), and field observations. The elevation data were based on the 1:2.500 topographic maps issued by Sendai City and 5 m DEM by Geospatial Information Authority of Japan (GSI).

Small terrace-like features and continuous shallow ditches are on the floodplain (Fig. 4.20). The depth of the ditches is shallower than 1 m (Fig. 4.21).

Damages of agricultural facilities, such as greenhouses, plastic small tunnels, plastic mulches and support posts, eroded top of small raised lines in vegetable field, newer sediment cover on the surface soil, buried vegetable roots, and growth of vegetable after the tsunami flood, showed the tsunami flood processes and the strength of the flow. First fieldwork was carried out at the beginning of May 2011, 50 days after the tsunami disaster. Although some fields began to be recultivated at that time, most of that was left to be able to observe the condition just after the tsunami disaster. There was no river flood event during the period from the disaster to the fieldwork. Fieldwork was carried out from the location of 2.5 km from the river mouth. Because the lowest 2.5 km section was not allowed to enter at that time. The upper extent of the fieldwork was the location of 6 km from the mouth. There was the upper limit of the tsunami flood on the riverside floodplain.

4.4.3 Tsunami Run-up Processes Along the Natori River

Based on the fieldwork, the tsunami-inundated riverside floodplain was divided into four sections (Fig. 4.20). The lower section was the lowest 3 km section. The

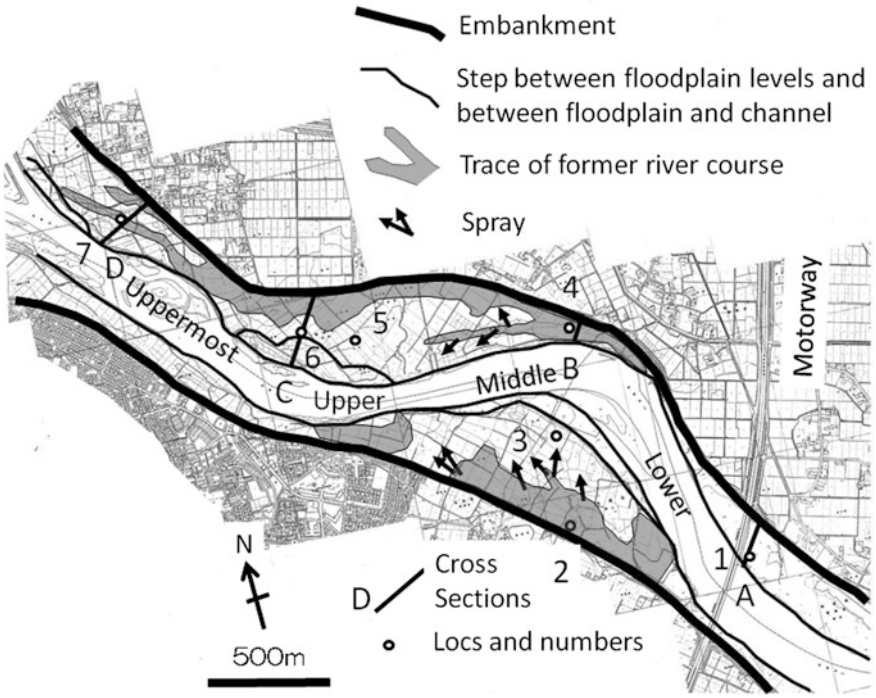

Fig. 4.20 Micro-landforms of river side floodplain of the Natori River and localities of observation and survey points. Four river sections of the tsunami inundation in the riverside floodplain are also shown in this figure

middle section was from 3 to 4.5 km from the mouth. The upper section was from 4.5 to 5 km from the mouth. The uppermost section was from 5 to 6 km from the mouth. Based on an interview from farmers who has one of the field areas on the riverside floodplain upper from 6 km from the mouth, the tsunami floodwater did not ascend on there. The elevation of that area is more than 3.5 m. The tsunami front ran up more in the river channel. The tsunami front was recognized in the river channel at about 8 km from the mouth, where the elevation is about 3.5 m.

In the lower section, erosional features were found. At the Loc. 1, surface was eroded less than 20 cm in depth (Fig. 4.22). Before the tsunami disaster, the surface was covered with grasses of Gramineae. Most surface vegetation was washed out and subsurface sediments outcropped. Only in some shallower eroded parts, from 1.5- to 3-cm-thick silty sand sediments including marine gravels and shells covered the subsurface sediments. Dunes indicating backwash direction were formed in some parts. In shallow hollows, thin salt incrustation was formed underlain by 3 cm of sandy sediments (Fig. 4.23).

In this section, destroyed house debris, furniture, household goods, small boats, and dead fishes were deposited on the river side floodplain. The live movie taken by

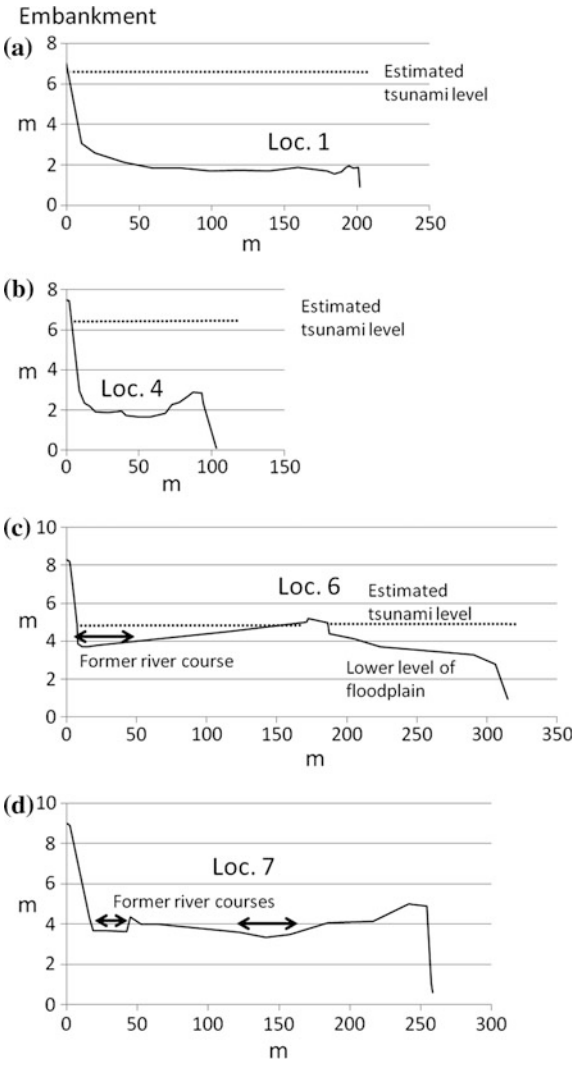

Fig. 4.21 Cross sections of the river side floodplain of the Natori River. Former river courses and estimated tsunami levels are shown in these figures

NHK showed that the tsunami floodwater in the habitation side went over the embankment of 5 m high into the riverside floodplain in lowest 1 km course. The flow brought the destroyed houses, house goods, and so on into the river. Much of those were deposited around the Loc. 1. The tsunami water level was below the top of the embankment in the upper section from here. Very strong flood flow caused erosion of the surface around this location, and it brought much debris from the habitation side floodplain up to here. Strong backwash also occurred at this point.

The middle section was characterized by slight erosion and strong impacts to the agricultural facilities. At the Loc. 2 in the wide river side floodplain near the embankment, the tsunami washed out most vegetables and agricultural facilities and

Fig. 4.22 Erosional feature in the lower section of the Natori River (Loc. 1)

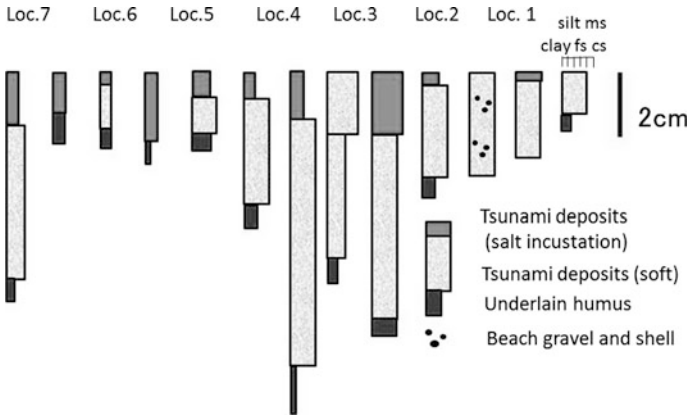

Fig. 4.23 Surface sediments induced by the tsunami flow

eroded ridges. Because the habitation side floodplain near this site was less affected by the tsunami flood, no house was washed out and recultivation had begun there. At the Loc. 3, top of ridges of the field was eroded. Some survival carrots on them indicated slight erosion. Most agricultural facilities were washed out. Many washed-out plastic sheets were found on grass along the channel. Woody debris was deposited on the surface of the field. Medium sand and finer sediments about 6 cm thick underlay 2-cm-thick salt-encrusted sediments of medium and coarse

Fig. 4.24 Washed-out plastic covers and leaned upward agricultural facilities in the vegetable field on the river side floodplain (Loc. 4). Sediments with surface incrustation buried a vegetable field. The tsunami ascended to right direction

sand on the pre-tsunami surface (Fig. 4.23). At the Loc. 4, most plastic tunnel covers were washed out and support posts leaned upstream direction (Fig. 4.24). In contrast, plants bordering the field leaned downstream. Top of ridges was eroded. Silty sand sediments of 8 cm or less underlay 2-cm-thick salt incrustation (Fig. 4.23). Although planted onions survived, growth was worth.

At the Loc. 5, plastic tunnel covers were washed out. On the other hand, support posts remained. Some of them leaned upstream and some stood as they were (Fig. 4.25). Live movies shot from the air by NHK show that the tsunami flood flow crushed all greenhouses around here. 1-cm-thick sediments of silty medium sand underlay hard and thin salty incrustation of fine sand sediments (Figs. 4.23 and 4.26). Growth of survived garlic was not enough. Although the river side floodplain was entirely affected by tsunami flood flow, influences were relatively weaker than the lower points in this section. Strong flood flow caused washout of the facilities and lean of the support posts, and relatively, weak ebb flow caused lean of flexible plants.

At the Loc. 6 in the higher level surface of the upper section, plastic tunnels survived tsunami and cabbages grew enough (Figs. 4.21 and 4.27). The lower level surface and the shallow ditch surrounding the higher level surface, growth of cabbages was poor. The surface of the shallow ditch was underlain by 2-cm-thick silty salt incrustation (Fig. 4.23). The lower surface was covered with granule and sand sediments with quite thin salt incrustation.

Fig. 4.25 Plastic tunnel covers were washed out, and support posts remained (Loc. 5)

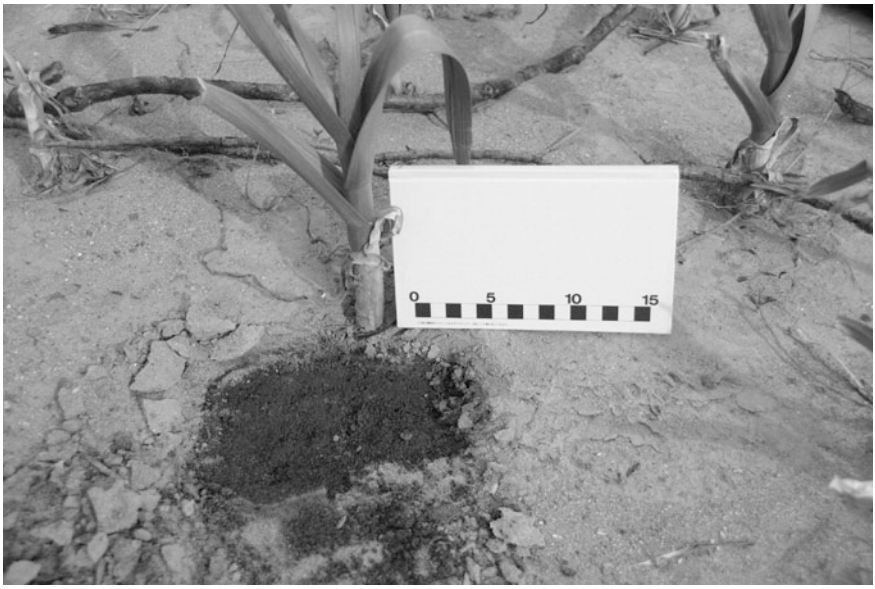

Fig. 4.26 Tsunami induced sediments with salt incrustation and buried vegetables (Loc. 5)

Fig. 4.27 Cabbages growing as usual on the higher level of the surface (Loc. 6)

At the Loc. 7, in the uppermost section, most fields had begun to be recultivated. The salt incrustation was observed in shallow ditches below 4 m in elevation (Figs. 4.28 and 4.21). The tsunami inundated only in these shallow ditches. The other part of the field where was more than 4 m in elevation was not flooded by the tsunami water.

4.4.4 Geomorphological Effects on Tsunami Inundation Processes Along the Natori River

Differences of tsunami inundation processes between sections are shown in Fig. 4.29.

In the lower section around the Locs. 2, 3, and 4, sedimentation stretching upward from the former river courses in the river side floodplain can be identified on the Google Earth images taken on March 27, 2011 (Fig. 4.20). These structures are similar to a spray caused by a strong overbank flow. In the lower section, very strong tsunami flow, whose depth was about 5 m as same as in habitation side floodplain, was less affected by the landforms. These flows caused the erosion and formation of spray-like structures. A strong backwash also affected the surface of the floodplain. It can be said that tsunami flow in this section formed landforms as Dawson (1994) and Nott (2006) mentioned.

Fig. 4.28 Salt incrustation found in a shallow ditch (Loc. 7)

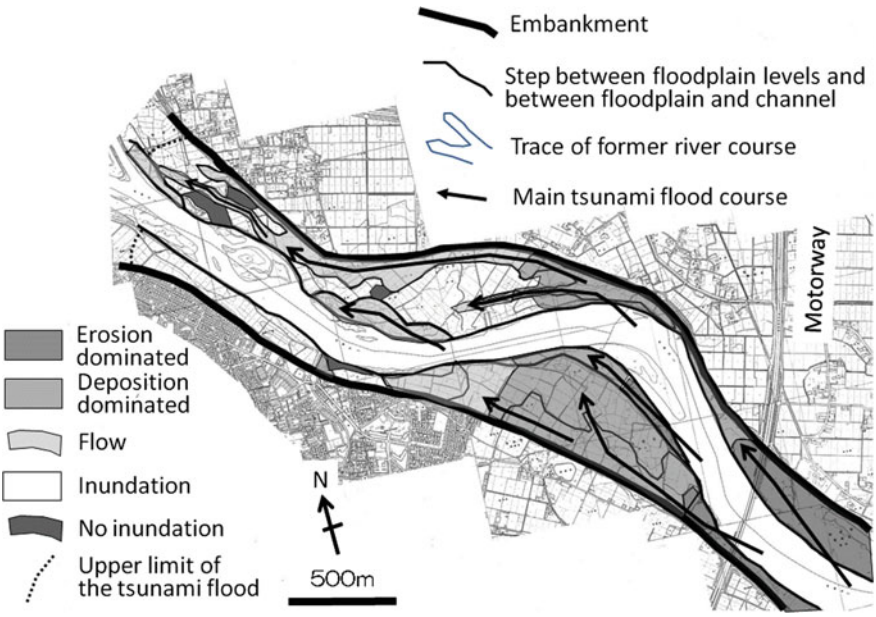

Fig. 4.29 Tsunami inundation processes in the riverside floodplain. *Arrows* show the main streams of flood flow of the tsunami

In the middle section, transported sediments were mainly deposited caused by a decrease of strength and depth of the flow. A similar effect was found in other tsunami event and in other area of this 2011 event. On the bank of the Usubetu River in Hokkaido, Japan, relatively thick tsunami sediments caused by the 1993 Hokkaido-Nansei-Oki earthquake were found in just upstream of erosion area (Nanayama 2008). The sediments were massive and less than 10 cm in thickness. These characteristics were similar to the single-bed deposits by one time sediment flow (Fujiwara 2008). This shows one time of the strong flood flow of the tsunami caused the sediments in this event. Saijo et al. (2013) showed that salt concentration in soil was thinner landward from the coast in this event in the Sendai Plain. Relatively thick incrustation being found in the middle section and tapering landwards supports the above-mentioned fact.

As the surface elevation of the floodwater was kept about 4 m in the upper and the uppermost sections, the depth of the tsunami flow on the floodplain decreased upstream gradually. In these sections, the tsunami ran up only in the shallow ditches and it deposited sandy sediments in the ditches and degree of damages depended on landforms. Geomorphological effects clearly appeared in these sections. Salt incrustation was formed by the concentration and evaporation of the salty floodwater. In the uppermost section, very thin silty salt incrustation was found only in the shallow ditches. The salty floodwater with thin sediments flowed in the shallow ditches and it also ponded. Goto et al. (2008) reported that in the coast of Thailand, salt incrustations were formed in restricted area beyond the limit of the flooded area of the tsunami event of the Indian Ocean. The salty tsunami water reached landward exceeding the tsunami-inundated area through continued lower landforms like former river courses

Koarai et al. (2015) showed landform effect on the tsunami flow changed step by step from coastal area to inland area in the 2011 tsunami event, the coastal plains of Sendai and Ishinomaki. The riverside flood plain also recognized gradual increase of landform effect on the tsunami flow and distribution characteristics.

4.5 Conclusions

Spatial characteristics of tsunami flow caused by the 2011 off the Pacific coast of Tohoku Earthquake were described in the four types of areas having different geomorphological characteristics. The Miyako City area is located in the valley bottom plain of the Hei River. Before the tsunami flow which inundated the coastal lowland reached the city center in the valley bottom plain, the banked river ascended tsunami flow got over the embankment. This flow severely damaged the city center. Otsuchi area is small coastal lowland with relatively small rivers. The town center in the coastal lowland was severely damaged by the tsunami got over the seawalls. The tsunami flows through two routes, ascended the banked river and inundated the lowland, joined upper area, and damaged buildings. Near the upper limit of the tsunami, the tsunami flow got over the embankment and inundated a

settlement. In these areas, the tsunami flow which ran up the banked river courses caused disaster in the upper areas. The Aneyoshi area is a tiny cove of the rias coast and a small and steep slope stream. Although the height of the tsunami was doubled by ascending the steep slope and small valley, the settlement, located in the upper valley floor of higher elevation, survived. The Natori River and its surroundings are in the Sendai Plain which is largest plain in Tohoku district. Although deep tsunami water directly inundated landward without landform effects, it caused geomorphological processes by erosion and sedimentation on land. The shallower water extent near the landward limit of the tsunami inundation was strongly affected by micro-landforms, especially former river courses. Artificial constructions, such as elevated roads and railways, also affected inundation processes of the shallower tsunami flow in a coastal plain and a valley bottom plain.

References

Association Japanese Geographers (2011) The tsunami disaster maps. http://map311.ecom-plat.jp/map/map/?mid=40

Dawson AG (1994) Geomorphological effects of tsunami run-up and backwash. Geomorphology 10:83–94

Fujiwara O (2008) Bedforms and sedimentary structures characterizing tsunami deposits. In: Shiki T (ed) Tsunamiites. Elsevier, Amsterdam, pp 51–62

Goto K, Imamura F, Keerthi N, Kunthasap P, Matsui T, Minoura K, Ruangrassamee A, Sugawara D, Supharatid S (2008) Distribution and significance of the 2004 Indian Ocean tsunami deposits: initial result from Thailand and Sri Lanka. In: Shiki T (ed) Tsunamiites. Elsevier, Amsterdam, pp 105–122

Haraguchi T, Iwamatsu A (2013) Detailed maps of the impacts of the 2011 Japan tsunami (revised edition). Kokon Shoin, Tokyo (in Japanese)

Iwafune M (ed) (2012) Tsunami overflowed into the city. Nature of tsunami on March 11, 2011 in Miyako City, Japan. Minamikyusyu Cable TV Net Inc., Kagoshima (DVD with narration in Japanese)

Japan Meteorological Agency (2011) First report of the earthquake and tsunami disaster of the 2011 off the Pacific coast of Tohoku earthquake. Natural phenomena report of disaster, 2011 No.1. http://www.jma.go.jp/jma/kishou/books/saigaiji/saigaiji_201101/saigaiji_201101_01.pdf (in Japanese)

Koarai M, Nakano T, Okatani T (2015) Relationship between tsunami hazard related to the 2011 off the Pacific Coast of Tohoku earthquake and geographical condition such as topography and land use on the Sendai Plain and Ishinomaki Plain. J Geogr (Chigaku Zasshi) 124:211–226 (in Japanese with English abstract)

Konno A, Yoshiki T, Sano Y (2011) Run-up height distribution of the 2011 Tohoku earthquake tsunami around the Omoe Peninsula and the Miyako Bay, Northeast Japan. Q J Geogr 63:147–152 (in Japanese with English abstract)

Matsumoto H (1981) Sea-level changes during the Holocene and geomorphic developments of the Sendai coastal plain, northeast japan. Geogr Rev Jpn 54:72–85 (in Japanese with English abstract)

Matsumoto H (1984) Beach ridge ranges on Holocene coastal plains in northeast Japan-The formative factors and periods. Geogr Rev Jpn 57(Ser.A)10:720–738 (in Japanese with English abstract)

Nanayama F (2008) Sedimentary characteristics and depositional processes of onshore tsunami deposits: an example of sedimentation associated with the 12 July 1993 Hokkaido-Nansei-oki earthquake Tsunami. In: Shiki T (ed) Tsunamiites. Elsevier, Amsterdam, pp 63–80

Nott J (2006) Extreme events. A physical reconstruction and risk assessment. Cambridge University Press, Cambridge

Otsuchi Town (2011) Plans for reconstructions of the Otsuchi Town from the East Japan earthquake tsunami disaster (in Japanese)

Saijo K, Endo R, Onodera S (2013) Characteristics of topsoil salinity in rice fields damaged by the 2011 Tohoku earthquake tsunami. Q J Geogr 64:173–177 (in Japanese with English abstract)

Shimazu H (1990) Segmentation of mountain rivers based on longitudinal change in gravel size of riverbeds in Tohoku district, northeastern Japan. Geogr Rev Jpn, 63-A:487–507 (in Japanese with English abstract)

Shimazu H (1996) Segmentation of Japanese mountain rivers and its causes based on gravel transport processes. Trans, Japan Geomorphol Union 15:111–128

Tani K (2012) Distribution of the number of deaths and the death rate on the Great East Japan earthquake. Occas Paper Depart Geogr Saitama Univ 32:1–26 (in Japanese)

Umitu M, Tanavud C, Boonrak P (2006) Spatial distribution of tsunami deposits and behavior of the tsunami flow in the Nam Khem Coastal Plain, Southern Thailand. E-Journal GEO 1:2–11 (in Japanese with English abstract)

Umitsu M, Takahashi M (2007) Geo-environmental features in the damages of the damages of the 2004 Indian Ocean tsunami I/around Banda Aceh, Indonesia. E-journal GEO 2:121–131 (in Japanese with English abstract)

Chapter 5
Distribution of Liquefaction Sites and Coastal Alluvium in Japan

Toshihiko Sugai and Keita Honda

Abstract In the Tohoku and Kanto regions, the 2011 off the Pacific coast of Tohoku Earthquake (2011 Tohoku earthquake) caused widespread sediment liquefaction along more than 600 km of the Pacific coast facing the Japan Trench. Liquefaction sites tended to be concentrated in reclaimed lands on the north side of Tokyo Bay, especially in sandy fill overlying thick alluvium, and along large rivers in alluvial lowlands. In Japan, alluvial deposits along the lower reaches of rivers often form coastal prisms (CPs) between the river profiles of the present and the last glacial. A basal gravel body (BG) generally forms the lower boundary of the CP. Within a thick CP, the period and duration of seismic shear waves (S-waves) are lengthened, and multiple S-wave reflections from the BG and the slow S-wave velocity increase the internal water pressure, leading to liquefaction of sand layers in the CP. The distributions of both liquefaction induced by the 2011 Tohoku earthquake and historic liquefaction sites correspond closely to the distribution of thick CP deposits. Large subduction-zone earthquakes have repeatedly caused liquefaction within CPs greater than 30 m thick, with liquefaction occurring as far inland as the upstream edge of the CP. In the long CPs in the Kanto region, along the Kinu, Ara, and Naka (Furutone) rivers, liquefaction induced by the 2011 Tohoku earthquake was particularly widespread. Mega-earthquakes can also cause liquefaction in sediment-filled basins inland of the CPs; the Tohoku earthquake liquefied the thick late Quaternary alluvium in the Koriyama and Aizu-Wakamatsu basins.

Keywords Alluvial plain · Coastal prism · Basal gravel · Liquefaction · Kanto Plain · Subduction-zone earthquakes

T. Sugai (✉)
Graduate School of Frontier Sciences, The University of Tokyo,
5-1-5 Kashiwanoha, Kashiwa, Chiba 277-8563, Japan
e-mail: sugai@k.u-tokyo.ac.jp

K. Honda
Musashi High School and Junior High School, Toshima, Tokyo 176-0011, Japan

S. Haruyama and T. Sugai (eds.), *Natural Disaster and Coastal Geomorphology*, DOI 10.1007/978-3-319-33814-9_5

5.1 Introduction

The 2011 off the Pacific coast of Tohoku Earthquake (2011 Tohoku earthquake) caused widespread sediment liquefaction along the Pacific coast of eastern Japan, from Aomori to Kanagawa prefectures (Wakamatsu and Senna 2013, 2014). In the Tohoku region, liquefaction occurred in alluvium along river channels and in swamps of the Kitakami Lowland and Sendai Plain. Soft, late Quaternary sediments in inland basins such as the Koriyama and Aizu-Wakamatsu basins also liquefied.

In the Kanto region, liquefaction occurred along many river channels and swamps in the Kinugawa, Nakagawa, and Tone-gawa lowlands (Seto 2011; Nakamura 2012; Senna et al. 2012; Aoyama et al. 2014; Komatsubara et al. 2014; Une et al. 2015). Alluvial lowlands along the lower reaches of the Kuji and Hitachi–Naka rivers, which flow into the Pacific Ocean, also liquefied. The most intensive damage occurred in areas of reclaimed land around Tokyo Bay in Urayasu and Chiba cities (Yasuda and Harada 2011; Ministry of Land, Infrastructure, Transport and Tourism, and the Japanese Geotechnical Society 2011; Koarai et al. 2011; Chiba Prefectural Environmental Research Center 2011, 2012).

In Tohoku and Kanto, liquefaction generally occurred in alluvial lowlands near the water area, suggesting that high groundwater table was an important factor controlling liquefaction potential and that lateral spreading to the water area may be promoted along the shore. On the other hand, Senna (2013) and Wakamatsu and Senna (2014, 2015) pointed out that, even with the same level of seismic intensity, liquefaction occurred at more sites in Kanto than in Tohoku in areas with similar geomorphic features (deltas, alluvial fans, natural levees, reclaimed lands) . This observation implies that liquefaction is controlled not only by geomorphic factors and seismic wave acceleration but by some other factor as well.

Liquefaction intensity depends partly on the basal topography beneath the coastal alluvium, and in the Tokyo Bay area, it depends on the thickness of the alluvium beneath reclaimed land (e.g., Kazaoka 2013). Therefore, in addition to groundwater table, geomorphology, seismic intensity, and land reclamation, the thickness of the coastal alluvium is another factor controlling liquefaction severity.

During the sea-level lowstand of the last glacial, incised valleys were formed by rivers in Japan, and during the post-glacial sea-level rise, these valleys were filled with sediments like in many regions of the world (e.g., Mattheus and Rodriguez 2011; Miall 2014, Chap. 6). During the subsequent sea-level highstand, alluvium continued to accumulate on top of the incised-valley fill. The thick, wedge-shaped layer of sediments deposited between the last glacial river profile (LGRP) and the present river profile (PRP) is called the coastal prism (CP; Honda and Sugai 2010, 2011; Sugai and Honda 2015; Fig. 5.1). A basal gravel body (BG) typically occurs at the bottom of the CP. In addition to the naturally formed CPs, during the past half century, the area of reclaimed land along the coast has increased along with the expansion of urbanization and industrialization in the coastal lowlands.

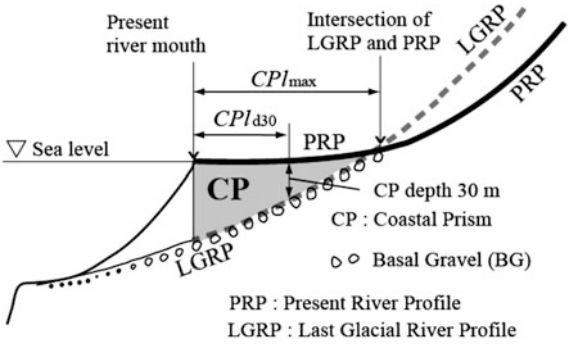

Fig. 5.1 Schematic longitudinal cross section of a coastal prism (CP). Modified after Sugai and Honda (2015)

As seismic shear waves (S-waves) enter the CP from below, their velocity slows and their period lengthens in the soft alluvium. Further, they are repeatedly reflected by the BG because of the high impedance between the BG and soft overlying sediments. These low-frequency, large-amplitude waves last a long time. As a result, the pore water pressure within the CP rises and eventually triggers liquefaction (e.g., Yoshida 2010).

In this chapter, we show by an analysis of 50 rivers in Japan (Table 5.1) that the distribution of the liquefaction sites induced by the 2011 Tohoku earthquake (e.g., Wakamatsu and Senna 2013, 2015) and historical submarine earthquakes (Wakamatsu 2011; Table 5.2) corresponds closely to CP distributions (Fig. 5.2) based on previous studies (Honda and Sugai 2010, 2011; Sugai and Honda 2015).

Table 5.1 List of the 50 rivers with their basin area, coastal prism area, and margin

River number	River name	Drainage basin area (km^2)	Coastal prism area (km^2)	Margin	Region
1	Toyohira	902	0.700	Sea of Japan	Hokkaido
2	Shiribeshitoshibetsu	765	0.884	Sea of Japan	Hokkaido
3	Yubetsu	1597	0.227	Okhotsk sea	Hokkaido
4	Tokoro	1923	0.591	Okhotsk sea	Hokkaido
5	Abashiri	1451	0.304	Okhotsk sea	Hokkaido
6	Tokachi	9025	0.953	Pacific	Hokkaido
7	Mu	1296	0.545	Pacific	Hokkaido
8	Saru	1428	0.452	Pacific	Hokkaido
9	Iwaki	2670	1.562	Sea of Japan	Tohoku

(continued)

Table 5.1 (continued)

River number	River name	Drainage basin area (km^2)	Coastal prism area (km^2)	Margin	Region
10	Yoneshiro	4100	1.093	Sea of Japan	Tohoku
11	Omono	4180	2.397	Sea of Japan	Tohoku
12	Koyoshi	1296	0.452	Sea of Japan	Tohoku
13	Mogami	7400	0.982	Sea of Japan	Tohoku
14	Mabechi	2091	0.370	Pacific	Tohoku
15	Hei	985	0.561	Pacific	Tohoku
16	Kitakami	10720	4.360	Pacific	Tohoku
17	Natori	769	0.165	Pacific	Tohoku
18	Abukuma	5480	1.357	Pacific	Tohoku
19	Natsui	770	0.673	Pacific	Tohoku
20	Hitachi–Naka	3270	1.096	Pacific	Kanto
21	Kinu	3153	5.276	Pacific	Kanto
22	Naka (Furutone)	7621[a] (2621)	3.988	Pacific	Kanto
23	Ara	8130[a] (3130)	3.445	Pacific	Kanto
24	Yoro	268	0.352	Pacific	Kanto
25	Tama	1066	0.931	Pacific	Kanto
26	Sagami	1647	0.878	Pacific	Kanto
27	Agano	8340	2.148	Sea of Japan	Chubu
28	Shinano	12260	7.349	Sea of Japan	Chubu
29	Kurobe	776	0.548	Sea of Japan	Chubu
30	Jintsuu	2780	0.414	Sea of Japan	Chubu
31	Sai	234	0.204	Sea of Japan	Chubu
32	Kuzuryuu	2580	0.632	Sea of Japan	Chubu
33	Tenryu	4890	0.871	Pacific	Chubu
34	Miyakoda	172	0.158	Pacific	Chubu
35	Toyo	714	0.123	Pacific	Chubu

(continued)

Table 5.1 (continued)

River number	River name	Drainage basin area (km^2)	Coastal prism area (km^2)	Margin	Region
36	Yahagi	1910	0.918	Pacific	Chubu
37	Kiso	5275	1.848	Pacific	Chubu
38	Maruyama	1387	1.035	Sea of Japan	Kinki-Chugoku
39	Chiyo	1155	0.456	Sea of Japan	Kinki-Chugoku
40	Kako	1850	0.063	Inland sea	Kinki-Chugoku
41	Chigusa	730	0.113	Inland sea	Kinki-Chugoku
42	Ota	1681	0.326	Inland sea	Kinki-Chugoku
43	Yoshino	3700	0.700	Inland sea	Shikoku
44	Naka	905	0.300	Inland sea	Shikoku
45	Monobe	509	0.040	Pacific	Shikoku
46	Onga	1033	0.783	Sea of Japan	Kyushu
47	Yamakuni	552	0.007	Inland sea	Kyushu
48	Oita	669	0.332	Inland sea	Kyushu
49	Omaru	501	0.171	Pacific	Kyushu
50	Kikuchi	1022	0.347	East China sea	Kyushu

[a]Including the half of the area of the upper drainage basin of the Tone River (i.e., ca. 5000 km^2); the river joined into the Watarase-Naka river (22) and Ara river (23) alternately during the Holocene

We first briefly review the relationship between liquefaction in Mihama (Chiba city) and basal topography, as reported by previous studies, and then, we discuss the relationship between liquefaction and CPs among the 50 rivers, focusing on the distance from the river mouth of the inland limit of liquefaction (ILL), because the alluvium thickness (i.e., CP depth) generally decreases monotonously inland from the river mouth.

Table 5.2 Earthquake name, occurrence date, magnitude, and locations of the earthquakes referred by this study (Fig. 5.7). Simplified after Wakamatsu (2011)

No.	Earthquake shown in Fig. 5.7	Name	The date of occurrence	Magnitude	Epicenter		Earthquake type	Liquefied river no. in Fig. 5.7
					Latitude (N°)	Longitude (E°)		
1	Ansei	Ansei Tokai and/or Ansei Nankai	1854.12.23 1854.12.24	8.4 8.4	34 33	137.8 135.0	SB	33, 35, 36, 37, 42, 43, 44
2	Shonai	Shonai	1894.10.22	7.0	38.9	139.9	C	13, 18
3	Kanto	Kanto	1923.9.1	7.9	35.3312	139.1357	SB	23, 24, 25, 26
4	N Tango	Kika Tango	1927.3.7	7.3	35.6318	134.9307	C	38
5	Tottori	Tottori	1943.9.10	7.2	35.4732	134.1840	C	39
6	Tounankai	Tounankai	1944.12.7	7.9	33.5733	136.1755	SB	37
7	Mikawa	Mikawa	1945.1.13	6.8	34.7027	137.1145	C	36
8	Nankai	Nankai	1946.12.21	8.0	32.9352	135.8488	SB	43
9	Fukui	Fukui	1948.6.28	7.1	36.1718	136.2905	C	32
10	Tokachi 1952	1952 Tokachioki	1952.3.4	8.2	41.7057	144.1512	SB	7
11	Niigata	Niigata	1964.6.16	7.5	38.3700	139.2117	S	27
12	Tokachi 1968	1968 Tokachioki	1968.5.16	7.9	40.7333	143.5833	SB	6, 14
13	Nihonkai M	Nihonkai chubu	1983.5.26	7.7	40.3600	139.0733	SB	12
14	Chiba E	Chiba toho oki	1987.12.17	6.7	35.3750	140.4933	SB	24
15	Hokkaido SW	Hokkaido Nansei oki	1993.7.12	7.8	42.7817	139.1800	SB	2
16	Tokachi 2003	2003 Tokachioki	2003.9.26	8.0	41.7785	144.0785	SB	1, 4
17	Chuetsu oki	Chuetsu oki	2007.7.16	6.8	35.5569	138.6095	S	28
18	(*shown as open circle*)	2011 Tohoku	2011.3.11	9.0	38.1003	142.8600	SB	16, 17, 18, 19, 20, 21, 22, 23

S Submarine earthquake
SB Subduction-zone earthquake
C Active fault-type shallow earthquake whose seirac center is below the coastal area

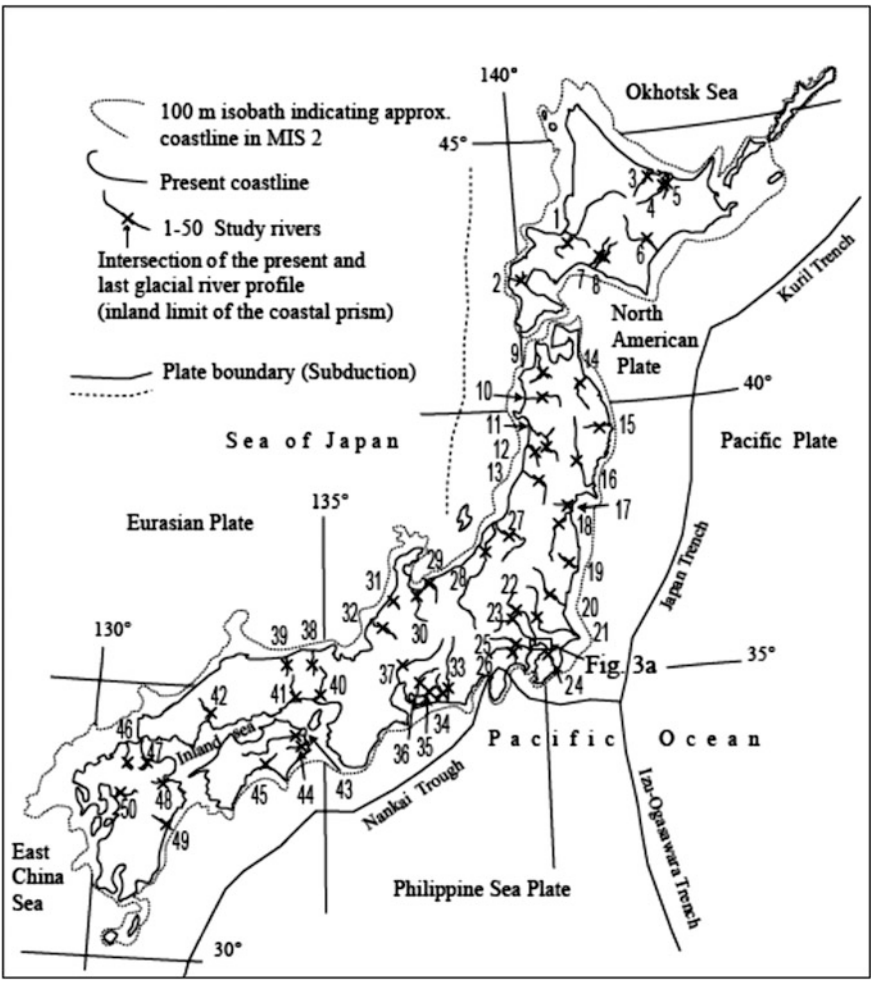

Fig. 5.2 Locations of the 50 studied rivers and the inland limits of their coastal prisms. *Notes* The Toyohira River (no. *3*) joins into the Ishikari River and then flow into the Japan Sea. The courses of the Kinu (no. *21*) and Naka (Furutone) (no. *22*) rivers are based on the inferred river system in the Kanto Plain before the Edo Period, about 500 years ago (Inazaki et al. 2014), and the buried basal topography of the latest Pleistocene (Hirai 1983; Endo et al. 1988, 2013)

5.2 Relationship Between Liquefaction During the 2011 Tohoku Earthquake and Alluvium

Land was reclaimed in Mihama in the 1970s (Fig. 5.3; Kumaki et al. 2013). From the original coastline (the northeastern edge of the reclaimed land) to the present coastline, the thickness of the fill increases from 0 to 5 or 8 m. When the reclaimed land overlies an incised valley, the total thickness of alluvium and fill is more than

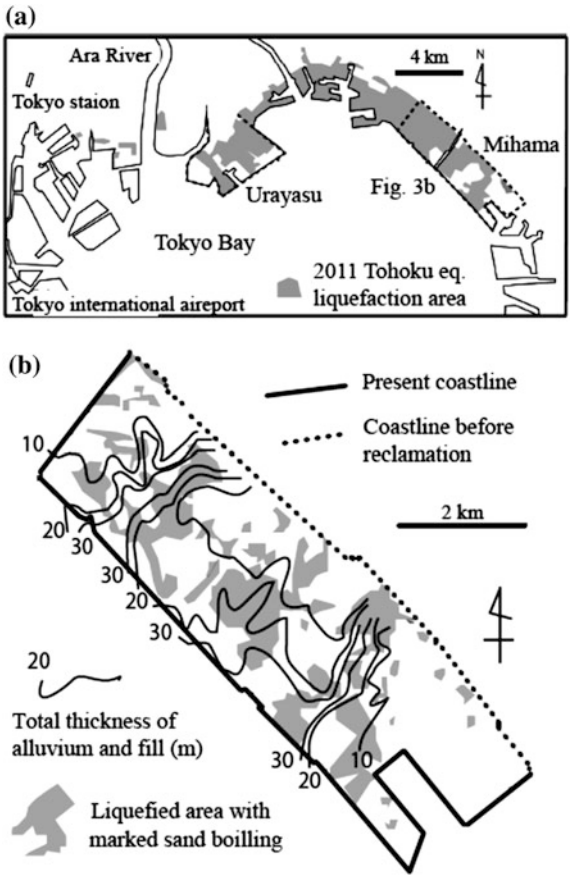

Fig. 5.3 **a** Distribution of liquefaction around Tokyo Bay during the 2011 Tohoku earthquake (Ministry of Land, Infrastructure, Transport and Tourism, and the Japanese Geotechnical Society 2011). **b** Areas of marked deformation and sand boils and the base depth of the alluvium in Mihama, Chiba city. Modified from Sekiguchi and Nakai (2012) and Chiba Prefectural Environmental Research Center (2012)

30 m; when it overlies a transgressive marine erosional surface, the total thickness is less than 20 m (Fig. 5.3b; Kaizuka et al. 1977).

The 2011 Tohoku earthquake tended to cause intense liquefaction of bodies of loose sand overlying thick muddy alluvium (Chiba Prefectural Environmental Research Center 2012) and fill within tidal channels (Koarai et al. 2011). Sand boils caused by the earthquake (Chiba Prefectural Environmental Research Center 2012; Sekiguchi and Nakai 2012) were concentrated near the head or margins of buried incised valleys with the depth of more than 30 m at their bottom to some extent (Fig. 5.3b). This result is consistent with the findings of Sekiguchi and Nakai (2012), who demonstrated by a simulation study of subsurface ground structures and a seismic response analysis that (1) areas deformed by sand boiling cannot be explained only by where ground acceleration or the ground motion velocity reached maximum values, (2) the predominant S-wave period tends to be proportional to the thickness of the alluvium, and (3) the sand boil distribution reflects the distribution of shear stress in sandy beds.

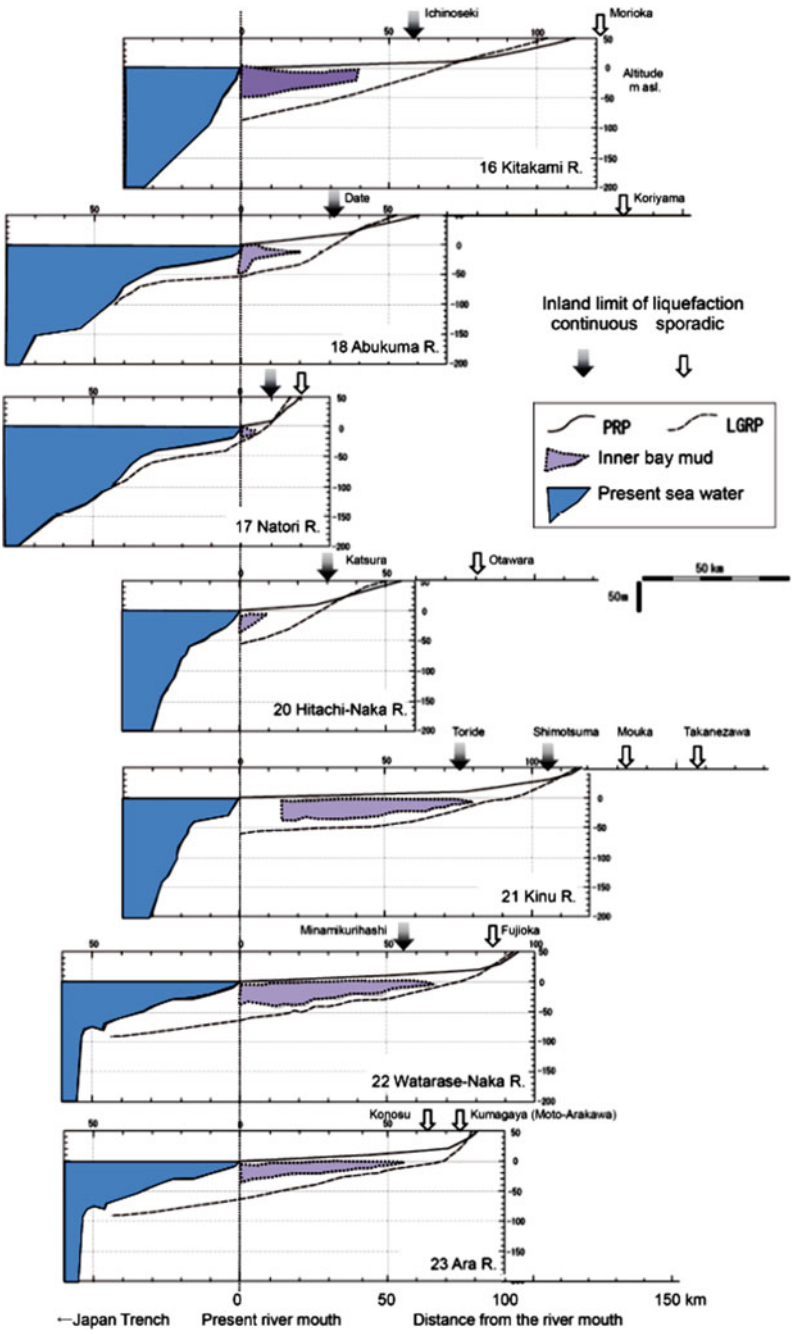

Fig. 5.4 Longitudinal profiles of seven rivers and their inland liquefaction limits. The locations of the rivers are shown in Fig. 5.2

The deeper the base is beneath reclaimed land, the longer the duration and predominant period of the S-waves will be; further, shear stress in reclaimed land and in sand bodies in the upper part of the alluvium is increased because of multiple reflections of the S-waves from the base of the alluvium.

The 2011 Tohoku earthquake produced few seismic oscillations with periods of 1 to 2 s, that is, long enough to damage low-rise structures. In many places where the alluvium was thick, however, a predominant S-wave period longer than 1 s was recorded. For example, the predominant period in the acceleration response spectrum observed at K-NET Urayasu, which is on reclaimed land on top of thick alluvium, was 1 s. Researchers have pointed out that the duration of earthquake shaking and aftershocks are more important for liquefaction than the seismic intensity or acceleration, and the duration of shaking tends to be longer in thick alluvium (e.g., Yoshida 2010; Urayasu City Liquefaction Countermeasure Technology Consideration Investigating Committee 2012). The upper part of the alluvium itself may become liquefied, depending in part on the thickness of the alluvium and the underlying basal topography. Cross sections along some coastal rivers (Fig. 5.4) show that the inland limit of continuous liquefaction caused by the 2011 Tohoku earthquake generally coincides with the upper edge of the CP, suggesting that under natural conditions, the thickness and length of the CP strongly influence the distribution of liquefaction. We explore this possibility further in the next section.

5.3 Geometric Character of Coastal Prisms in Japan

We determined the length and thickness of the CPs of 50 rivers in Japan (Fig. 5.2) by comparing the basal topography beneath their modern channels (i.e., the LGRP) with the PRP, using data published by Honda and Sugai (33 rivers; 2010) and Sugai and Honda (17 rivers; 2015) (Fig. 5.5). The gradient of the PRP is typically gentle, scarcely rising above the present sea level, especially where deltas have formed at the river's mouth, whereas the LGRP tends to have a steep gradient and very little concavity; almost all LGRPs have slope greater than 1 ‰ at the downstream end (at 10 km section from the present river mouth) if post-glacial crustal deformation was considered in the reconstruction of the LGRP (Honda and Sugai 2011). The groundwater table in the present alluvial plain is generally very shallow, and the presence of the BG at the base of the CP suggests that the tractive force on the steep slope was large enough to transport gravel and form gravel body. Shallow groundwater table, the presence of the BG, and thickening CP toward river mouth are important factors controlling liquefaction potential. Moreover, in Japan, rivers generally transport large amounts of coarse sediment to the coastal area, leading to the formation of deltas, natural levees, beach ridges, and sand dunes. As a result, the upper part of the CP often contains large amounts of sand, which can become a source of liquefied material.

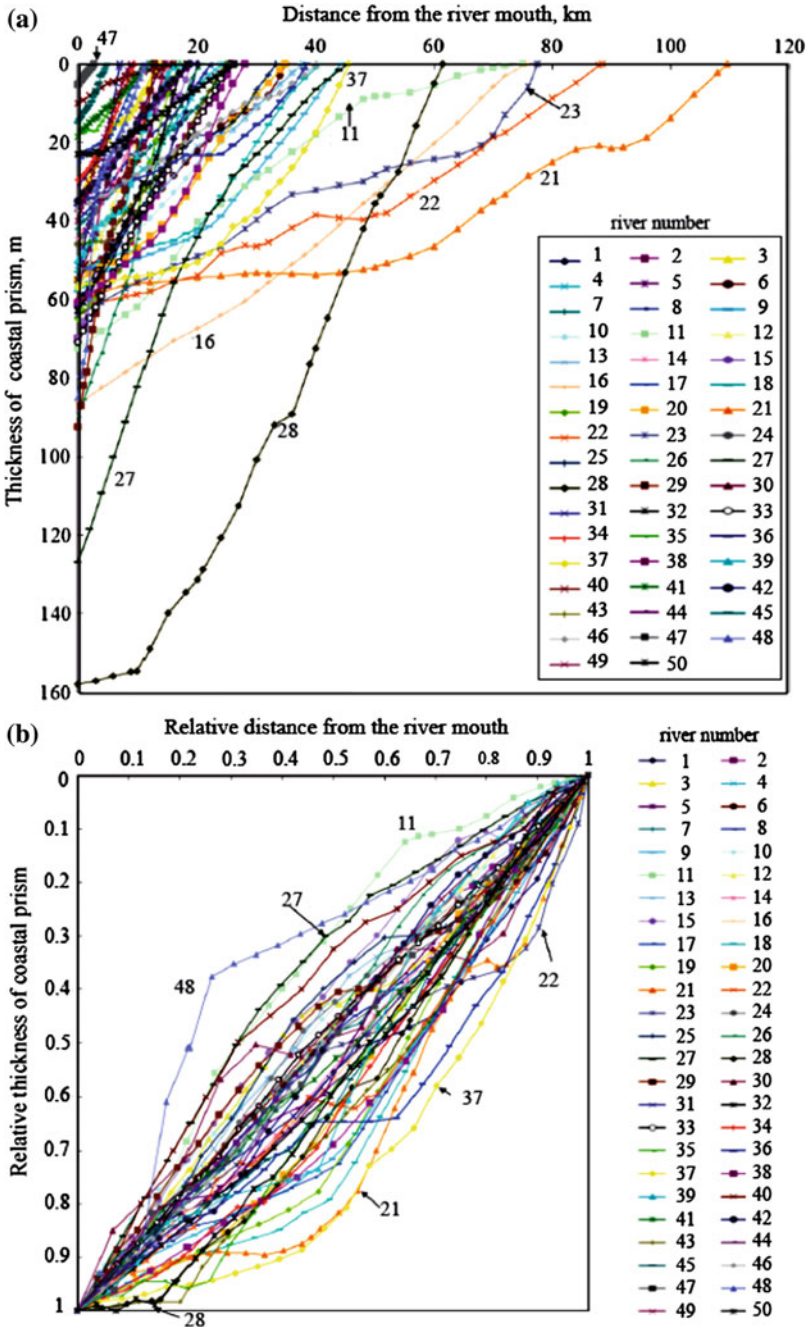

Fig. 5.5 Relationships between **a** the coastal prism (CP) thickness and distance from the river mouth along the 50 studied rivers, and **b** the normalized CP thickness and the normalized distance from the river mouth. CP thickness is defined as the difference in elevation between the present river profile (PRP) and the last glacial river profile (LGRP) (see Fig. 5.1). The locations of the rivers are shown in Fig. 5.2. Modified after Sugai and Honda (2015)

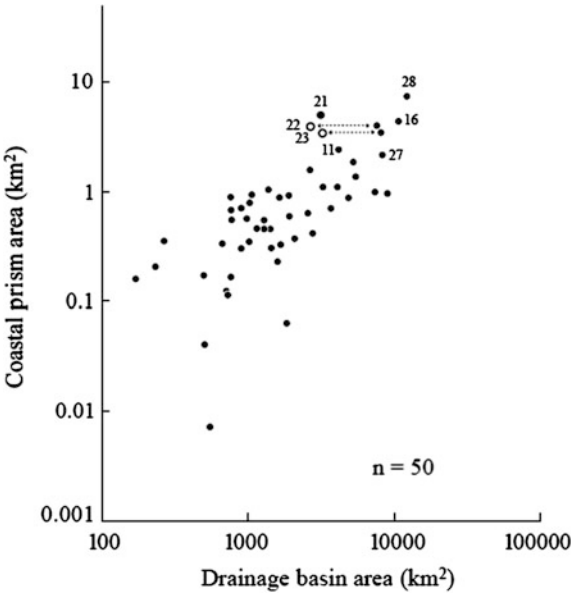

Fig. 5.6 Relationship between the coastal prism area and the drainage basin area of the 50 studied rivers. The locations of the rivers are shown in Fig. 5.2. *Open circles* (river no. 22, 23) indicate the drainage basin area when the upper Tone river basin does not join into the Ara and Naka (Furutone) rivers

To evaluate dimensions of the CP, we define a CP's area as integrated value of the thickness of CP from river mouth to upstream edge of CP along the river valley (Fig. 5.5a and Table 5.1) for simplicity, although the CP is 3-dimensional. The area of a river's CP is proportional to the river basin area for 50 rivers (Fig. 5.6).

In general, rivers with a larger drainage basin tend to deposit alluvium further inland, so they have a longer CP. The rate at which CP depth decreases inland varies, depending on the river. The CP of the Agano and Shinano rivers (nos. 27 and 28), which is very thick near the river mouth, decreases rapidly in thickness with distance inland from the river mouth (Fig. 5.5a), because rapid (several millimeters annually) tectonic subsidence and compaction have occurred along the coast (Niigata Geotechnical Survey Association 2002). In contrast, the Kinu, Naka (Furutone), and Ara rivers in the Kanto region (nos. 21, 22, and 23) have a different CP geometry; the CP remains relatively thick even far from the river mouth (Fig. 5.5a). In the Kanto basin (area about 17,000 km^2), tectonic subsidence has occurred at a rate of about 0.1 mm/y, but the sedimentation rate has exceeded the subsidence rate (Sugai et al. 2013). As a result, the CPs of these rivers are thick. The Kinu River CP is thicker in the downstream region of the Ryugasaki Lowland (Kaizuka 1987), whereas the Ara River CP is thicker in upstream Menuma Lowland (Hirai 1983; Ishihara et al. 2012; Fig. 5.5b); both lowlands are known as local tectonic subsidence centers. This indicates local tectonic subsidence has modified the shape of coastal prism.

5.4 Liquefaction and Coastal Prisms

5.4.1 Relationship Between the Inland Limit of Liquefaction and CP Length and Thickness

In Mihama and Urayasu, where the alluvium depth exceeds 30 m, liquefaction was extensive. Hence, we focus here on parts of the CPs that are at least 30 m thick. We defined CPl_{d30} as the distance from the present river mouth to the point where the CP thickness (depth) was 30 m (km) and measured this distance along 44 of the 50 rivers. The maximum CP depth of the remaining six rivers (i.e., the Natori, Kako, Chigusa, Monobe, Yamaguni, Kikuchi rivers; nos. 17, 40, 41, 45, 47, and 50, respectively) was less than 30 m. We defined the ILL during targeted earthquakes as the distance to furthest inland liquefaction site from the river mouth, among the sites listed by Wakamatsu (2011) and Wakamatsu and Senna (2013).

Targeted earthquakes were the 2011 Tohoku earthquake and historical earthquakes that, according to Wakamatsu (2011), caused liquefaction in our targeted river basins. For simplicity, we ignored inland earthquakes (those with epicenters upstream of the CPs). We examined the relationship between the ILL and CPl_{d30} of each river for each earthquake (Fig. 5.7a). Many ILLs are plotted above the dashed line in Fig. 5.7a; these are further inland than the CPl_{d30} point.

Along seven rivers with a maximum CP thickness of over 30 m, there is no record of liquefaction (i.e., the Yubetsu, Saru, Hei, Kurobe, Onga, Oita, and Omaru rivers; nos. 3, 8, 15, 29, 46, 48, and 49, respectively). Records of previous liquefaction along the Hei River (no. 15) may have been destroyed by the tsunami that was generated by the 2011 Tohoku earthquake.

Among the 50 rivers, only five had CPl_{d30} values that exceeded 40 km (i.e., the Kitakami, Kinu, Naka (Furutone), Ara, and Shinano rivers; nos. 16, 21, 22, 23, and 28, respectively). Liquefaction was induced along all of these rivers, except along the Shinano River, by the 2011 Tohoku earthquake.

5.4.2 Inland Limit of Liquefaction and the Distance from River Mouth to the Upper Edge of the Coastal Prism

We next examined the relationship between ILL and the distance from river mouth to the upper edge of the CP (CPl_{max}) for the 50 rivers (Fig. 5.7b). Liquefaction occurred beyond the upper edge of the CP only during huge subduction-zone earthquakes, which sometimes liquefied sediments in inland basins such as the Koriyama basin along the Abukuma River (e.g., no. 18).

Among the 50 rivers, the Kinu, Naka (Furutone), and Ara rivers (nos. 21, 22, and 23) in the Kanto basin had the longest CPs, which remained thick far upstream.

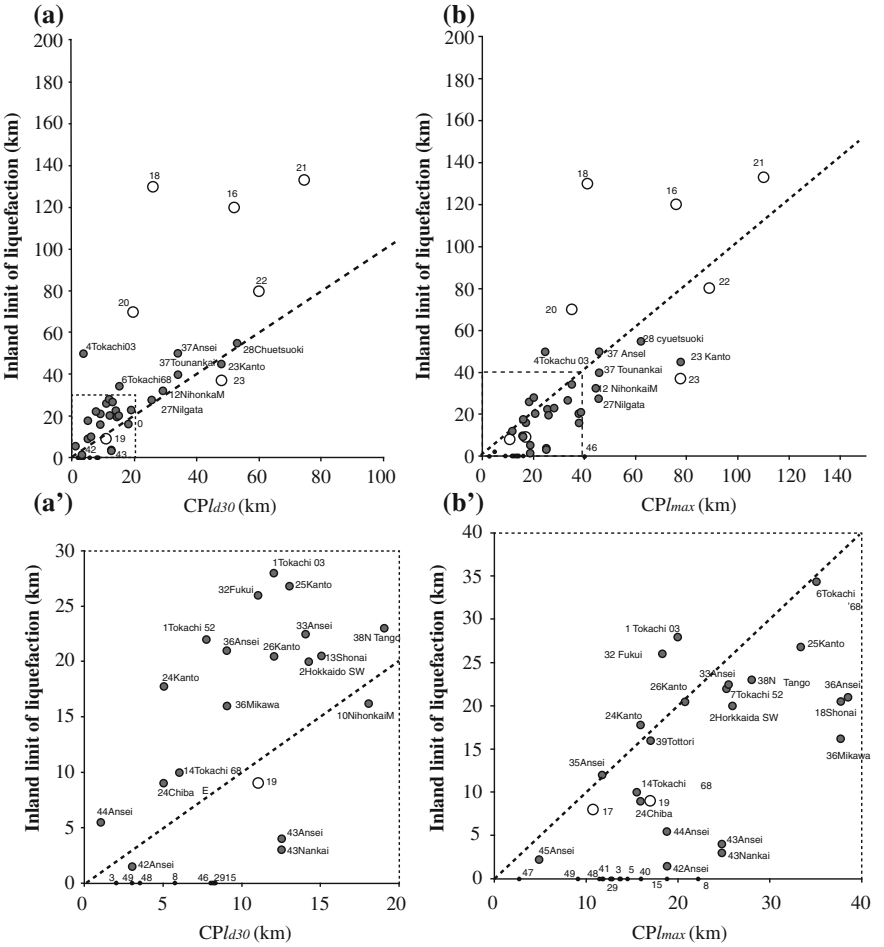

Fig. 5.7 Relationships between (a and a') the inland limit of liquefaction (ILL) and the distance from the river mouth to the point where the alluvium thickness was 30 m (CPl_{d30}), and (b and b') the ILL and the distance to the upper end of the coastal prism (CPl_{max}). The *dashed lines* are 1:1 lines. Sites of liquefaction induced by the 2011 Tohoku earthquake are indicated by *open circles* labeled with the river number. Sites of liquefaction induced by other submarine earthquakes, including subduction-zone earthquakes and other earthquakes in coastal areas, are indicated by *small gray circles* labeled with the river number and earthquake name; the earthquakes are listed in Table 5.2. For each river, only the furthest two earthquake-induced liquefaction sites are plotted. The *black dots* along the horizontal axis (i.e., ILL = 0 km) indicate rivers along which there is no record of liquefaction induced by any earthquake. Liquefaction in the Omono, Mogami, and Agano river basins (no. 10, 13, and 27) is not shown in Fig. 5.7 because these rivers drain into the Japan Sea. Modified and simplified from Sugai and Honda (2015)

Along these rivers, muddy inner bay sediments also extended far inland. Along with the extensive land reclamation, these natural conditions in the Kanto region may have enabled extensive liquefaction during earthquakes.

5.4.3 Relationship Between Liquefaction and CP Dimensions and Facies

Pore water pressure in sandy sediments tends to increase as the duration of incident S-waves in the CP increases. The duration is controlled by the dimensions of the CP and the mechanical impedance of its basal surface. In Japan, the bottom of a CP (the LGRP) is generally a BG; a clast supported gravel body of high ground strength with a steep longitudinal gradient (e.g., Honda and Sugai 2011), whereas the CP itself is characterized by soft sediments and a high water content. These facts suggest that, in addition to geomorphology and land reclamation, CP thickness and length are important factors contributing to liquefaction. Thus, we think the liquefaction risk at coastal sites on an alluvial plain above a thick CP is higher than the risk further upstream where a thin layer of alluvium overlies the basement rocks.

For CPs of the same thickness, however, the presence of inner bay mud may make liquefaction more likely. Along the Kitakami River, which has a long, thick CP, inner bay mud extends 40 km inland from the river mouth (Fig. 5.4) (Ito 1999). Along the Kinu and Naka (Furutone) rivers, inner bay mud extends nearly to the upstream edge of the CP.

If tectonic subsidence and fluvial sedimentation were negligibly small in comparison with the post-glacial sea-level rise, then the Holocene eustatic sea-level curve (Fig. 5.8) implies that seawater invaded incised valleys that were deeper than −30 m relative to the present mean sea level at around 9.5 kyr BP and in the resulting inner bay environment deposited soft muddy sediments. Figure 5.8 also implies that seawater hardly invaded the river valleys shallower than −20 m with the slowdown of the sea-level rise at around 9 kyr BP. Japanese rivers with a CP thickness of more than 20 m sometimes contain inner bay muddy sediments, and those with a CP thickness exceeding 30 m usually have inner bay mud (Fig. 5.9).

In addition to loose, sandy incised-valley fill, sandy sediments in natural levees, river channels, dunes, and beach ridges in the uppermost part of the CP may become liquefied during an earthquake. If such sand bodies are buried under muddy flood deposits, they may not be visible as microscale landforms, but the overlying mud may effectively increase the pore pressure within them during earthquakes,

Fig. 5.8 Holocene sea-level changes modified and simplified after Siddall et al. (2003)

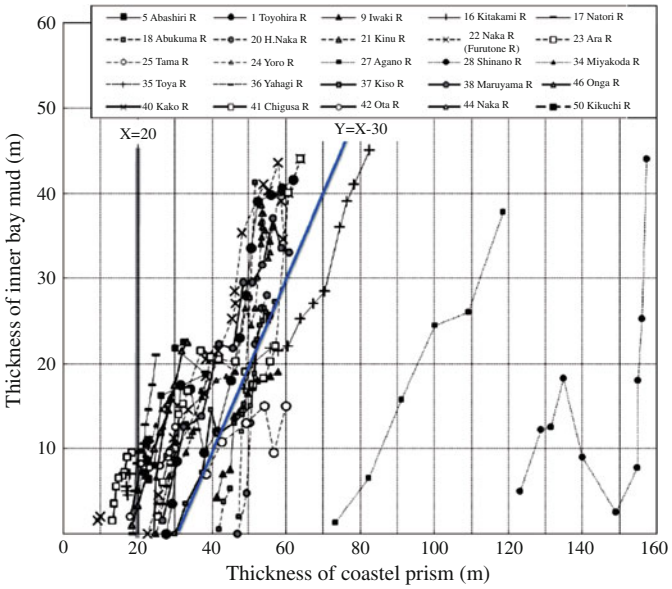

Fig. 5.9 The relationship between the thickness of inner bay mud and alluvium thickness within the CPs of 25 rivers in Japan

making their liquefaction more likely. Therefore, to evaluate liquefaction risk, the buried microtopography of a CP, as well as whether artificial fill is present, must be known.

5.5 Conclusions and Future Study

Severe liquefaction occurred in the Kanto region during the 2011 Tohoku earthquake. The main cause is considered to be intense human modification of landforms. Thus, land reclamation and the filling of shallow marine, lakes, and river channels with sandy sediments caused the liquefaction damage to be more serious because the artificial fill sediments liquefied (e.g., Wakamatsu and Senna 2014; Une et al. 2015). Moreover, microscale geomorphic features such as natural levees, swamps, and river channels also controlled the local distribution of sand boils (e.g., Senna et al. 2012; Nakano et al. 2015). In addition to such surface features, it is also important to consider buried landforms that formed during the last 20 ka.

This chapter focused on the geometry of coastal prisms composed mainly of incised-valley fills. The tectonic movements that formed the Kanto basin, coupled with a large fluvial sediment supply, caused the CPs in the Kanto region to be long, thick, and relatively weak; these subsurface conditions probably led to intensified liquefaction damage there. The Kinu, Naka (Furutone), and Ara rivers on the Kanto

Plain have the longest CPs among the studied rivers, and their CP thicknesses decrease only slightly inland.

We targeted only 50 rivers, and their incised-valley geometry is not known in detail. High-resolution reconstruction of the buried valley topography is an important future task toward mitigating liquefaction disasters.

Four plates converge in and around the Japanese archipelago, and deep ocean trenches in the Pacific Ocean run parallel to the Japanese islands. The continental slope is steep, and the continental shelf is narrow. As a result, during the glacial sea-level lowstand, rivers became deeply incised. Then, as sea level rose during the post-glacial periods, the fluvial sediment supply increased, and thick coastal prisms composed of unconsolidated sediments formed during the Holocene. Large cities and important infrastructure have been constructed on the coastal prisms. Submarine earthquakes, especially huge subduction-zone earthquakes, along with high precipitation due to the monsoonal climate, increase the vulnerability of these cities to natural disasters such as soil liquefaction, tsunamis, and flooding. For future natural disaster prevention and mitigation, knowledge of the three-dimensional geometry of coastal prisms and the evolutionary processes that produced them is essential.

Acknowledgments This study was supported in part by Japan Society for the Promotion of Science grants-in-aid for Scientific Research (A 2424011, B2628207). We would like to thank Tokyo Geographical Society for permission to reproduce in part for Figs. 5.3, 5.5, and 5.6.

References

Aoyama M, Koyama T, Une H (2014) Geomorphological condition and land history of liquefaction damaged sites in the lower part of the Tone river lowland induced by the 2011 off the Pacific coast of Tohoku earthquake. Geogr Rev Jpn 87:128–142 (in Japanese with English abstract)

Chiba Prefectural Environmental Research Center (2011) Liquefaction-fluidization phenomena and its damages in Chiba Prefectural at the 2011 earthquake off the Pacific coast of Tohoku, Central Japan. Part 3 Urayasu district (1) Research Report G8-3:1–25. (in Japanese). (http://www.pref.chiba.lg.jp/wit/chishitsu/ekijoukahoukoku/)

Chiba Prefectural Environmental Research Center (2012) Liquefaction-fluidization phenomena on Boso peninsula at the 2011 earthquake off the Pacific coast of Toholu, Central Japan. Part 5 eastern part of Research Report G8-5:1–8. (in Japanese). (http://www.pref.chiba.lg.jp/wit/chishitsu/ekijoukahoukoku/)

Endo K, Kosugi M, Hishida R (1988) Holocene and latest Pleistocene deposits and their basal topography in the, central Japan. Proc Inst Nat Sci Nihon Univ 23:37–48 (in Japanese with English abstract)

Endo K, Ishiwata S, Hori S, Nakao Y (2013) Tokyo lowland and chuseki-so formation of the soft ground and Jomon transgression. J Geogr (Chigaku Zasshi) 122:968–991

Hirai Y (1983) Geomorphic development of the alluvial lowlands in the central part of the Kanto Plain, Japan. Geogr Rev Jpn 56:679–694 (in Japanese with English abstract)

Honda K, Sugai T (2010) Distribution of alluvium in the Japanese archipelago: geomorphologic development models for evaluating the vulnerability of alluvial lowland to natural disasters. J Geogr (Chigaku Zasshi) 119:924–933 (in Japanese with English abstract)

Honda K, Sugai T (2011) Late quaternary change in the longitudinal profiles of rivers in Japan. Trans Japanese Geomorphological Union 32:293–315 (in Japanese with English abstract)
Inazaki T, Ota Y, Maruyama S (2014) The largest and longest project in Japan—spanning over 400 years: river improvement works in the Kanto plain and constraints of tectonic setting. J Geogr (Chigaku Zasshi) 123:401–433 (in Japanese with English abstract)
Ishihara T, Sugai T, Hachinohe S (2012) Fluvial response to sea-level changes since the latest Pleistocene in the near-coastal lowland, central Kanto Plain, Japan. Geomorphology 147–148:49–60
Ito A (1999) Holocene geomorphic development of the Kitakami river Lowland, Northeastern Japan. Q J Geogr 51:1–18 (in Japanese with English abstract)
Kaizuka S (1987) Quaternary crustal movements in Kanto, Japan. J Geogr (Chigaku Zasshi) 96:223–240 (in Japanese with English abstract)
Kaizuka S, Naruse Y, Matsuda I (1977) Recent formations and their basal topography in and around Tokyo Bay, central Japan. Q Res 8:32–50
Kazaoka O (2013) Liquefaction-fluidization horizons and geological structure in man-made strata: examples of geological survey for elucidation of mechanism and defense against liquefaction fluidization. GSJ Chishitsu News 2:371–375 (in Japanese)
Koarai M, Nakano T, Otoi K, Une H, Kawamoto R, Daigo K (2011) Liquefaction damages of the East Japan great earthquake and evaluation of liquefaction risk using geospatial information. J Geospatial Inf Auth Jpn 122:127–141 (in Japanese with English abstract)
Komatsubara J, Mizuno K, Ishihara Y, Ishihara T, Yasuhara M, Inamura A, Kazaoka O (2014) Relationship between liquefaction and geology in the downstream basin of the Tone River. Research Planning Office for Geological Survey and Applied Geoscience (ed) Reports of research and investigation on multiple geological hazards caused by huge earthquakes. GSJ Interim Report 66:245–272 (in Japanese with English abstract)
Kumaki Y, Koarai M, Nakano T (2013) Land transformation in Tokyo and its surrounding regions. J Geogr (Chigaku Zasshi) 122:992–1009 (in Japanese with English abstract)
Mattheus CR, Rodriguez AB (2011) Controls on late quaternary incised-valley dimension along passive margins evaluated with empirical models. Sedimentology 58:1113–1137
Miall A (2014) Fluvial depositional systems. Springer, Berlin, 316 p
Ministry of Land, Infrastructure, Transport and Tourism, and the Japanese Geotechnical Society (2011) Report on the liquefaction phenomena in the Kanto region during the 2011 off the Pacific coast of Tohoku earthquake, 69 p (in Japanese). http://www.ktr.mlit.go.jp/bousai/bousai00000061.html
Nakamura Y (2012) Ground liquefaction in Tochigi Prefecture due to the 2011 Tohoku earthquake. Utsunomiya University project report toward reconstruction and recovery from the Great East Japan earthquake—Elucidation of the ground disaster and its mechanism in the northern part and eastern part of Tochigi Prefecture, Chapter 6:50–68 (in Japanese)
Nakano T, Koarai M, Une H (2015) Reconsideration of hazard assessment standard for land liquefaction using landform classification data. J Geogr (Chigaku Zasshi) 124:259–271 (in Japanese with English abstract)
Niigata Geotechnical Survey Association (2002) Sub-ground map of Niigata Prefecture and its explanatory book. 4- Sheets and 66 p. (in Japanese)
Senna S (2013) Relationship between liquefaction occurrence ratio and strong ground motion duration for the 2011 off the Pacific coast of Tohoku earthquake. GSJ Chishitsu News 2:367–370 (in Japanese)
Senna S, Hasegawa N, Maeda T, Fujiwara H (2012) Liquefaction damage of the Tonegawa basin caused by the 2011 off the Pacific coast of Tohoku earthquake. J Jpn Assoc Earthq Eng 12–5:143–162 (in Japanese with English abstract)
Sekiguchi T, Nakai S (2012) Effects of surface soil structure on liquefaction damage in Mihama Ward of Chiba City. J Jpn Assoc Earthq Eng 12–5:21–25 (in Japanese)
Seto M (2011) Liquefaction in the Watarase flood control pond and Minami-kurihashi, Saitama Prefecture. In: Annual report of Geosphere Research Institute of Saitama University 10:x–xii (in Japanese)

Siddall M, Rohling EJ, Almogi-Labin A, Hemleben Ch, Meischner D, Schmelzer I, Smeed DA (2003) Sea-level fluctuations during the last glacial cycle. Nature 423:853–858

Sugai T, Matsushima (Ogami) H, Mizuno K (2013) Last 400 ka landform evolution of the Kanto plain: under the influence of concurrent glacio-eustatic sea level changes and tectonic activity. J Geogr (Chigaku Zasshi) 122:921–948 (in Japanese with English abstract)

Sugai T, Honda K (2015) Distribution of alluvium, historic liquefaction sites, and liquefaction following the 2011 Great East Japan earthquake. J Geogr (Chigaku Zasshi) 124:273–286 (in Japanese with English abstract)

Urayasu City Liquefaction Countermeasure Technology Consideration Investigating Committee (2012) Urayasu city liquefaction countermeasure technology consideration investigation report. The 2nd piece grasp of ground property and attribution analysis of liquefaction. 81 p (in Japanese). (http://www.city.urayasu.chiba.jp/menu11324.html)

Une H, Aoyama M, Koyama T, Hasegawa T (2015) Improvements to hazard map of Abiko city based on liquefaction damage. J Geogr (Chigaku Zasshi) 119:287–296 (in Japanese with English abstract)

Wakamatsu K (2011) Maps for historic liquefaction sites in Japan, 745–2008. Univ. Tokyo Press. 71 p + DVD-ROM. (in Japanese with English abstract)

Wakamatsu K, Senna S (2013) Liquefaction by the 2011 off the Pacific coast of Tohoku earthquake and historic liquefaction. Geology and Survey (Chishitsu to chosa: Japan Geotechnical Consultants Association) 138:6–11 (in Japanese)

Wakamatsu K, Senna S (2014) Liquefaction and their site conditions in Tohoku region during the 2011 Off the Pacific coast of Tohoku earthquake. J Jpn Assoc Earthq Eng 14:124–143 (in Japanese with English abstract)

Wakamatsu K, Senna S (2015) Liquefaction and their site conditions in Kanto region during the 2011 Off the Pacific coast of Tohoku earthquake. J Jpn Assoc Earthq Eng 15:25–44 (in Japanese with English abstract)

Yasuda S, Harada K (2011) Liquefaction-induced damage in the reclaimed lands along Tokyo Bay. Geotech Eng Mag JGS 59:38–41 (in Japanese)

Yoshida N (2010) Earthquake response analysis of ground. Kajima Institute Publishing, Tokyo, 256 p. (in Japanese)

Chapter 6
Landform and Vulnerability for Disaster in Land Use Changing

Shigeko Haruyama

Abstract The fluvial and coastal landforms have important roles causing natural disaster and had influence on disaster-stricken area of liquefaction under the expansion of land use changing in the Tone River lowland. In this chapter, the disaster vulnerability, specific liquefaction, is designated upon several mesh maps of risk levels, landform, land use, and vulnerability transformation of liquefaction on land use changing in the case of the lower Tone River floodplain. The liquefaction vulnerability is brought by physical dimensions as the scale of earthquake, the distance from hypocentral region, landform and sedimentation, underground water table, etc., and the other hand, the human dimensions as recent rapid land use change and regional planning without knowledge of geomorphology are accelerating higher vulnerable level, low resilience, and longer period for resuscitation from disaster. The land use changing with urban sprawl on site has been inducing to be new and transforming vulnerability level. Geomorphology demonstrates landform process and explaining the former natural disaster occurrence history and vulnerability level of disaster; therefore, understanding disaster vulnerability on site in the fluvial and coastal plain would support future regional planning toward to secure from disaster mitigation and appropriate land use pattern planning should be discussed in future. The essential of risk reduction needs appropriate sustainable education, and the geomorphology should be core subject due to secure for lives.

Keywords Vulnerability · Fluvial landform · Coastal landform · Land use change · Liquefaction · Risk · Landform · Mesh map

S. Haruyama (✉)
Graduate School of Bioresource, Mie University, 1577 Kurimachiyacho,
Tsu Mie Prefecture, Japan
e-mail: haruyama@bio.mie-u.ac.jp

S. Haruyama and T. Sugai (eds.), *Natural Disaster and Coastal Geomorphology*, DOI 10.1007/978-3-319-33814-9_6

6.1 Review of Previous Research into Liquefaction During Earthquakes in Japan

The 2011 East Japan earthquake (*Mw* 9.0) and tsunami caused major damage along Pacific coast of northern Japan. Damage due to seismic shaking, liquefaction, tsunami intrusion, inundation in web and tide after tsunami and subsidence was severe in specific urban and industrial areas, and production loss in agriculture production area, isolation of rural residential areas, and fishing village swept away in Tohoku region. Taresawa and Haruyama (2013) pointed out that the local response of earthquake and tsunami at 2011 East Japan earthquake was different in each community activity and in each landform because of different understanding disaster. Damage due to liquefaction was widespread on the fluvial and coastal plain of the lower Tone River Basin and the worst damage on the coastal plain around Tokyo Bay because of density population on widespread reclaimed lands. In Katori city (Chiba Prefecture) where is located on the lower Tone River floodplain, liquefaction destroyed residential area during the 2011 East Japan earthquake and disaster-stricken were to stop important lifelines (water supply, gas supply, electricity supply, etc.) for long period after earthquake (Haruyama and Naruse 2013).

Wakamatsu has studied historical liquefaction events in Japan and proofed evidences in Geographical Information System, and liquefaction evidence in Kanto plain was also reported by Wakamatsu in the 1987 Eastern Chiba earthquake, and she emphasized that the boundary area between natural levee and back marsh was vulnerable zones for these liquefaction outbreaks, and reported that natural levee zone along the lower Shinano River was severe damaged by liquefaction in 1964 Niigata earthquake (Wakamatsu 1993) and recurrent liquefaction in the lower Tone River floodplain induced by the 2011 East Japan earthquake (Wakamatsu 2012). Kotoda et al. (1993) proved that surface geology contributed to increase risk potential of liquefaction during earthquakes, and they developed the method of preparing of maps for showing the distribution areas susceptible to this phenomenon. Oya et al. (1989a, b) identified that the appropriate knowledge of landform as important key for understanding had the likely locations and processes of earthquakes in a study of the distribution of liquefaction in the lower Mogami River floodplain (Yamagata Prefecture in Japan). The large damaged Hanshin region in Japan effected by 1995 Hanshin-Awaji earthquake was explained to be related to fault existence (Suzuki et al. 1996) and Takahashi (1996) pointed out that the house collapsed zones were strongly related to liquefaction points on the landform classification map of Hanshin region. Komatsubara (2006) analyzed the relationship between micro-topography and earthquake damage for the 1894 Meiji earthquake to show that 30 % of the houses destroyed by the earthquake were proved in three geomorphologic environments: along former meanders of the Mogami River, on Holocene marine terraces, and on the landward edge of coastal sand dunes where springs were plentiful and soils were weakly stratified.

Following the 2011 East Japan earthquake, Asano et al. (2011) reported on damage to irrigation systems along the lower Tone River as a result of liquefaction.

They also reported liquefaction in Inasaki city (Ibaraki Prefecture) and Kozaki region (Chiba Prefecture). Asano et al. (2011) recognized the following five damage types of liquefaction in agricultural production areas: (1) sand boils and substantial cracking of the surface in rice fields; (2) flow of liquefied sand into drainage canals; (3) uplift or inclination of drainage canals; (4) relative gaps between drainage and irrigation facilities, etc.; and (5) water leakage from broken asbestos pipes. Severe damage to asbestos pipes was observed at Yotsuya region (Inasaki city). Damage to be piping due to liquefaction in agricultural production areas was 3.7 times greater than that in the total area of reticulated water distribution.

Wakamatsu (2012) reported the widespread liquefaction associated with the 2011 East Japan earthquake within a 650-km-long zone along Pacific Ocean coast, including 85 sites where liquefaction had occurred during previous earthquakes (e.g., 1987 Chibaken-Toho-Oki earthquake and 1978 Miyagiken-Oki earthquake). Liquefaction during that period occurred in low-lying areas underlain by water-saturated Holocene sediments, and repetitive liquefaction was occurred in response to five or more successive earthquakes in Nobi plain, Akita plain, Niigata plain, Kanto plain, Osaka plain, Kanazawa plain, Tsugaru plain, Sendai plain, and Shizuoka plain as a large floodplain in Japan.

Regarding former river courses related to liquefaction under 2011 East Japan earthquake, Koarai (2013), Koarai et al. (2015), and Koarai and Nakano (2013) reported the specific liquefaction areas in the Kanto plain, especially near Tokyo Bay and along the lower Tone River, where damage was concentrated in areas of modern land reclamation on the former river courses where sandy sediments are water-saturated using landform classification map for flood control. They checked the liquefaction points on the rapid survey map published by the Imperial Japanese Army in the early Meiji period and the specific landforms were damaged. Honma (2013) described surface evidence of liquefaction in Kanto plain including bulging and sinking of roads, uplift of manholes, leakage of water supply pipes, and disruption of vital communication and transport systems by sand boils. Responses by local residents to a questionnaire (Haraguchi and Iwamatsu 2011) about damage caused by liquefaction were different with each local community, and social and human analysis for damage is important research in this study area during the 2011 East Japan earthquake.

6.2 Landform History of the Lower Tone River

The surface and subaqueous landform units shown on the 1:30,000 scale geomorphologic land classification map of the Kasumigaura lacustrine plain was surveyed and classified fluvial and lacustrine landforms in 1983–1986 (Oya et al. 1986). The southern lacustrine lowland of this was open to Pacific Ocean and is considered to have developed under the influence of global sea-level change during the Holocene (Saito et al. 1990; Saito and Inouchi 1993; Hirai 1989; Oya et al.

1987a, b; Toyota and Ikeda 2003). On the basis of work of the author cited above, there were six stages in Holocene in geomorphologic evolution as followings; stage (I) 10,000–9000 yBP was a period of rapid sea-level rise during which a brackish inland embayment formed in connection to a branch of the Tone River. During stage (II) 9000–5500 yBP, the brackish embayment reached its maximum at Holocene high stand giving rise to transgression. Sea level fell slowly during stage (III) 5500–4000 yBP, the mouth of the embayment closed and tidal delta developed. Stage (IV) 4000–2500 yBP was a cooler period when lake was a closed lagoon confined by sand dunes. Stage (V) 2500–500 yBP was lagoon stage. After that, a cool period is included with minor fluctuations of sea level. The geomorphologic evolution was marked with landform in the bottom of lake and surrounding lowlands. The present-day floor of Lake Kasumigaura is flat (−4 to −7 m depth), and there are littoral shelves recorded sea-level change and relics of former rivers.

Starting on sixteenth century, the river-control projects were undertaken in the lower Tone River including river bed dredging, floodway construction, building new channels to connect rivers, embankment construction, and diversion channel construction. An important river management project was the construction of Akaborigawa channel joining the Tone River, where the narrow valley plain is dissected by terraces (Haruyama and Oya 1993). The past Tone River flowed mainly into Tokyo Bay until sixteenth century and the channel management projects between 1594 and 1809 joined the main Tone River with the Kinu and Kokai rivers, so that the Tone flowed through the southern Kasumigaura lacustrine plain into Pacific Ocean, as it does today. These projects are remodeling of nature of Kanto Plain supported by engineering works. This is flood mitigation project and flood prevention for conservation of the Edo castle townships located on the former Tone floodplain and to provide a secure inland transportation route between the Edo castle townships and the present lower Tone River Basin. After the project of new channel construction, the flooding events in the present lower Tone floodplain had been increasing because of rapid sedimentation in the present lower Tone and the river as progressed widely fluvial plain (Oya 1969; Kataoka 1998; Haruyama 1987; Oya and Haruyama 1987a; Oya and Haruyama 1987b; Haruyama and Oya 1993; Haruyama 1994). The reshaping of nature had been amending the driving force of disaster for man-made disaster.

Katori region has the former lagoons and wetlands associated with paleo-embayment existed until the medieval periods and the low-relief landscape with shallow groundwater was affected by repeated severe flooding between sixteenth century and nineteenth century. Although the lower Tone River has been uplifted during Holocene, the river gradient has been decreased, resulting in large volume deposition of the lower Tone. The accelerating expansion of agricultural production has increased the frequency of severe floods by shrinking the flood-retarding buffer zone of the lower plain (Oya et al. 1986; Oya and Haruyama 1987b). Because of food shortages in the middle twentieth century, the national governmental land reclamation

projects have been expanded the amount of rice fields to improve with drainage and irrigation engineering works in the lower Tone River.

The geomorphologic land classification maps of the Lake Kasumigaura and its Vicinity (1) and (2) published in 1986 (Oya et al. 1986) were bound together with purpose of description local landform and lacustrine environment for that reason why flood prevention around the lowlands of lakes and building up harmonious natural environment toward to lacustrine conservation planning in the case of changing the water level of lakes under the water resource management. There are micro-landforms on the bottom of the lake, lacustrine landforms, and Holocene terrace that provided to be the sea-level change. The author modified the above-mentioned geomorphologic land classification map and put the supplement with the geomorphologic land classification map of the Tone River lowland published by Haruyama and Oya (1993) using additional topographic data, boring data, aerial photographs taken in different periods, land condition maps, and disaster history showing lowland affected by floods and explains the lower Tone River with Kasumigaura lacustrine lowland (Figs. 6.1, 6.2).

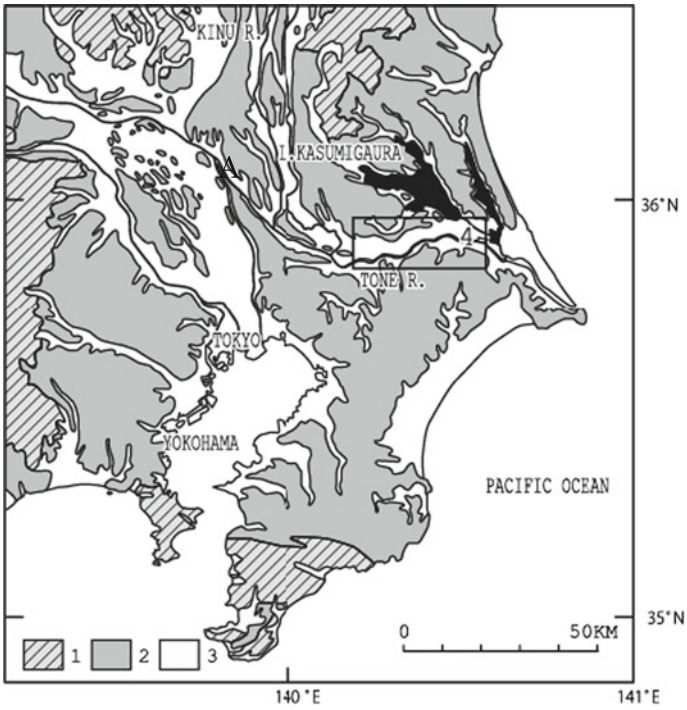

Fig. 6.1 The Tone River basin and location of study area of the lower Tone River. *Explanatory note 1*. Coastal and fluvial plain, *2*. Terrace, *3*. Hill and mountain, **a**. Akaborigawa channel (The *square* is showing the study area of this chapter and same area of Fig. 6.2.)

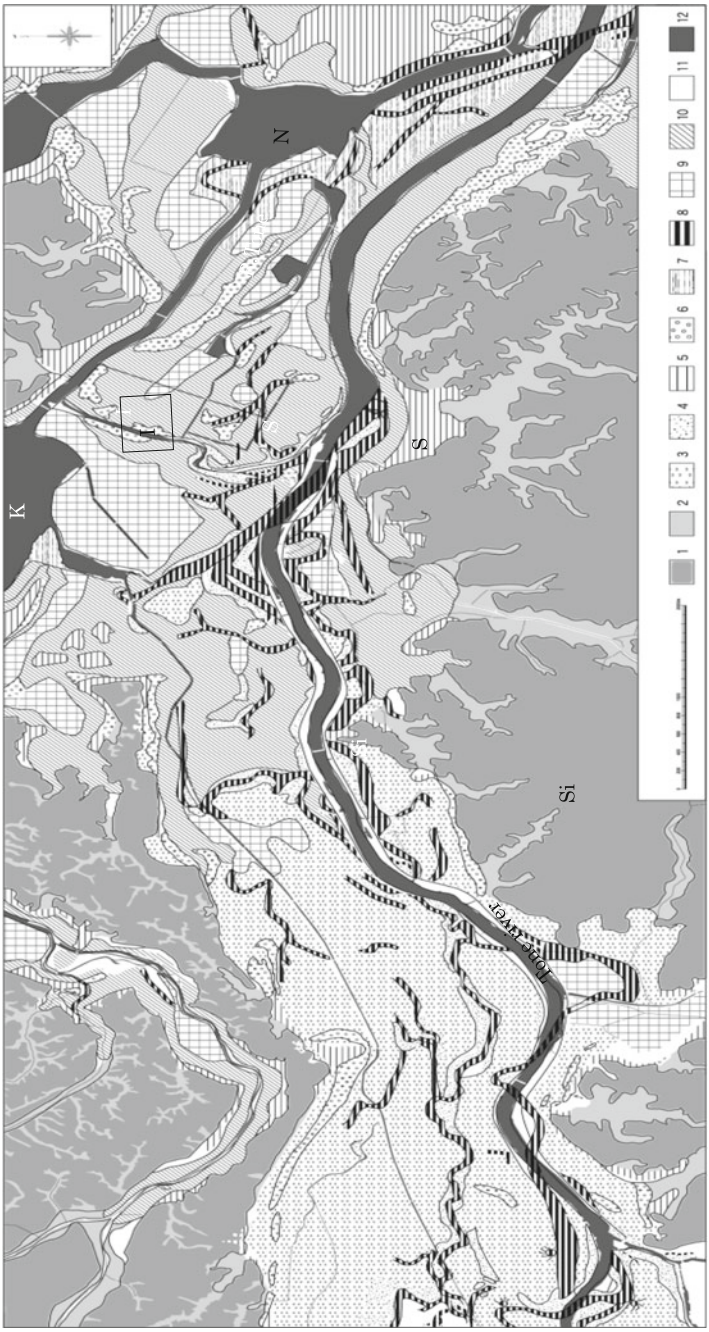

Fig. 6.2 Geomorphologic land classification map of the lower Tone River. *Explanatory note* Landform unit as followings; *1*. Terrace, *2*. Valley plain, *3*. Sand ridge, *4*. Natural levee, *5*. Lower terrace, *6*. Back swamp and flood plain, *7*. Delta, *8*. Former river course, *9*. Former lagoon, *10*. Lacustrine terrace, *11*. River Bed, *12*. Water surface (Local names are as followings; I: Isoshima, K: Kasumigaura Lake, N: Nasakaura, S: Sawara city, Si: Shimofusa terrace)

The typical landform combination of coastal and fluvial plains in Japan is given to [alluvial fan +natural levee (with back swamp) + delta], and there are several landform combination types as followings in Japan; [alluvial fan + sand dune], [natural levee (with back swamp) + delta], [large natural levee (with back swamp) + fan delta + sand dune], [fan + fan delta], etc. The location of the coastal and fluvial plain, the depth of fluvial and coastal sedimentation, geologic and geomorphologic condition of the upper and middle reaches, and local climate condition, and the other natural environmental factors are forming different landform combination types. The landform combination type was usable as subjects for understanding specific flooding types and planning of engineering for river management (Oya 1993). The lower Tone River plain proves one of the models of landform combination, [natural levee (back swamp) + delta + sand dune]. The alluvial terraces or lacustrine terraces formed during the Holocene lie adjacent to and below the Shimofusa terrace, and they are categorized as fluvial sedimentation process under the middle Holocene higher sea level. Lacustrine terraces are classified in each elevation, 4–8 m and 1.8–3.0 m, respectively, and these are relics of remarkable sea-level fluctuations. Lacustrine lowlands are developed around Lake Kasumigaura and there are reclaimed land between lakes and the Tone River. The alluvial plain includes as following landform: alluvial terrace, dissected valley plain, sand spit, sand dune, natural levee with back swamp, former river course, lagoons, and reclaimed land. Related to sea-level changes in Holocene, there are littoral shelves in Lake Kasumigaura and lacustrine terraces around the lakes as followings: littoral shelves (200–500 m wide) are developed along the lake shores, littoral shelf I lies at water depths of 1–1.5 m, and littoral shelf II at depths of 2–3.5 m. Small cliffs or steep slopes commonly separate Littoral shelf types I and II. The elevation of lacustrine terrace is 5–8 m and 2–3 m in generally Oya et al (1986).

6.3 Landform and Liquefaction of the Lower Tone

Comparing geomorphologic land classification map with liquefaction zones in the lower Tone River after 2011 earthquake (Fig. 6.3), the greatest liquefaction occurrence areas were generally located on built-up areas in former lagoons, such as Hinode and Motoshin, and the other remarkable damages were occurred in the reclaimed former river courses and reclaimed land in the geomorphologic view. The boundary between natural levee and back marsh was another target area of liquefaction point. Some liquefaction points were located on the lowland under the buffs around terrace and hills. Photo 6.1 shows an example of liquefaction point on the reclaimed former river course of the lower Tone River, and Photo 6.2 is the occurrence point on the reclaimed former lagoon (Fig. 6.3). The paddy fields are

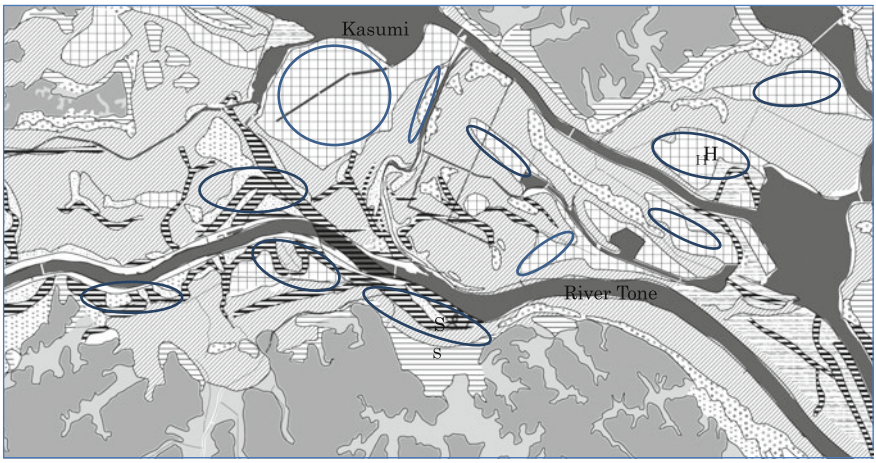

Fig. 6.3 The studied liquefaction indications on the geomorphologic land classification map of the lower Tone River basin. *Explanatory note Circles* are indication of liquefaction, H; Hinode, S; Sawara

Photo 6.1 Liquefaction point at Sawara located in the former river course (taken in July 2011)

target areas of liquefaction with small damage, but the differential settlement and boiling sand with water gave damage to the economy in urban area.

The boiled sand at several points related to the following landform in the lower Tone River as reclaimed and refilling former lagoon, the reclaimed former river course, the boundary between natural levee, and flood plain under 2011 earthquake in this study area, and the spout out sands were collected for analysis of grain size distribution in each landform. The grain size distribution curves of liquefaction points

Photo 6.2 Differential settlement landscape at Hinode reclamation area in the former lagoon (taken at July 2011)

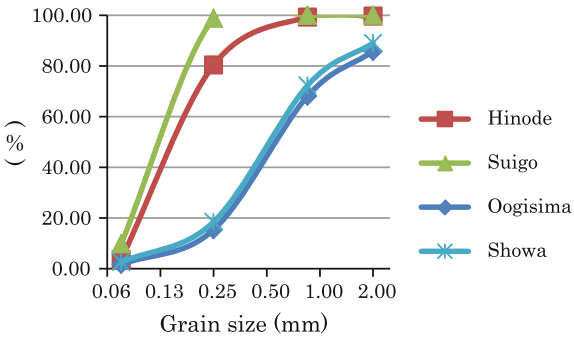

Fig. 6.4 Grain size distribution of liquefaction sand in the lower Tone River

are similar in sand ridge and natural levee boundary, and former lagoons in this study area (Fig. 6.4). The damages by liquefaction are shown in Photos. 6.3, 6.4, 6.5, 6.6, and the some buildings showed differential settlement, and electric pillars were lean because of boiling sand with water in the lower Tone River Basin. The emission of spray of sand and water was in paddy field and the line of holes with cracks buried by sands in the study area. The median grain size was investigated in the range from 0.05 to 0.9 mm and sandy. The grain size distribution of sediment on natural levee is difference from those of former lagoons. Average grain size is 0.66 mm at Sawara, 0.578 mm at Hinode, 0.059 mm at Showa, and 0.071 mm at Oogisima, and the grain size is larger on reclaimed former river course. There appears to be a relationship between areas of liquefaction and depth to the underground water table. The underground water level in this study area is generally shallower in the former river course related to sedimentation such as fine sand in the bottom of the channel landform.

Photo 6.3 Liquefaction of the boundary between natural levee and flood plain at Oogisima (taken in July 2011)

The former river courses are concentrated in liquefaction, specific reclamation or refilled area. There appears to be a relationship with depth to the underground water table, and the underground water level is generally shallower in former river course related to sedimentation such as fine sand in the bottom of the channel landform. The combined effect of shallow underground water table and grain size appears to contribute for vulnerability of liquefaction. The geomorphologic land classification

Photo 6.4 Liquefaction points on the boundary line between sand ridge and flood plain at Showa (taken in July 2011)

Photo 6.5 Liquefaction at Hinode reclaimed land and boiling sand (taken in July 2011)

Photo 6.6 Gymnasium hall of elementary school in Hinode getting sand bald of building (taken in July 2011)

map shows a close relationship between landform, grain size distribution, and liquefaction occurrence points.

6.4 Land Use Changes Linked with Vulnerability in this Study Area

The recent land use pattern has been decided to be convenience of transportation and the pleasant of life with living condition, and the nature-oriented land use has been exchanged with urban sprawl in the absence of order. In the lower river basin, natural levee zones have been developed for livelihood zone and swampy areas have been continuing to be natural resources or paddy field remaining to be

wetland. After collecting the land use data comparing with the recent 50 years land use change, the different two land use patterns were done for clarifying the distribution transform of land use changes in the lower Tone River.

The first land use pattern is shown in the 1960s rural land scape (Fig. 6.5) and there are former lagoon and back swamp widely covered by paddy fields, and natural levee and sand ridge covered by upland crop fields and specific mulberry fields with rural residences, and some dotted rural landscapes. These land use patterns are nature-oriented. The hill and terraces were used to be upland crop field with hedge and the secondly forest. The lacustrine terraces and sand ridges were occupied by rural landscape with hedges, and the urban core of Sawara was located on sand ridge. The urban area has been extended to more inland moving forward to land reclamation and exploitation of natural resource in hinterland. The land reclamation projects have allowed wetland and lagoon near Sawara to be urbanized. Hinode region was reclaimed in the 1960s for develop of backward regions of new industrial zone. The land use situation of the study area is one of the typical regional development styles under the period when the economy progressed and the early

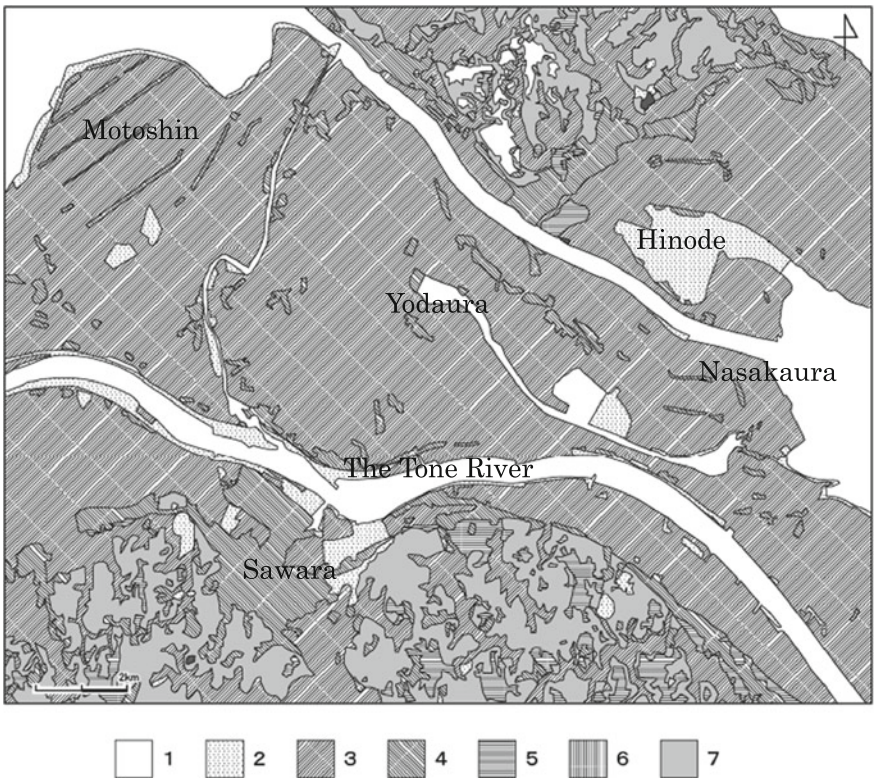

Fig. 6.5 Land use map at the 1960s in the lower tone. *Explanatory note 1*. Water surface and inland lake water surface, *2*. Reclaimed land with surface water, *3*. Paddy fields, *4*. Residential place, *5*. Upland crop field, *6*. Mulberry field, *7*. Forest H. Hinode, M. Motoshin, N. Nasakaura

stage of urban sprawls. However, there are rural districts where nature still thrives in this area.

In the second land use pattern in the 2010s (Fig. 6.5), the paddy fields are still widely distributed in back swamp and former lagoon in the lower Tone River; however, the national development project for food security has pushed to be extended polder and create upland crop fields in Motoshin with land reclamation projects including drainage and irrigation system. The transformation trend of land use pattern has two dimensions as traditional–nature-oriented and engineering-oriented. The former nature-oriented land use pattern is resident on sand ridges and natural levees. Urban core of Sawara town has been spreading to east and south on sand ridges. The urban fringe of Sawara has been expanding to north with land reclamation of the former river courses. Several former lagoons and wetlands have been reclaimed for building houses. The golf courses are increasing in Simofusa terrace and hill with cutting slopes. For conservation of natural

Fig. 6.6 Land use map at the 2010s in the lower Tone River (Explanatory note is same as Fig. 6.5). *Explanatory note 1* Water surface and inland lake water surface, *2* Reclaimed land with surface water, *3* Paddy fields, *4* Residential place,*5* Upland crop field,*6* Mulberry field, *7* Forest H. Hinode, M. Motoshin, N. Nasakaura

environment, there are some small lagoons with wetland vegetation and the lagoons are providing wet land for tourism destinations (Fig. 6.6).

The disaster vulnerability showing each state is concerned with local micro-landform, and land use changing with reclamation and raising ground level are second affixation of damage level of liquefaction in evidence based in 2011 earthquake. Generally, the local community activity and community networking toward to disaster prevention mitigation is the other risk reduction factor (Haruyama and Mizuno 2007; Haruyama and Yoshida 2014; Haruyama and Taresawa 2014), and the accelerating land use changing has been transforming the higher disaster scale with useless lifeline; therefore, the suitable land use planning would guide to be sustainability and to be secure from disaster (Haruyama 2001; Haruyama and Hayashi 2013). The potential vulnerability of liquefaction varies due to land use change and shifting indiscretion utility purpose in unsuitable laws governing nature.

Three vulnerabilities of liquefaction of the study area were assigned, such levels as (1) vulnerable, (2) more vulnerable, and (3) the most vulnerable (Figs. 6.7, 6.8) and liquidizing damage level is increasing with land use changing and reclamation process of the same location. To weigh landform with land use changing, the vulnerable of liquefaction was transforming and taking landform features into vulnerability is shown in Fig. 6.9. Even though same landform unit, the vulnerability is transformed in land use change.

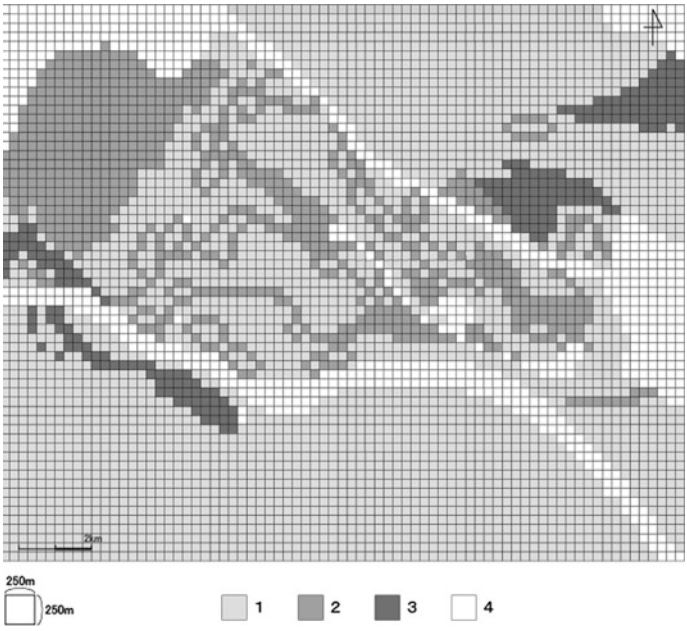

Fig. 6.7 Mesh map of vulnerability level of liquefaction in the study area

The disaster vulnerability has been increasing in land use changing with urban sprawl and reclamation with massive refilling of sand in each landform. Toward to long-term sustainability, regional planning should be included appropriate land use on each landform because artificial landform, such as refilling, reclamation, and cutting, has weakness for bringing about disaster. The refilling works and reclamation projects should take into account local landform units, and their likely response to natural disasters. Taking geomorphologic information into consideration, vulnerability mapping for regional planning with mitigation should be based on each landform changing land use because geomorphologic process is important role of damage (Fig. 6.10).

Fig. 6.8 Mesh map of liquefaction vulnerability level in land use changing

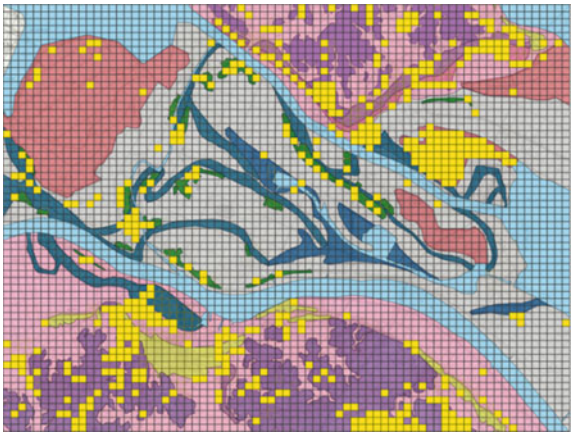

Fig. 6.9 Mesh map showing transformation of liquefaction vulnerability in changing land use on the same landform (The *yellow* color meshes were changed land use for residences)

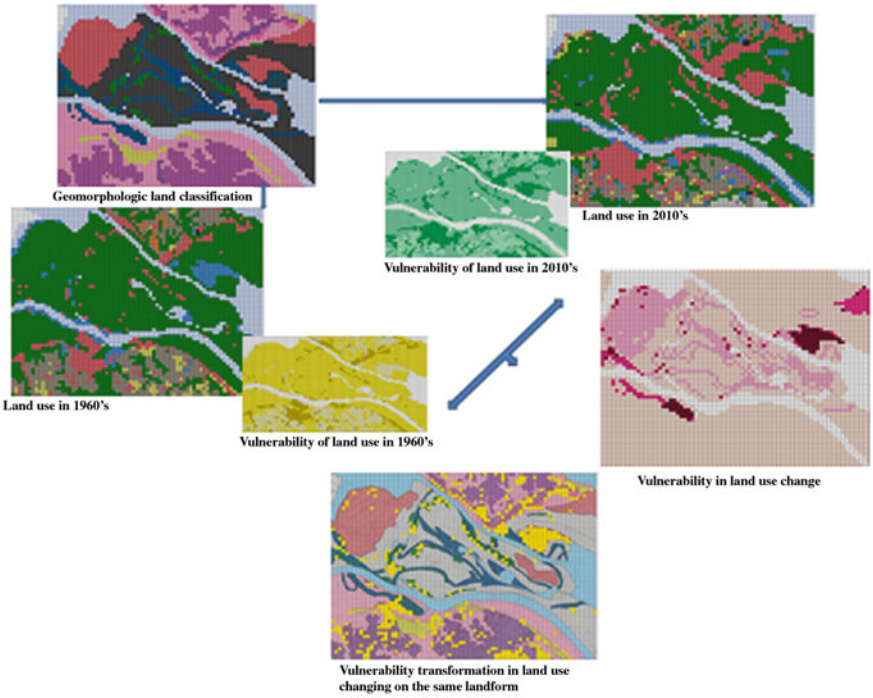

Fig. 6.10 Transformation of vulnerability within land use changing and landform

6.5 Future Vulnerability Reduction

The fluvial and coastal landforms have been important roles causing natural disaster and had influence on disaster-stricken area of liquefaction under the expansion of land use changing. The disaster vulnerability, specific liquefaction, is designated upon several mesh maps of risk levels, landform, land use patterns and vulnerability transformation of liquefaction on land use changing in the lower Tone River floodplain. The liquefaction vulnerability is brought by physical dimensions, and the human dimensions are accelerating vulnerable level, low-resilience, and longer period for resuscitation from disaster. The rapid land use change without knowledge of geomorphology has been inducing to be transforming risk. The future regional planning toward to disaster mitigation needs geomorphologic knowledge for basic component and land use change and also hazard mapping. The essential of risk reduction needs appropriate sustainable education and the geomorphology should be core subject due to secure for lives.

Disaster of "low-probability but high-consequence-scale (LPHC)" type brings large-scale economic losses; on the other hand, the governmental policy would enhance the LPHS-type disaster weakening the resilience. To prepare resilience of the local society to LPHC-type disaster by regenerating resilience of the local

community is important. In lessons from the Japanese experience 2011.3.11 earthquake, to achieve a sustainable reduction in disaster risk, it is requisite to deepen the understanding of the complexity of disaster management and to be augured comprehensive and integrated risk management system promoting various measures throughout an entire basin and strengthening the social resilience by nurturing preparedness by local community and residents. Such a system should incorporate all stakeholders, including governments, local communities, and local residents. Urbanization has changed resident's awareness to disaster risk in their habitat, and no land use management policy in floodplain has increased damage potential.

The geomorphologic structure will predict the future disaster damage because of the fluvial and coastal landform including past natural disaster and availability of interpretation of disaster in the geomorphologic evolution, and the geomorphologic land classification map shows hazardous area and risk area for explaining the past repeated natural disaster. To understand disaster risk in fluvial plain should be used for effective regional planning for land reclamation and the other sustainable land development projects require appropriate knowledge of current land use and background of land history, and the local geology, local landform, soil type, hydrology, and also ecology. Prepared to provide these data, the sustainable land use planning toward to disaster mitigation would be optimal. Development plans prepared with appropriate consideration of the natural environmental data and capacity building for transformation as described above will reduce the likelihood of future natural disasters.

Acknowledgement I should offer my thanks for Mr. Sho Naruse who supported for my research of liquefaction assessment along the lower Tone River in 2011 and 2012. The late Dr. Masahiko Oya who was a superior fluvial geomorphologist and the author studied with him the lower Tone River and prepared geomorphologic land classification map of Lake Kasumigaura and surrounding. These joint researches are important groundwork of this chapter and the author should express my thanks for Dr. Masahiko Oya.

References

Asano I, Tokashiki M, Mori M, Nishihara M (2011) Damage to irrigation and drainage canals along the Tone River downstream by the 2011 off the Pacific coast of Tohoku earthquake. Nokouken Rep 213:145–173

Haraguchi T, Iwamatsu A (eds) (2011) Great eastern Japan earthquake tsunami detail map, Aomori, Iwate and Miyagi edition (p 168) and Fukusima, Ibaragi and Chiba edition (p 98). Kokon-Shoin Publisher, Tokyo, Japan (Japanese)

Haruyama S (1987) Land use of the Tone River basin. Agriculture waster use of the Tone River basin, Agriculture Engineering Association, Tokyo, Japan, pp 25–35 (Japanese)

Haruyama S (1994) Development and environmental conservation in the lake and surroundings - Songklar lake, Laguna lake and Kasumigaura lake. J Int Relat Res 20:25–36 (Japanese)

Haruyama S (2001) Land use planning for disaster mitigation. J Rural Plann 20(2):87–90 (Japanese)

Haruyama S, Hayashi K (2013) Tsunami 2004 disaster impacted by recent land use change in Phuket, Thailand. Haruyama S (ed) Coastal geomorphology and vulnerability of disaster towards disaster risk reduction, TERRAPUB Publisher, Tokyo, Japan, pp 69–86

Haruyama S, Mizuno S (2007) Disaster features and resilience of each local community under 2004 Fukui flooding. J Nat Disaster 26(3):307–322 (Japanese)

Haruyama S, Naruse S (2013) Liquefaction and landform structure in 2011 mega earthquake at Katori city, Chiba Prefecture, Japan. SLUAS science report 2013 towards sustainable land use in Asia (IV), JSPS Science Fund Basic Research (S) No.2122200, pp 100–399

Haruyama S, Oya M (1993) Physical geographical analysis of the Tone River management -lesson from the Akaborigawa channel excavation. J Acad Stud Geogr Hist Soc Sci 41:1–19, The School of Education of Waseda University (Japanese)

Haruyama S, Taresawa Y (2014) Local community activities for disaster reduction in regard to the 2011 tsunami. Geographia Polonica 87(3):299–306

Haruyama S, Yoshida A (2014) Flood risk under recent land use change in the lower Syonai river basin. SLUAS science report 2014 towards sustainable land use in Asia (V), JSPS Science Fund Basic Research (S) No.21222003, pp 177–188

Hirai Y (1989) Land form feature and geomorphologic development of lagoon in Japan. Geogr Rev 62:145–159 (Japanese)

Honma M (2013) Utilization plan for geological data in real estate transactions and recovery status from liquefaction damages in Urayas city. GSJ Chisitsu News 12(12):357–360 (in Japanese)

Kataoka E (1998) Sawara city history. Sawara city office, p 163

Koarai M (2013) Liquefaction damage of the east Japan great earthquake and evaluation of liquefaction risk using geospatial information. GSJ Chisitsu News 12(12):166–361 (in Japanese)

Koarai M, Nakano T (2013) Liquefaction damage in the Kanto region caused by 2011 of the Pacific coast of Tohoku earthquake in Japan, and the land condition of damaged areas detected by time-series geospatial information. In: The proceedings of 26th International Cartographic Conference, pp 21–32

Koarai M, Nakano T, Okatani T (2015) Relationship between tsunami hazard related to the 2011 off the Pacific coast of Tohoku earthquake and geographical Condition such as topography and land use on the Sendai plain and Ishinomaki plain. J Geogr 124(2):211–226 (in Japanese)

Komatsubara T (2006) Relationship between micro-topography and damage by the 1894 Meiji Shonai earthquake. J Hist Earthq 21:249 (in Japanese)

Kotoda K, Wakamatsu K, Midorikawa R (1993) Seismic microzoning on soil liquefaction potential based on geomorphological land classification. J Geotech 28(2):127–143 (in Japanese)

Oya M (1969) Geomorphology and flooding of the plain in the middle and lower reaches of the Tone River in Kanto plain. J Geogr 78(5):43–56 (in Japanese)

Oya M (1993) Fluvial geography. Kokonshoin Publisher. 221–239 (in Japanese)

Oya M, Haruyama S (1987a) Flooding and urbanization in the lowlands of Tokyo and Vicinity. Nat Disaster Sci 9(2):1–12

Oya M, Haruyama S (1987b) Landform of the Tone River basin and the southern part of Kasumigauwa lake. J Ootone. 9(2):2–4 (in Japanese)

Oya M, Kato Y, Haruyama S, Hirai Y, Kobayashi K, Inoue Y, Oshizawa N (1986) Geomorphologic land classification map of Kasumigaura lake. No.1 and No.2. Kasumigaura River Engineering Office, Ministry of Construction, Kanto region construction office (in Japanese)

Oya M, Kinoshita T, Wakamatsu K, Hadori T, Ishii Y (1989a) Shizensaigai wo Shiru and Fusegu (How to know and how to prevent of natural disaster). Kokon-shoin Publisher, Tokyo, Japan, p 236 (in Japanese)

Oya M, Haruyama S, Hirai Y (1989b) Geomorphologic land classification map of lake Kasumigaura, Kitaura and their Vicinity, East of Tokyo. GEOGRAFIA FISICA E DINAMICA QUATERNARIA. Bollettino del Comitato Glaciologico Italiano. Ser.3 12 (1):47–50

Saito Y, Inouchi Y (1993) Kasumigaura. Urban Kubota 32:56–64 (Japanese)
Saito Y, Inouchi Y, Yokota S (1990) Geologic history of Kasumigaura- transition history of coastal lake environment effected by sea level changes. J Geol 36:103–118 (in Japanese)
Suzuki Y, Watanabe M, Azuma T, Okada A (1996) Active tectonics of the Rokko-Awaji, and earthquake fault of the southern Hyogo prefectural earthquake of 1955: tectonic geomorphological and paleo-seismological studie and problems. Geogr Rev Japan 69A(7):469–482 (in Japanese)
Takahashi M (1996) Geo-environment analysis of the Hannshinn-Awaji great earthquake disaster. Geogr Rev Japan 69A(7):504–517 (in Japanese)
Taresawa Y, Haruyama S (2013) Coastal landform in the southern part of Miyagi prefecture and 2011 tsunami disaster, coastal geomorphology and vulnerability of disaster towards disaster risk reduction. TERRAPUB Publisher, Tokyo, Japan, pp 87–96
Toyota M, Ikeda H (2003) The formation of lacustrine lowlands around lake Kaumigaura. Geologic environment information bank of Chiba. http://wwwp.pref.chiba.lg.jp/pbgeogis/servlet/infobank.index (in Japanese)
Wakamatsu K (1993) The study of liquefaction vulnerable assessment related with geological condition and geomorphologic condition using historical liquefaction in Japan. Ph. D Dissertation of Waseda University, p 228 (in Japanese)
Wakamatsu K (2012) Recurrent liquefaction induced by the 2011 great east Japan earthquake. Japan Earthq Eng J 12(5):69–88 (in Japanese)

Chapter 7
Reconstructing Areas Affected by the Great East Japan Earthquake Disaster: Progress and Challenges

Shizuka Hashimoto

Abstract The Great East Japan Earthquake devastated the Pacific coast of Tohoku and Kanto, inundating approximately 561 km^2 of coastal areas across six prefectures with 142 billion USD of economic damage as well as 18,682 deaths and 2674 missing. The damages caused by the disaster vary between Sanriku and Sendai-Fukushima, according to their geographical differences. In response to the Great East Japan Earthquake, the governments, both national and local, have been making great efforts to smoothly recover and reconstruct the disaster-affected areas, first by setting up the Reconstruction Design Council to formulate prefectural reconstruction plans and provide the municipalities of tsunami-affected areas with reconstruction guidance, and then by preparing institutional framework to facilitate reconstruction efforts. Among the various reconstruction measures, the Reconstruction Grant Project has been playing an important role with strong financial support from the national government to reconstruct infrastructures and recover the livelihoods of local people by designating the first five years, starting from 2011, as the intensive reconstruction period. However, the tight time frame set to facilitate reconstruction seems to have been causing various issues, such as a rise of construction cost, limited time for decision making and building consensus, and environmental impacts.

Keywords Tsunami inundation · Land use regulation · Nuclear disaster · Reconstruction · Reconstruction measures

S. Hashimoto (✉)
Graduate School of Agricultural and Life Sciences, The University of Tokyo,
1-1-1, Yayoi, Bunkyo-Ku, Tokyo 113-8657, Japan
e-mail: ahash@mail.ecc.u-tokyo.ac.jp

S. Haruyama and T. Sugai (eds.), *Natural Disaster and Coastal Geomorphology*, DOI 10.1007/978-3-319-33814-9_7

7.1 Characteristics of Damage Caused by the Great East Japan Earthquake and Geography of the Disaster-Affected Areas

7.1.1 Overview of the Damage Caused by the Great East Japan Earthquake

The Great East Japan Earthquake (also known as the 2011 earthquake off the Pacific coast of Tōhoku) with a magnitude 9.0 *Mw* occurred at 14:46 JST on Friday, March 11. The epicenter of this earthquake was approximately 70 km east of the Oshika Peninsula of Miyagi prefecture. A strong seismic intensity at a maximum of 7 on the Japan Meteorological Agency's seismic intensity scale was observed in Kurihara, Miyagi Prefecture, and in the upper 6 range in 37 municipalities across three prefectures: Fukushima, Ibaraki, and Tochigi (Japan Metrological Agency 2011). The earthquake triggered huge tsunami waves at a maximum wave height of 16.7 m in Ofunato, Iwate, and devastated the Pacific coast of Tohoku and Kanto. The estimated tsunami inundation area is approximately 561 km^2 across 6 prefectures: Aomori, Iwate, Miyagi, Fukushima, Ibaraki, and Chiba. In addition to the huge tsunami wave, it caused liquefaction, subsidence, a rip in the dam, and paralysis of the transportation network from Hokkaido to the Tokyo metropolitan area. The Fire and Disaster Management Agency of Japan confirmed 18,682 deaths and 2674 people missing due to the earthquake disaster as well as the complete collapse (*zenkai*) of 126,273 buildings, a further 269,726 buildings half collapsed (*hankai*), and another 644,946 buildings partially damaged (*ichibu-sonkai*) as of September 1, 2014. The number of refugees reached approximately 470,000 people at maximum, of which, according to the Reconstruction Agency of Japan, 209,862 people are still living in temporary housing as of February 12, 2015. According to the Cabinet Office of Japan, the total damage from the earthquake disaster was estimated to be 169 trillion JPY (142 billion USD) (Table 7.1).

The damage caused by the earthquake is concentrated in three prefectures, namely Iwate, Miyagi, and Fukushima, in the Pacific coast area of East Japan. These three prefectures alone account for 87 % of the tsunami inundation (497 km^2) and over 99 % of the dead and missing (21,262 people); 67 % of the dead were people at least 60 years old, shedding light on the vulnerability of the elderly to tsunami. Drowning was the principal factor responsible for death, accounting for 77 % of the causes of death, followed by injury, which accounted for 22 %. In addition, 97 % of the buildings that were totally collapsed (122,539 buildings) as well as 87 % of buildings that were "half collapsed" (234,683 buildings) were concentrated in this area, leaving 22.5 million tons of debris. For

Table 7.1 Victims and damages of the Great East Japan Earthquake

	Dead people	Missing people	Minor and serious injuries people	Inundation area (km^2)	*Building damage*		
					Completely collapsed buildings	Half-collapsed buildings	Partially damaged buildings
Aomori	3	1	111	24	308	701	1005
Iwate	5086	1145	212	58	18,460	6563	14,191
Miyagi	10,449	1299	4145	327	82,889	155,099	222,781
Fukushima	3057	226	182	112	21,190	73,021	166,758
Ibaragi	65	1	712	23	2625	24,225	185,332
Chiba	22	2	256	17	801	10,117	54,879
Total	18,682	2674	5618	561	126,273	269,726	644,946

Source Ministry of Internal Affairs and Communication of Japan (September 17, 2013)

these three prefectures alone, the number of refugees reached 368,000 people with a blackout of 2.6 million households, a disrupted gas supply for 2.1 million households, and a disrupted water supply for 1.3 million households.

In addition to the earthquake disaster, Fukushima and its surroundings have severely suffered from radionuclides released by the Fukushima Daiichi Nuclear Power Station accident triggered by the earthquake and tsunami. Approximately 22 % of the radionuclides released from the power station are estimated to have been deposited on land (Morino et al. 2011). In response to the accident, a 20 km radius around the nuclear plant was designated by the Japanese government as a "Restricted Area" to which entry is prohibited. The area beyond the 20 km radius, where the estimated cumulative doses of radiation reached 20 mSv within a year, was designated as a "Deliberate Evacuation Area." In total, nearly 154,000 people have been evacuated from Fukushima, of which 109,000 are from the "Restricted Area" (Reconstruction Agency 2013a). The destinations of nuclear accident refugees range from other Fukushima areas outside the restricted area to other prefectures across Japan. The number of evacuees to other prefectures increased gradually after the accident and reached a maximum number of 63,000 in March 2012, a year after the accident. Still, around 47,000 people are forced to live outside Fukushima. The nuclear disaster made recovery of Fukushima more challenging than other disaster-affected areas as it requires decontamination of radioactive cesium deposited on the ground along with reconstruction of tsunami and earthquake-affected areas.

The primary focus of this chapter is to provide an overview of the recovery and reconstruction efforts and challenges of the tsunami-affected areas of the Great East Japan Earthquake with special attention to the most severely damaged prefectures—Iwate, Miyagi, and Fukushima—while trying to cover the major findings and challenges associated with the nuclear disaster wherever possible.

7.1.2 Characteristics of Damage and Geography of the Tsunami-Affected Areas of Iwate, Miyagi, and Fukushima

Tsunami-affected areas of Iwate, Miyagi, and Fukushima can be classified into two areas from the viewpoint of terrains and land use: the Sanriku coastal area and Sendai-Fukushima coastal area. The Sanriku coastal area is characterized by steep topography and a deeply indented coastline with the Kitakami mountain range in its background, whereas the Sendai-Fukushima coastal area is characterized by a wide-ranging flat plain with a predominantly straight coastline (Fig. 7.1). As such, although the total lengths of the coastal lines between the two areas are not largely different, the Sendai-Fukushima coastal area experienced significantly larger inundation by the tsunami (356 km^2) due to its extensive plains, which is approximately four times greater than that experienced by the Sanriku coastal area

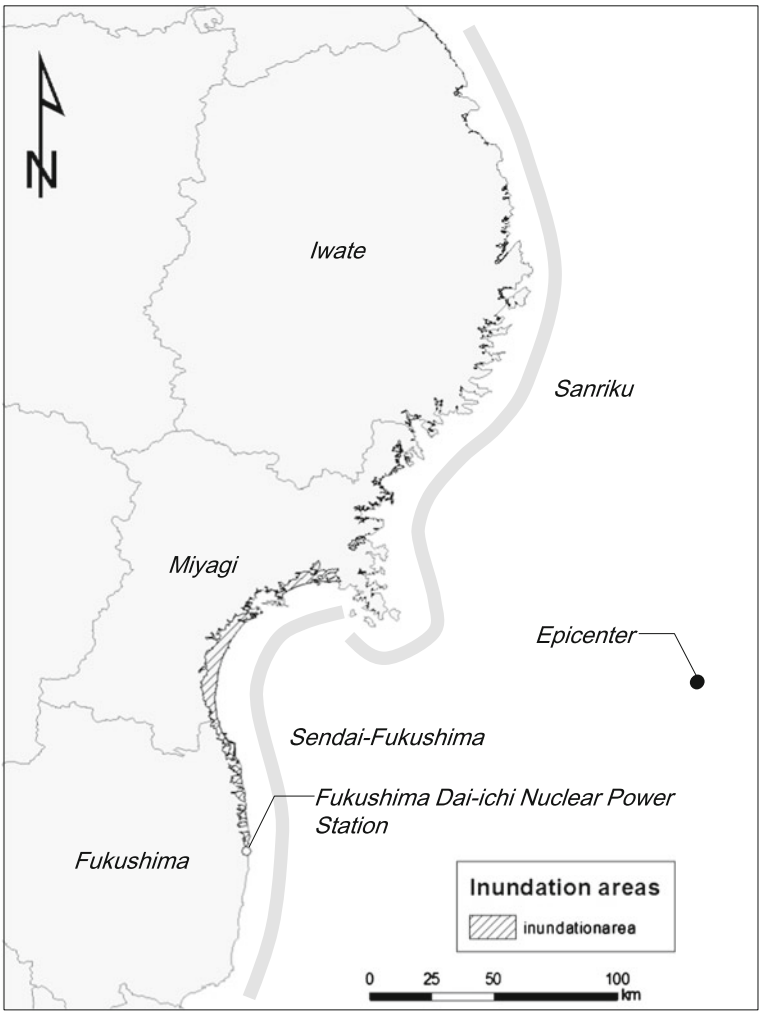

Fig. 7.1 Epicenter of the Great East Japan Earthquake, tsunami inundation areas, the location of Fukushima Daiichi nuclear power station, and the boundary of Sanriku and Sendai-Fukushima coastal area

(90 km^2). The tsunami reached several kilometers inland from the foreshore in the Sendai-Fukushima area and roughly 80 % of the inundation area is located below an altitude of 6 m (Fig. 7.2). Inundation area that is 10 m above sea level accounts for less than 1 % in this area. Contrarily, 44 % of the inundation area is located below an altitude of 6 m in the Sanriku coastal area and inundation that is 10 m above sea level accounts for 29 %, demonstrating tsunami penetration is relatively higher in areas along a hill slope (Hashimoto forthcoming).

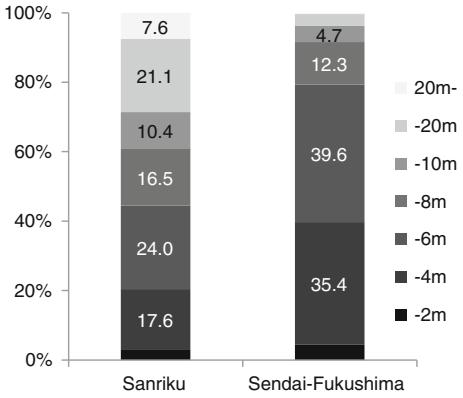

Fig. 7.2 Elevation profile of tsunami inundation area (%). *Note* GIS data on the tsunami inundation area and digital elevation model (30 m mesh) were cross-tabulated with ArcGIS 10.2 to derive the elevation profile

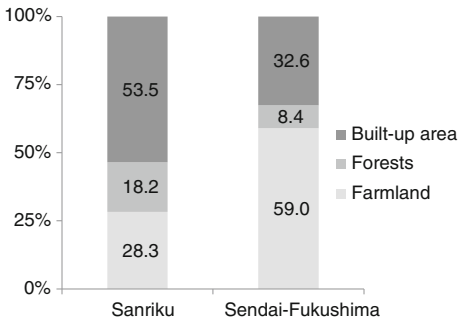

Fig. 7.3 Land use composition of tsunami inundation area (%). *Note* GIS data on the tsunami inundation area and land use data for the year 2006 (100 m mesh) were cross-tabulated with ArcGIS 10.2 to derive the land use profile

Land use was also largely different between the two tsunami inundation areas. The Sanriku inundation area was predominately built-up areas, such as residential land, roads, and industrial sites, constituting 54 % of the total, followed by farmland (28 %) and forests (18 %). In contrast, the Sendai-Fukushima inundation area was predominately farmland, constituting 59 % of the total, followed by built-up areas (33 %) and forests (8 %) (Fig. 7.3). In addition, the Sanriku inundation area exhibited a higher concentration of public facilities (3.7 facilities/km^2) than that of the Sendai-Fukushima area (1.2 facilities/km^2) (Hashimoto forthcoming). Surprisingly, the Sanriku inundation area was one-fourth of the spatial scale of Sendai-Fukushima, but the number of public facilities located in the inundation areas was approximately 1.4 times larger. There were many inundated community centers, welfare-related facilities, schools, post offices, police stations, and national

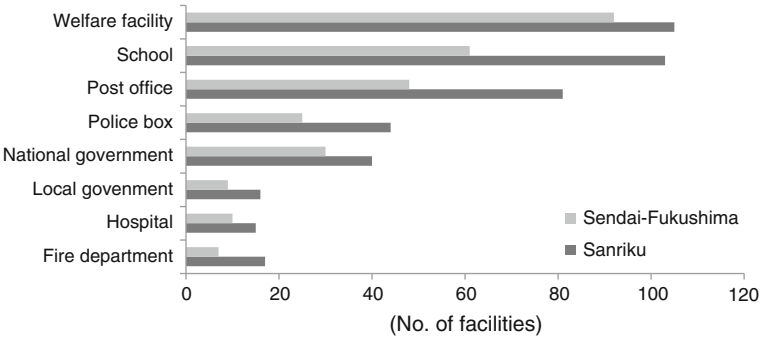

Fig. 7.4 Number of public facilities located in the tsunami inundation area. *Note* GIS data of (1) tsunami inundation area (polygon), location data of (2) public facilities (point) (2006), and (3) local governments and other public meeting places (2010) were overlaid with ArcGIS 10.2 to derive the type and number of public facilities located in the tsunami inundation area

government branches in both areas (Fig. 7.4). The inundation of local governments and fire departments was frequent in the Sanriku coastal area. All of these caused a delay of emergency response by the local governments after the earthquake and tsunami. Severe inundation damage to community centers also often prevented local people from meeting later to discuss the restoration of tsunami-affected areas.

The number of dead and missing in the Sanriku coastal area was 9152 people, whereas it was 11,697 people in the Sendai-Fukushima coastal area; no significant differences were observed, despite the significant differences in the spatial scale of the inundation area between the two. However, when we look at the number of victims per inundation area, there is a large difference between them: 102 people in Sanriku and 33 in Sendai-Fukushima (Table 7.2). This can be attributed to the geographical differences and land use of the two areas. Similarly, the number of completely collapsed buildings was 1.6 times greater in the Sanriku coastal area than that of Sendai-Fukushima, whereas the number of half-collapsed buildings is 5.7 greater in the Sendai-Fukushima coastal area.

On the Sanriku coast, since there is little land suitable for built-up areas due to its precipitous geography, urban functions have been situated at valley plains near the coast. Accordingly, the population has also been concentrated in and around the valley plains, which resulted in much more severe damage in terms of both human suffering and building damage inflicted when struck by the tsunami.

Table 7.2 Victims and damages of the Great East Japan Earthquake by the coasts

	Dead people	Missing people	Inundation area (km^2)	Completely collapsed buildings	Half-collapsed buildings	Dead and missing per inundation area (people/km^2)	Completely collapsed buildings per inundation area (buildings/km^2)	Half-collapsed buildings per inundation area (buildings/km^2)
Sanriku	7586	1566	90	32,502	7977	84.3	361	89
Sendai-Fukushima	10,902	795	356	82,941	179,482	30.6	233	504

Source Ministry of Internal Affairs and Communication of Japan (September 17, 2013)

7.2 Government's Reconstruction Efforts

7.2.1 Reconstruction Design Council

The Great East Japan Earthquake revealed the existence of a tsunami that could not be fully repelled by breakwaters, coastal dikes, and tide barriers. The government of Japan established the Reconstruction Design Council, an advisory committee to Prime Minister Naoto Kan, in April 2011 to outline a foundation for the efforts to recover and reconstruct disaster-affected areas.

The Reconstruction Design Council submitted a final report as a set of recommendations to the prime minister on June 25, 2011, which introduced the concept of "disaster reduction" to cope with a tsunami that is physically impossible to defend against. This concept is a departure from the traditional idea of disaster prevention that has exclusively relied on coastal defensive structures. The concept of disaster reduction calls for people-oriented approaches to disaster management. The Council categorized a variety of reconstruction measures from two different perspectives: (1) soft (people-oriented)/hard (infrastructure-oriented) measures and (2) direct (protection-oriented)/indirect (escape-oriented) measures (Fig. 7.5). The Council indicated the importance of soft and indirect measures, such as disaster-prevention education with stress on the concept of "escape," the use of hazard maps, and community building that facilitates emergency response. As for hard and direct measures, the Council also encouraged the construction of setback levees and elevated land with embankments to supplement other conventional defensive structures such as breakwaters and dikes. The importance of land use regulation from the viewpoint of risk management is also stressed in the final report (RDC 2011).

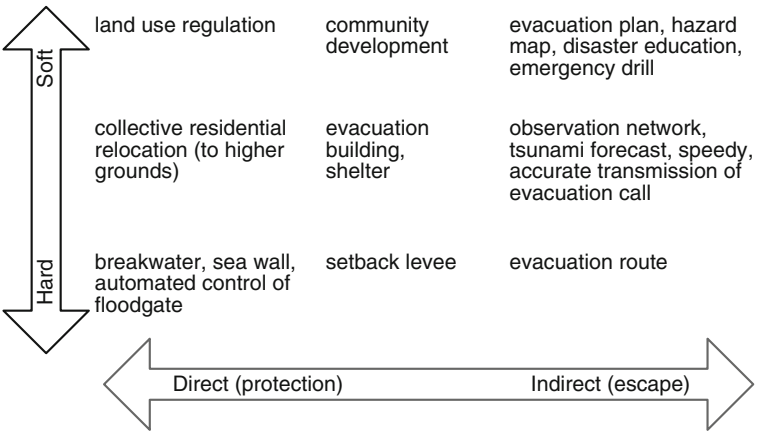

Fig. 7.5 Types of reconstruction measures (RDC 2011)

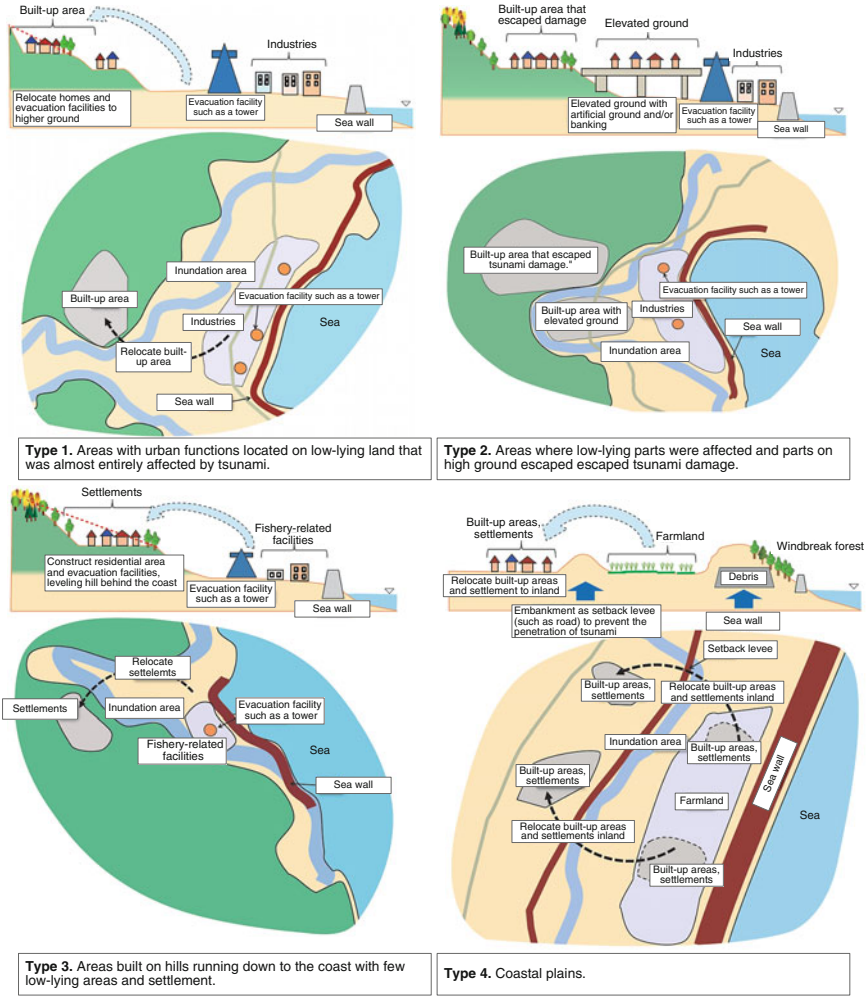

Fig. 7.6 Types of disaster-affected areas with reconstruction measures [translated from RDC (2011)]. *Note* Figures are prepared only for types 1–4 in the final report

The Council presented reconstruction measures, classifying disaster-affected areas into five types (Fig. 7.6). Type 1 is areas with urban functions located on low-lying land that was almost entirely affected by the tsunami. Type 2 is areas where low-lying parts were affected and parts on high ground escaped tsunami damage. Type 3 is areas built on hills running down to the coast with few low-lying areas and settlements. Type 4 is coastal plains. Type 5 is inland areas that were damaged due to liquefaction triggered by the earthquake.

Although the Council did not mention which specific area falls into which type, it is clear that most of the tsunami-affected areas on the Sanriku coast fall into types

1–3, while those on the Sendai-Fukushima coast fall into Type 4. Type 5 seems to refer to the disaster-affected areas of Ibaragi and Chiba, where serious liquefaction was observed.

For the four types associated with tsunami, types 1–4, the measures involved are land use regulation, relocation of homes and core urban functions, and construction/improvement, though the point of focus for each is slightly different. To be more precise, for types 1–3 (Fig. 7.6, types 1–3), relocation of the built-up areas from low-lying areas to safe, higher ground is a high-priority task in reconstruction. However, due to limited land available for relocation, not all of the buildings and facilities could be relocated. Commercial needs, such as those of fisheries, are also likely to become an obstacle in relocation. Hence, basically, the priority is given to the relocation of homes. In addition, land use regulation needs to be implemented to prohibit residential development in low-lying areas that are vulnerable to tsunami while allowing only those with special needs, such as fishery industries, to be re-established in low-lying areas. In contrast, Type 4 requires a mixed approach, combining items such as setback levees, land use regulation, and relocation of houses and other facilities. Setback levees, utilizing transport infrastructure, and other means would work as multiple protections against tsunamis in combination with coastal defensive structures. As for relocation, since Type 4 is blessed with a wide-ranging coastal plain, there is abundant land for relocating houses and facilities in the vicinity of the coast (Fig. 7.6, Type 4). As with types 1–3, land use regulation needs to be combined with relocation of houses and other facilities and residential development should be prohibited at the coast while allowing farmland and other industries in those areas with special treatments, such as evacuation routes and buildings.

7.2.2 Iwate Prefecture

Iwate prefecture proposed a concept of "multiple protections" in the reconstruction of tsunami-affected areas, which combines (1) disaster-prevention infrastructures such as breakwaters, dikes, and setback levees, (2) disaster-prevention/evacuation facilities such as evacuation routes, artificial ground, and residential relocation, (3) buildings such as a breakwater building and evacuation buildings, and (4) land use regulation with special focus on tsunami risk (Iwate 2011). It took a similar approach to the Reconstruction Design Council in formulating a post-disaster reconstruction plan; the plan classifies tsunami-affected areas into four categories, combining two axes: (1) the scale of damage by the tsunami (entirely affected/partially affected) and (2) land use pattern (predominantly urban/predominantly rural) (Fig. 7.7). It provided three reconstruction patterns for them (Fig. 7.8), but Iwate prefecture did not propose which pattern was preferred for each area.

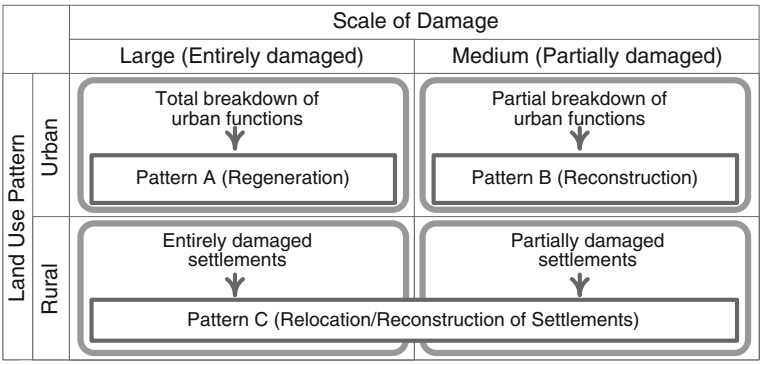

Fig. 7.7 Classifications of tsunami-affected areas and corresponding reconstruction patterns [translated from Iwate (2011)]

Pattern A is for those areas with a wide baymouth, which were entirely devastated by the tsunami (Fig. 7.8, Pattern A). This pattern calls for fundamental changes of the urban structure from scratch: (1) relocate homes and other facilities where a number of people visit, such as commercial and public facilities, (2) construct evacuation routes, buildings, and towers within walking distance of people who work at or visit coastal areas, and (3) utilize coastal areas as tsunami-buffer zones, allowing farmland, fishery industries, parks, and other large-scale buildings to be established there. Pattern B is for those areas with a narrow baymouth, where a part of the built-up areas was destroyed by the tsunami (Fig. 7.8, Pattern B). Thus, Pattern B suggests using existing urban structures, which allows commercial and business to be re-established at the coast; relocation focuses mainly on residential buildings at the coast. Construction of evacuation routes, buildings, and other tsunami-protection facilities are also encouraged to enact the approach of multiple protections. Pattern C is for those small settlements at the coast that were entirely or partially destroyed by the tsunami (Fig. 7.8, Pattern C). For those communities entirely devastated, relocation of settlements to safe, higher ground is encouraged. For those with limited damage at the coast, land elevation is suggested so that settlements are reconstructed on higher ground.

7.2.3 Miyagi Prefecture

Miyagi prefecture also classified the coastal area into three regions from the north to south for the purpose of proposing reconstruction measures (Miyagi 2011): (1) Sanriku region, (2) Ishinomaki-Matsushima region, and (3) the south region of the Sendai Bay (Fig. 7.9).

The Sanriku region is predominated by steep topography with an indented coast line. In this region, the basic policy for reconstruction is a combination of relocation

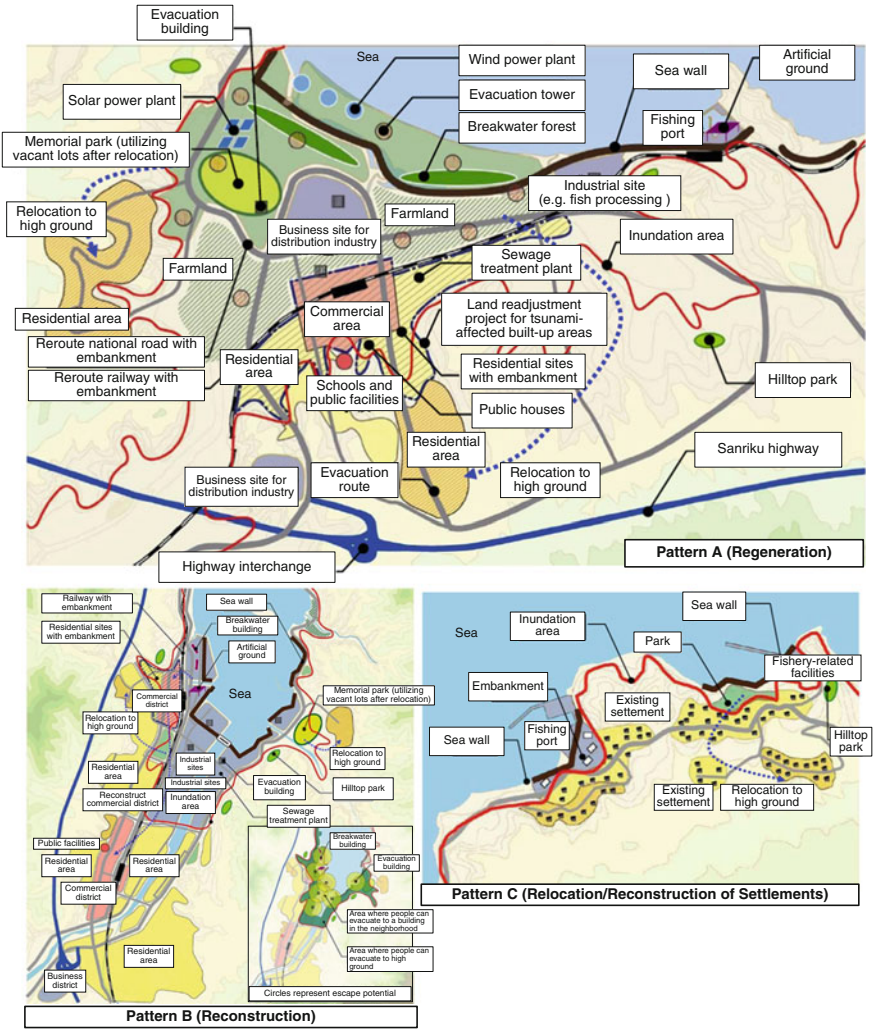

Fig. 7.8 Proposed reconstruction patterns for tsunami-affected areas of Iwate [translated from Iwate (2011)]

of homes/other facilities and separation between residential and working places (Fig. 7.10, upper image). Coastal areas are to be redeveloped with evacuation routes and buildings for industrial use, parks, and tourism. The south region of Sendai Bay is comprised of a wide, low-lying plain with a long, straight coast. In this region, the importance of multiple protections from setback levees utilizing road and railway, in combination with seawalls and green spaces, is proposed (Fig. 7.10, lower image). Low-lying coastal areas are to be transformed or re-developed to be more flood resistant for residences, agriculture, and other

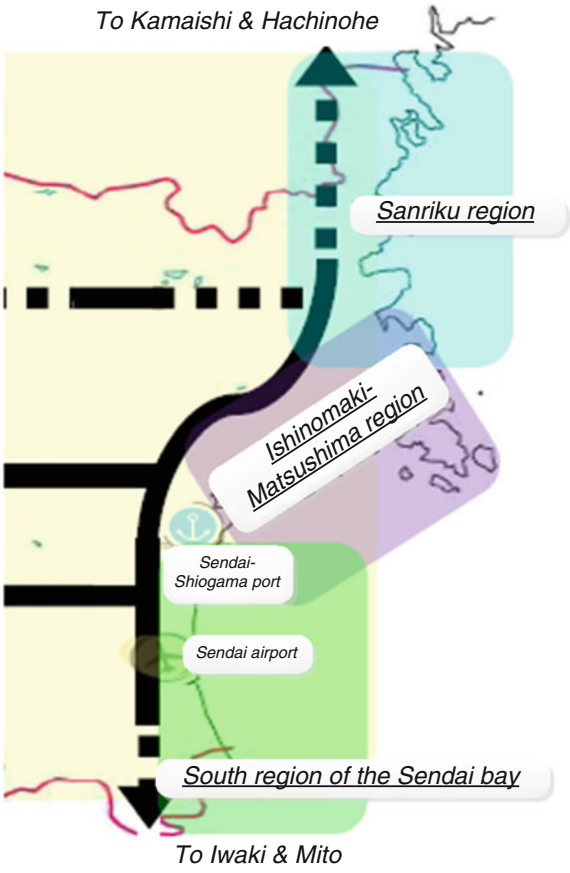

Fig. 7.9 The three coastal regions of Miyagi prefecture [translated from Miyagi (2011)]

industries. The Ishinomaki-Matsushima region is located in between the other two regions and shares their geographical characteristics. Accordingly, the reconstruction measures for this region became a mixture of the other two: relocation of homes/other facilities, separation of residential and working places, and multiple protections utilizing transportation infrastructures.

7.2.4 Commonalities of Reconstruction Measures

Substantial land use reform, unconstrained by past land use patterns, is necessary to build more tsunami-resistant areas. Accordingly, despite large geographical differences among tsunami-affected areas, there exist commonalities among reconstruction measures proposed by governments located at different areas. They are (1) to relocate residential buildings and other people-gathering facilities from

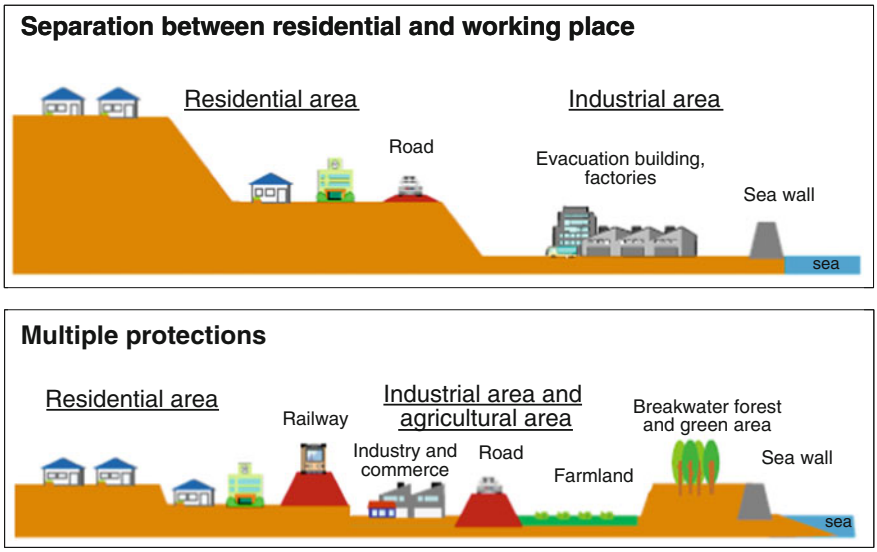

Fig. 7.10 Two representative images of reconstruction [translated from Miyagi (2011)]

low-lying, coastal areas to safer, inland or higher grounds, (2) to introduce multiple protections with setback levees utilizing transportation infrastructures combined with conventional defensive structures and spaces, (3) to implement land use regulations that prohibit residential development at the tsunami-vulnerable coast while allowing those areas to be utilized for industrial sites and agricultural production, and (4) to develop evacuation routes and buildings for people who work at or visit coastal areas so that they can smoothly evacuate from hazardous areas in case of an emergency.

To be more precise, the point of focus in implementing these measures is different from place to place. Presumably, the difference would be closely related to geographical constraints such as land availability and topography. For those areas located in the Sanriku coast, only a limited amount of land is available for reconstruction. Thus, governments tend to put a higher priority on relocation of residential buildings and people-gathering facilities and development of evacuation routes and towers for those facilities that are difficult to relocate. The construction of a setback levee was seldom mentioned, as it often requires a vast area of land for embankment. In contrast, for those located in Sendai coast, governments tend to utilize a mixed approach of relocation, combining land use regulation and multiple protections with defensive structures. Since governments need to deal with a wide stretch of land, the construction of huge seawalls that are adequate to prevent large-scale flooding caused by tsunami is not economically viable. Thus, the construction of setback levees that utilize existing and/or new transportation infrastructures seemed to emerge as a more promising approach if it is effectively combined with land use regulation and residential relocation.

7.3 Institutional Framework to Facilitate Recovery and Reconstruction Efforts in Response to the Great East Japan Earthquake

The government of Japan enacted the Basic Act on Reconstruction in response to the Great East Japan Earthquake on June 24, 2011, to promote a smooth and prompt reconstruction following the Great East Japan Earthquake. In addition, the government issued the "Basic Guidelines for Reconstruction in response to the Great East Japan Earthquake" on July 29, 2011, under the Basic Act, embracing proposals made in the final report of the Reconstruction Design Council to support the formulation and implementation of reconstruction plans to be formulated by disaster-affected local governments. The guidelines stipulated a reconstruction period from 2011 to 2021, with the first 5 years being the intensive reconstruction period for swift recovery, and also provided a framework to support reconstruction efforts that included the establishment of the Reconstruction Agency with a 10-year mission responsible for planning, coordination, and implementation of measures for reconstruction, special zones for reconstruction,, and grants for the reconstruction projects planned by local governments. According to the guidelines, at least 23 trillion JPY are necessary as public expenditure, including both national and local, for reconstruction of the disaster-affected areas, of which 19 trillion JPY, 83 % of the total is the budget for the intensive reconstruction period. However, the estimate of the reconstruction budget for the intensive reconstruction period was revised in 2014 from 19 to 25 trillion JPY (Table 7.3). In reality, the reconstruction budget exceeded 19 trillion JPY in the first two years and gradually increased to 32 trillion JPY by the fiscal year of 2015. It should be noted that the public expenditure described here does not include compensation for those affected by the Fukushima Daiichi Nuclear Power Station accident paid for by the Tokyo Electric Power Company (TEPCO), which alone accounted for 4.9 trillion JPY as of May 2015 (TEPCO 2015).

The special zone for reconstruction has been put in place by enactment of the Act on special zones for reconstruction in response to the Great East Japan Earthquake in August 2011 as a framework to offer a set of measures to support reconstruction efforts by local governments. The special zone covers 227 municipalities affected by the Great East Japan Earthquake that range across 10 prefectures from Hokkaido to Nagano.

The reconstruction measures prepared for the special zone include: (1) mechanisms to ensure reduced regulations and statutory procedures, such as easing eligibility requirements for public housing for disaster-affected people and granting special permits for certain business establishments (regulations and procedures); (2) a range of tax breaks to stimulate investment and employment in the afflicted areas (taxation); (3) special grant for reconstruction projects and interest rate compensation for lenders (financial and fiscal assistance); and (4) measures to facilitate land use restructuring of disaster-affected areas (land use restructuring) (Table 7.4).

Table 7.3 Reconstruction budget in response to the Great East Japan Earthquake (billion JPY)

	FY2011	FY 2012	FY 2013	FY 2014	FY 2015
Support for disaster victims (life support, health, education, etc.)	1579	279	218	112	129
Reconstruction of disaster-affected area (infrastructures, land readjustment, waste management, etc.)	6034	1247	1830	1339	1349
Reconstruction of industries (industrial development, employment, etc.)	3193	442	438	131	168
Restoration from the nuclear disaster (decontamination, measures against reputational damage, etc.)	1241	651	898	910	781
Disaster-related local allocation tax	2141	670	605	572	590
National disaster prevention	609	606	277	138	201
Other	323	199	681	705	692
Total	15,120	4093	4948	3906	3908

Source Reconstruction Agency (2015a)

Table 7.4 Examples of reconstruction measures available for municipalities located in the special zone for reconstruction upon their request

(1) Regulations and legal procedures • Reduced requirements to be eligible as public housing for disaster-affected people • Special measures in farmland conversion to develop facilities for food/forestry/fishery processing and sales
(2) Tax breaks • Special depreciation/tax credit • Tax credit equivalent to 10 % of the combined amount of salaries and other payments for employees from severely damaged areas • Exemption from corporate tax for 5 fiscal years for new enterprises and so forth
(3) Financial and fiscal assistance • Grants for reconstruction (funding for reconstruction projects) • Interest rate compensation for reconstruction projects
(4) Land use restructuring • Special arrangements for land use restructuring beyond existing land use frameworks (urban area, farming area, forests, etc.) • Relaxed requirements for floor area ratio for buildings constructed to facilitate evacuation from tsunamis

Source Reconstruction Agency (2013b)

If local governments are to employ reconstruction measures in an effective manner, municipalities within the special zone need to formulate special plans (Table 7.5). To be more precise, there are three types of plans prepared by the Japanese government under the Act on special zones for reconstruction in response to the Great East Japan Earthquake: (1) the reconstruction promotion plan to utilize

Table 7.5 Types of plans and reconstruction measures available for municipalities within the special zone for reconstruction

Type of plan	Reconstruction promotion plan	Land restructuring plan	Plan for funding reconstruction grant projects
Reconstruction measures available	• Deregulation and simplified procedures for such sectors as housing, industry, community building, medical services, and nursing care • Tax breaks to promote employment and industrial activities • Interest rate compensation for lenders	• Special permits needed to conduct reconstruction projects • Unified contact for municipalities in seeking approval or authorization • Creation of new types of projects to facilitate land use	• 40 projects for municipalities consolidated into a package of core projects • Resources secured to enable flexible use for local governments • Central government funds the reconstruction projects entirely • Flexible implementation with simplified procedures
Organization responsible for formulating a plan	• Formulated by prefectures alone or jointly with municipalities • Private enterprises are entitled to submit proposals to local governments	• Formulated by municipalities alone or jointly with a prefecture	• Formulated by municipalities alone or jointly with a prefecture
Conditions to be enacted	Approval by the Prime Minister	• Public hearings, announcement and display for public when necessary • Consultation for subsequent agreement on the plans in the meeting on land restructuring • Public disclosure	Submission to the Prime Minister

Source: Reconstruction Agency (2013b)

deregulation, simplified legal procedures, tax breaks, etc.; (2) the land restructuring plan to employ measures on approval/authorization and procedures for land restructuring; and (3) the plan for funding reconstruction grant projects to utilize the Reconstruction Grant for projects designed to recover and reconstruct disaster-affected areas. These plans are, of course, not independent but interrelated because each of them deals with a different aspect of reconstruction (Suzuki and

Kaneko 2013). Among others, the plan for funding reconstruction grant projects is especially important for the local governments in accelerating the reconstruction of disaster-affected areas with strong financial support from the national government. To be more precise, the Reconstruction Grant Projects fall into two different categories: core projects and associated projects. The core projects comprise 40 "hardware" projects from five ministries, such as road construction and infrastructure development, to physically reconstruct disaster-affected areas. All of the expenses of the core projects will be covered by the national government in the form of subsidies and local allocation tax. In contrast, associated projects are "software" projects, often carried out in connection with the core projects to facilitate their implementation, which include participatory planning of local vision, small-scale facility development, and counseling for disaster victims, of which 80 % of the project expenses will be covered by the national government. The share of infrastructure and other public works for the disaster-affected areas accounts for more than 30 % of the reconstruction budget, highlighting the significance of financial supports for Reconstruction Grant Projects (Table 7.3). It should be noted that the Reconstruction Grant Projects were not established as permanent measures but time-bound measures for the intensive reconstruction period meant to accelerate recovery and reconstruction of the disaster-affected areas, which is valid until March 2016.

In addition, the government of Japan enacted the "Act on Special Measures for the Rebirth of Fukushima" in March 2012 to cope with the serious situation caused by the Fukushima Daiichi Nuclear Power Station accident. The Cabinet formulated the "Basic Guidelines for Fukushima Reconstruction and Revitalization" under the Act in July 2012, which introduced a number of special measures: (1) special measures for reconstruction and revitalization of areas where evacuation orders have been lifted, (2) special measures to secure a safe living environment regarding radiation exposure, (3) reconstruction and revitalization of local industries affected by the nuclear disaster,, and (4) promotion of a framework that contributes to the creation of new industries.

7.4 Current Status of Reconstruction

7.4.1 Reconstruction of Tsunami-Affected Areas

Great efforts have been made so far by stakeholders, including the national and local governments, for the swift reconstruction of the disaster-affected areas making best use of institutional supports established by the national government.

The number of refugees due to the disaster reached approximately 470,000 people at maximum three days after the earthquake (Reconstruction Agency 2015b), and half of them were still living away from their houses and more than 80,000 people are living in temporary, prefabricated houses (Fig. 7.11). Approximately, 110,000 households rebuilt their houses themselves after receiving

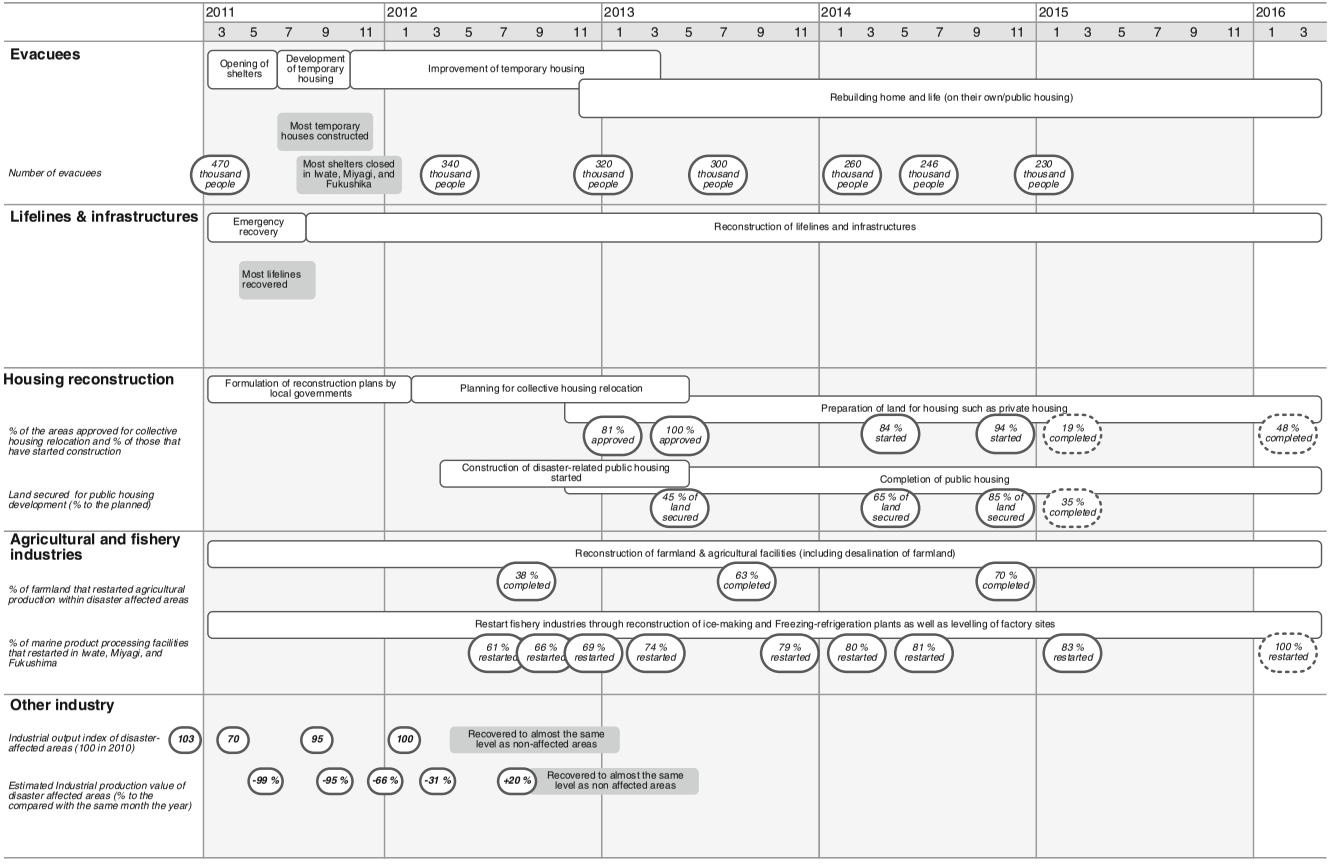

Fig. 7.11 Progress of reconstruction from 2011 to 2016 with selected indicators (numbers in a dashed box are projected values) [translated and modified from Reconstruction Agency (2015b)]

the grant for disaster victims from the national government. More than 340 plans for collective housing relocation to uplands have been formulated by the municipalities of Iwate, Miyagi, and Fukushima for 21,000 households. However, only about 4000 houses are scheduled to be completed by the end of March 2015. Similarly, about 30,000 disaster-related public houses are planned to be built but only 10,000 are to be completed by the end of March 2015. Although the number of houses constructed, including both through collective relocation and public housing, to be completed will increase greatly in the fiscal year of 2015 and will reach approximately 30,000 units by the end of the intensive reconstruction period, it accounts for only 60 % of the total construction plan, implying that 20,000 households will still be forced to live in small, temporary houses (Fig. 7.11).

In contrast to the slow speed of housing construction, the waste management of disaster-related debris, which was approximately 29.3 million tons in Iwate, Miyagi, and Fukushima, was almost completed by March 2015. Recovery and reconstruction of lifelines and infrastructures such as roads, railways, water supply and sewerage systems, electricity, and communications were also mostly completed by March 2015 (Fig. 7.11). Along with the recovery of the existing road network, the government has planned to construct an additional 42 km of road to support and facilitate reconstruction efforts by increased and smoother distribution of resources. Although the reconstruction of infrastructures has been proceeding smoothly on average, the reconstruction of the seawall to protect coastal areas shows sluggish progress with 98 coasts completed and 361 coasts under construction out of 468 damaged coasts. There have been fierce conflicts between governments and local people over the height of the seawall, which will be described later in this chapter.

Local industries, including agriculture and fishery, are also gradually recovering. The mining and manufacturing industrial production index of the disaster-affected areas decreased by more than 30 points due to the earthquake but it recovered to almost the same level as the non-disaster-affected areas by early 2012. For those managers and employees who lost their places of employment, temporary factories and shops were constructed at 577 locations across the disaster-affected areas and about 2700 business operators restarted their business by the end of December 2014. However, the recovery of the agriculture and fishing industries is a bit behind this (Fig. 7.11). Out of 319 fishing ports affected by the disaster, 208 ports had been completely recovered and 97 were partially recovered. Landing of fish and other fishery products have rebounded to about 80 % to their pre-quake levels. Regarding the marine product processing facility, 83 % of the 812 facilities wishing to restart their operation were recovered and had restarted. However, many of the marketing channels of marine products have also been lost due to the disaster, and their recovery is slow; therefore, only 40 % of the marine product processing business had rebounded to about 80 % to the pre-quake sales level. For agriculture, more than 20,000 ha of farmland was inundated by the tsunami, causing soil salinization, and, in addition, many of their irrigation and drainage facilities were severely damaged by the tsunami, of which 15,000 ha of farmland and associated facilities had been recovered by January 2015, accounting for approximately 70 % of the disaster-affected farmland. Tourism industries in the disaster-affected areas,

generally speaking, are benefiting from increased visitors, which is in large part due to increased reconstruction project labor. In fact, the number of visitors who stayed in Iwate, Miyagi, and Fukushima was from 7 to 8 % greater in 2013 than they had been pre-quake in 2011.

7.4.2 *Decontamination of the Nuclear Disaster-Affected Areas*

For those areas severely affected by the nuclear disaster of the Fukushima Daiichi Nuclear Power Station accident, the demarcation of the radiation-contaminated areas provided by the national government was revised under the Special Measures Law on Radioactive Material Environmental Pollution Management, enacted December 2011, to specify who was responsible for decontamination. Under this law, the Restricted Area and Deliberative Areas were reformulated into the Special Decontamination Area, which consists of three different areas based on cumulative dose within a one-year period: (1) Evacuation-order-cancel Preparation Area (annual cumulative dose equal to or smaller than 20 mSv/year), (2) Restricted Residential Area (annual cumulative dose greater than 20 mSv/year and equal to/smaller than 50 mSv/year), and (3) Difficult to Return Area (annual cumulative dose greater than 50 mSv/year). The national government is responsible for the decontamination work in these three areas. In addition, the Special Measures Law provided one more category for those areas with an average radiation dose rate of 0.23 μSv/h, so-called the Priority Survey Area, where decontamination will be the responsibility of municipal governments. The Special Decontamination Area covers 11 municipalities centered on the Fukushima Daiichi Nuclear Power Station while the Priority Survey Area covers 102 municipalities across 8 prefectures, of which 40 are located in Fukushima.

The progress of the decontamination work has been monitored by the type of land use and building, such as public facility site, residential land, road, farmland, and forest (near living area), by the Ministry of the Environment. Decontamination of most of the Priority Survey Area has been completed outside Fukushima while their progress is slow within Fukushima; 90 % of public facility sites, 60 % of residential land, 50 % of roads, 80 % of farmland, and 60 % of forests near living areas were decontaminated by March 2015 (Ministry of the Environment 2015a). Decontamination of the Special Decontamination Area was completed for four municipalities by March 2014, of which the evacuation order for Tamura was lifted, and the remaining seven municipalities are still under operation (Table 7.6).

Table 7.6 Progress of decontamination of the special decontamination area

Municipalities	Population within decontamination site (people)	Area to be decontaminated (ha)	Schedule	
			Residential land	Other land
Tamura	400	500	By March 2014	
Kawauchi	400	500	By March 2014	
Naraha	7700	2100	By March 2014	
Okuma	400	400	By March 2014	
Katsurao	1400	1700	By mid-2014	By December 2015
Kawamata	1200	1600	By mid-2014	By December 2015
Iidate	6000	5600	By December 2014	By December 2016
Minamisoma	13,300	6100	By March 2016	By March 2017
Namie	18,800	3300	By March 2016	By March 2017
Tomioka	11,300	2800	By March 2016	By March 2017
Futaba	300	200	By March 2016	By March 2017

Source translated from Ministry of the Environment (2015b)

7.5 Present and Future Challenges

7.5.1 Tight Time frame for the Reconstruction Grant Project

The Reconstruction Grant Project was originally designed as time-bound measures for use during the intensive reconstruction period to accelerate recovery and reconstruction of the disaster-affected areas with strong financial support. Starting in fiscal year 2016, a new framework for the Reconstruction Grant Project will be put in place but the continuation of strong financial support by the national government is uncertain. If the national government reduces or ceases support for the Reconstruction Grant Project in the future then local governments, both municipal and prefectural, have to bear the great amount of project expenditure by themselves, which would naturally slow down the pace of reconstruction. As such, the temporary framework of the Reconstruction Grant Project, with its unclear future, has been urging local governments within the special zone for reconstruction to implement as many reconstruction projects as possible by March 2016, the end of the intensive reconstruction period.

7.5.2 Rise of Construction Costs

Pressures, such as the aforementioned, on government officials as well as on stakeholders bring about various issues associated with the reconstruction process. Although the number of skilled laborers had been decreasing since 1997 across Japan with a medium- to long-term shrinking of public works, the construction demand suddenly expanded due to the need to reconstruct after the Great East Japan Earthquake. The tight time frame of reconstruction grants has naturally increased the price of construction materials, such as concrete and asphalt, and labor cost, resulting in an increase in the total cost of construction work by 5–8 % (Hashimoto 2013). This has also contributed to an increase in the construction budget (Table 7.3). The situation is further exacerbated by the decision made in September 2013 that the 2020 Summer Olympics would be organized in Tokyo, which also spurred construction demands for items such as athletic facilities and infrastructures. Due to the rise of the construction cost combined with the shortage of labor, it has been often reported in disaster-affected areas that reconstruction bidding ended up in failure. As a result, although the national government provides local governments with enough subsidies to carry out the Reconstruction Grant Projects, responding to their request for each year, not all reconstruction grants from the national government could be fully utilized.

7.5.3 Decision and Consensus Regarding Building in Haste

The tight time frame set for the reconstruction grant project often renders local governments incapable of providing as much opportunity and time for consensus building with stakeholders as normal construction projects provide. Disaster victims need more time to prepare for involvement in decision making and consensus building efforts for reconstruction, in large part because many of them have lost their homes, workplaces, means of labor, and, sometimes, even their family and friends. Immediately after the disaster, for victims, it is necessary to ensure a safe living place such as a shelter, and then, after several months, they move into temporary housing constructed by local governments and can start to consider the restoration of their homes and incomes. Before they start recovering their livelihood and redeveloping their outlook on life, at least for the short term, people lack the emotional capacity necessary to participate in making decisions about the reconstruction of disaster-affected areas, even when they are invited to by the local government. In fact, government officials were often criticized by disaster victims when the government invited them to a public hearing to prepare a reconstruction plan. This was especially true in the early stage of disaster reconstruction when disaster victims were struggling to recover their livelihoods. However, this does not mean that local governments are only interested in their business and are indifferent to the livelihood recovery of the local people. Rather, faced with the tight time

frame of the Reconstruction Project Grants, local governments were also strongly urged to promote the reconstruction of the disaster-affected areas.

7.5.4 Stereotypical Reconstruction of the Seawall

There were approximately 300 km of seawalls constructed along the coast from Iwate to Fukushima, of which about 190 km were destroyed by the tsunami. The national government stated that those seawalls were to be reconstructed within the intensive reconstruction period. The Central Disaster Prevention Council of the national government prepared a tsunami scale to be utilized for the reconstruction of the seawall: L1 and L2. While L1 refers to tsunamis that occur several decades to 100 years apart, L2 tsunamis are those that occur several hundred years apart, like the Great East Japan Earthquake. The guidance from the Central Disaster Prevention Council calls for protection from an L1-scale tsunami by reconstruction of the seawall. For an L2-scale tsunami, assuming not all the tsunami damage could be prevented by the seawall, the Council called for more compressive disaster reduction measures including land use regulations.

In response to the guidance from the council, the national government notified local governments of disaster-affected areas about the height of the L1-scale tsunamis that the seawall is meant to mitigate, which is then utilized as the standard to decide the height of the seawall, which, in the case of Miyagi prefecture, for example, ranges from 2.6 to 11.8 m (Miyagi 2014). For most cases, the height of the new seawall is from a few to more than 7 m higher than the previous embankments. However, uncertainties exist in tsunami simulations conducted for the purpose of setting the height standards for new seawalls, which sometimes prevents local government and experts from convincing local stakeholders. Also, too often, new seawalls are larger than the previous ones and necessitate a larger site for construction, which results in a decrease in the size of sites originally used for local industries, such as fisheries, causing conflicts. In addition, local stakeholders are concerned about environmental impacts due to the construction of larger embankments, such as impacts on fisheries and local ecosystems. These uncertainties and doubts about local governments result in opposition campaigns against the construction of the seawall in some areas.

7.5.5 Lack of Land Available for Residential Relocation

Under the Building Standard Act, approximately 13,000 ha of coastal land in 37 municipalities from the three prefectures of Iwate, Miyagi, and Fukushima were designated as “disaster hazard areas,” as of March 2013, where the construction of residences and welfare facilities are permanently prohibited to avoid future risk of disaster. If the residential land of tsunami victims is designated as a disaster hazard

area, he/she, in exchange, is able to take part in the collective residential relocation project operated by the local government that relocates residents from low-lying coastal areas inland to higher grounds to avoid risks associated with future tsunami disasters. The project costs, including the cost of land acquisition, infrastructure construction, and land preparation, are fully subsidized by the national government. In addition, for land owners participating in the collective residential relocation project, the national government provides moving costs and a part of the expense of purchasing a new house or land through the project. There are 182 plans of the collective residential relocation project formulated as of March 2014, of which 120 plans are in Miyagi, followed by 52 in Iwate, 9 in Fukushima, and 1 in Ibaraki, creating enormous land demand.

When we observe land use composition of the tsunami inundation areas of Sanriku and Sendai-Fukushima, the residential area within 200 m of the Sanriku coast is 860 ha, which is greater than the 750 ha of Sendai-Fukushima. The residential area within the tsunami inundation area decreases significantly with distance from the Sanriku coast; the scale of residential area peaks from 200 to 400 m from the Sendai-Fukushima coast, which gradually decreases, but the tendency is gentler than that of Sanriku (Fig. 7.12). How much land is available for relocation if we relocate all of the residential buildings from the coast to the safer inland area within the tsunami inundation area? Table 7.7 shows the answer to this question, which

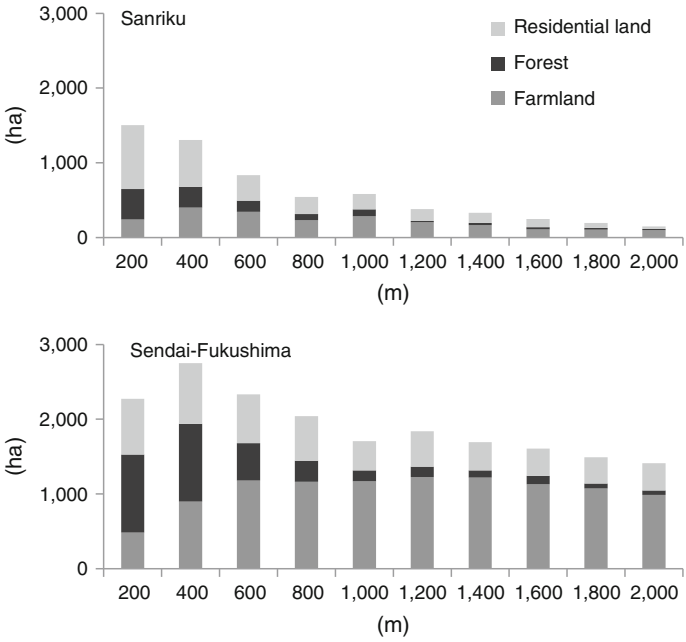

Fig. 7.12 Land use composition of tsunami inundation area in 200 m increments from the coast. *Note* GIS data of tsunami inundation area and land use data for the year 2006 (100 m mesh) were cross-tabulated with ArcGIS 10.2

Table 7.7 Land areas available for residential relocation within 200 m increments from the coast

Distance from the coast (m)	Sanriku			Sendai-Fukushima		
	Residential area to be relocated (a)	Supply potential (b)	Balance (b − a)	Residential area to be relocated (a)	Supply potential (b)	Balance (b − a)
0–200	860	2670	1810	750	12,490	11,740
0–400	1480	1990	510	1560	10,550	8990
0–600	1820	1490	−330	2210	8870	6660
0–800	2050	1180	−870	2810	7420	4610
0–1000	2260	800	−1,460	3200	6110	2910
0–1200	2420	580	−1840	3680	4740	1070
0–1400	2550	380	−2170	4060	3430	−630
0–1600	2660	250	−2420	4420	2190	−2240
0–1800	2730	120	−2610	4770	1050	−3730

Note GIS data of tsunami inundation area and land use data for the year 2006 (100 m mesh) were cross-tabulated with ArcGIS 10.2. This estimate supposes that we need the same land area for relocation as that of residential land to be relocated from the coast

demonstrates the balance between (a) residential area to be relocated and (b) supply potential of the land as a sum of farmland and forest areas available, which is between 0 and 2000 m from the coast in 200 m increments. If the balance (b − a) has a negative value, it is impossible to supply as much land for relocation as that of the previous residential land nearer the coast. For example, if we relocate all the residential area within 1000 m of the coast of Sanriku, we need to prepare 2260 ha of land. However, the land available for relocation between 1000 and 2000 m from the coast is only 800 ha. We lack 1460 ha of land, which means that we need to fill this gap by relocation to more inland areas or to higher ground; the latter necessitates a great amount of tree-clearing and earthwork. Table 7.7 clearly demonstrates the difficulties of residential relocation in the Sanriku area. In contrast, the Sendai-Fukushima area demonstrates a greater amount of land available for relocation to inland areas. However, it has been causing a sharp rise in land prices, which makes it difficult for disaster victims to find land to build their homes upon at a reasonable price.

7.5.6 Future Use of the Empty Spaces Left by the Residential Relocation

The residential relocation project leaves extensive empty spaces in the coastal areas designated as “disaster hazard area” where the construction of residences and welfare facilities are permanently prohibited. If we relocate all the residential areas within 1000 m of the coast, the relocation will leave approximately 2260 ha of

empty area in Sanriku and 3200 ha in Sendai-Fukushima. Local governments operating the collective residential relocation project are also bothered about the future use of these empty spaces. Reconstruction plans formulated by local governments of the disaster-affected areas often stipulate that these empty spaces that are left by the residential relocation are to be utilized for planting windbreak forests, farmlands, parks, industrial sites, and renewable energy production such as wind and solar power (e.g., see Fig. 7.8). However, it is very difficult to attract new businesses to operate in those areas even with various economic incentives, such as tax exemptions, especially if those empty lands are located in remote areas. Also, as for the use as windbreak forests and parks, local governments have to take care of their long-term maintenance costs.

7.5.7 Environmental Impacts Due to Reconstruction Projects

In order to facilitate the reconstruction of disaster-affected areas, various preferential measures are applied to reconstruction projects stipulated by local governments in their land restructuring plans. One such measure is simplification of the environmental impact assessment mandated by the national government under the Act for Assessment of Environmental Impacts. While normal environmental impact assessment obliges developers to carry out an in-depth field survey for the project site throughout the year as part of impact assessment procedure and usually takes from 3 to 4 years in total to complete the assessment, under the simplified process, this time-consuming assessment is replaced with a review of existing literature and most of the evaluation process is to be conducted by local governments, cutting the total evaluation times remarkably. Prefectural governments also take similar attitudes about the application of the environmental impact assessment even if they have their own ordinance to supplement national legislation. For example, the Miyagi prefectural government, to facilitate the reconstruction efforts, amended their environmental impact assessment ordinance. This amendment is to exempt reconstruction projects from environmental impact assessment if the governor admits the smooth execution of these projects is necessary. In addition to this amendment, land adjustment projects, collective residential relocation projects, and reconstruction and improvement of existing railways have been also exempted from the environmental impact assessment. Thus, a large part of the reconstruction projects, regardless of their large expected environmental impacts, is exempted from impact assessment, and the rest of the projects, though assessed, go thorough lax procedures. Here, we are also faced with the challenges of balancing the reduction of environmental impacts with the promotion of reconstruction of disaster-affected areas.

7.5.8 Accelerated Trend of Population Decrease

The populations of Iwate, Miyagi, and Fukushima were on a declining trend that started from late 1990s to the mid-2000s with an annual population decline of a few thousand in Miyagi to more than 10,000 in Iwate and Fukushima. Given the fact that the national population has been on a decline since 2005, these trends are not surprising information, but they have been accelerated by the Great East Japan Earthquake of 2011. The population has decreased by approximately 160,000 in these three prefectures as a whole from 2010 to 2014, of which 94,000 were in Fukushima, followed by 46,000 in Iwate and 20,000 in Miyagi. Out of 42 municipalities located in the coastal areas of Iwate, Miyagi, and Fukushima and within the Deliberative Evacuation Area around the Fukushima Daiichi Nuclear Power Station, 39 municipalities experienced population decline with a total decrease of 92,000 people (Asahi 2015). Only three municipalities showed an increase in population, which are Sendai (+27,000), Natori (+3000), and Rifu (+1000) in large part due to migration from disaster-affected areas; these municipalities are geographically connected, comprising the prefectural capital and its satellites. Population decrease is especially severe in Yamada (−14 %), Otsuchi (−22 %), and Rikuzentakada (−16 %) of Iwate; Minamisanriku (−21 %), Onagawa (−29 %), and Yamamoto (−26 %) of Miyagi; and Minamisoma (−10 %), Namie (−11 %), Futaba (−11 %), and Tomioka (11 %) of Fukushima from March 1, 2011, until February 1, 2015. Presumably these are in large part due to the loss and slow recovery of workplaces and the slow progress of collective residential relocation projects. The population decline is also influenced by other factors such as the convenience of life or remoteness from densely populated areas, which, although independent from the disaster, influences the pattern of out-migration from the disaster-affected areas. The municipalities of Fukushima that suffered from the nuclear disaster are faced with another difficult situation as they need to carry out the decontamination of radioactive materials from their territory in order to ensure a safe living environment for local people and promote the return of those who are currently evacuated.

References

Japan Metrological Agency (2011) Disaster earthquake and tsunami Bulletin of the 2011 Tohoku Pacific Ocean Earthquake. http://www.jma.go.jp/jma/kishou/books/saigaiji/saigaiji_201101/saigaiji_201101.html. Accessed 15 May 2015 (in Japanese)

Hashimoto S (2013) Two-years trend of the construction materials and construction cost and their prospects. Build Cost Res 81:34–41

Hashimoto S (forthcoming) Land use of Tsunami inundation areas: challenges of the coastal areas of Sanriku and Sendai-Fukushima. In: Investigation Report Editing Committee for the Great East Japan Earthquake (eds) Investigation report 9: architecture-society system and disaster/rural community planning, Architectural Institute of Japan (in Japanese)

Iwate Prefecture (2011) Basic plan for the Great East Japan Earthquake and tsunami reconstruction efforts. http://www.pref.iwate.jp/dbps_data/_material_/_files/000/000/008/990/kihonkeikaku.pdf. Accessed 28 May 2015 (in Japanese)

Ministry of the Environment (2015a) Progress of decontamination conducted by the municipal government. http://josen.env.go.jp/zone/. Accessed 28 May 2015 (in Japanese)

Ministry of the Environment (2015b) Progress of decontamination conducted by the national government. http://josen.env.go.jp/material/pdf/josen_gareki_progress_201504.pdf. Accessed 28 May 2015 (in Japanese)

Miyagi Prefecture (2011) Miyagi prefecture basic plan for disaster reconstruction (draft). http://www.pref.miyagi.jp/uploaded/attachment/36636.pdf. Accessed 28 May 2015 (in Japanese)

Miyagi Prefecture (2014) Height of sea walls in Kesennuma region. http://www.pref.miyagi.jp/uploaded/attachment/108393.pdf. Accessed 28 May 2015

Morino Y, Ohara T, Nishizawa M (2011) Atmospheric behavior, deposition, and budget of radioactive materials from the Fukushima Daiichi nuclear power plant in March 2011. Atmos Sci 38(7):L00G11. doi:10.1029/2011GL048689

Reconstruction Agency (2013a) The status in Fukushima. www.reconstruction.go.jp/english/topics/2013/03/the-status-in-fukushima.html

Reconstruction Agency (2013b) Current status and path toward reconstruction. http://www.reconstruction.go.jp/english/130528_CurrentStatus_PathToward_FINAL.pdf. Accessed 28 May 2015

Reconstruction Agency (2015b) Reconstruction efforts and institutions to date. http://www.reconstruction.go.jp/topics/main-cat1/sub-cat1-1/20150310_torikumi_seido.pdf. Accessed 28 May 2015

Reconstruction Agency (2015b) Overview of the Great East Japan Earthquake: progress of reconstruction and recent efforts. http://www.reconstruction.go.jp/topics/main-cat7/sub-cat7-2/201503_pamphlet.pdf. Accessed 28 May 2015 (in Japanese)

Reconstruction Design Council (2011) Towards reconstruction—hope beyond the disaster. Report to the Prime Minister of the Reconstruction Design Council in response to the Great East Japan Earthquake. http://www.cas.go.jp/jp/fukkou/english/pdf/report20110625.pdf. Accessed 28 May 2015

Suzuki I, Kaneko Y (2013) How the 3.11 emergency responses for the gigantic natural disasters were actually organized. In: Japan's disaster governance: how was the 3.11 crisis managed? Springer, Berlin, pp 39–48

TEPCO (2015) Payment for nuclear damage compensation. http://www.tepco.co.jp/fukushima_hq/compensation/images/jisseki01-j.pdf. Accessed 28 May 2015 (in Japanese)

Index

S. Haruyama and T. Sugai (eds.), *Natural Disaster and Coastal Geomorphology*, DOI 10.1007/978-3-319-33814-9